جمهورية العراق
وزارة التعليم العالي والبحث العلمي
جامعة بابل
كلية العلوم
قسم الفيزياء

تحسين الخصائص الفيزياوية في خليط بوليمري المشوب لجسيمات الغير عضوية نانوية للتطبيقات الطبية الحيوية

أطروحة مقدمة إلى

مجلس كلية العلوم- جامعة بابل

وهي جزء من متطلبات نيل درجة الدكتوراه فلسفة في العلوم / الفيزياء

من قبل

سرور فاضل عبيد هلال

بكالوريوس علوم في الفيزياء / 2015

ماجستير علوم في الفيزياء / 2019

بأشراف

أ.د. رحيم كعيد كاظم حسين

2022 م **1444هـ**

Republic of Iraq
Ministry of Higher Education and Scientific Research
University of Babylon
College of Science
Department of Physics

Improving Physical Properties of Polymer Blend Doping with Inorganic Nanoparticles for Biomedical Applications

A Thesis
Submitted to the Council of the College of Science University of Babylon in Partial Fulfillment of the Requirements for the Degree of Doctor of Philosophy in Science/Physics

By

Sroor Fadhil Obaid Hilal

B.Sc. in physics / 2015

M.Sc. in physics / 2019

Supervised by

Prof. Dr. Raheem G. Kadhim Hussein

2022 A.D. **1444 A.H.**

﴿نَرْفَعُ دَرَجَاتٍ مَّن نَّشَاءُ وَفَوْقَ كُلِّ ذِي عِلْمٍ عَلِيمٌ﴾

صدق الله العلي العظيم

سورة يوسف الآية (76)

Acknowledgments

Praise be to Allah, and thanks to His Majesty the Almighty who enable and helpe me to accomplish this thesis, O Allah, bless Muhammad and his family. And yet ..

I would like to express my gratitude to my supervisor Prof. Dr. Raheem G. Kadhim Hussein for their valuable support & guidance throughout this study.

I want to extend special thanks to Prof. Dr. Abdulazeez O. Mousa AL-Ogaili, the Head of Department of Physics, College of Science, University of Babylon, and all the members of the Department, for their support and advice during the entire course of my study.

I would also thank Prof. Dr. Ahmed Hashim Mohaisen and Prof. Dr. Ehssan Dhiaa Jawad, University of Babylon, College of Education for their help in using the laboratories at the Department of Physics.

Finally, my thanks go to whoever offered a help whatsoever. Especially my family for their support and encouragement throughout the work of these research. I extend my wishes, thanks and gratitude.

Sroor

Dedication

I dedicate this thesis

To the symbol of giving who support me all the time

(My Father and My Mother)

To my princess…. (my daughter is a malk)

To my loving……..(My Brothers and Sisters)

(To My friends)

Sroor

الخلاصة

يتضمن العمل الحالي تحضير المتراكبات النانوية ($PVP-PVA-Ag_2O-NbO_2$) ($PVP-PVA-Al_2O_3-NbO_2$) بطريقة صب المحلول. وحضر الخليط البوليمري (PVP-PVA) بتركيز (50 wt.%) من بولي فينيل بيروليدون و (50 wt.%) من بولي فينيل الكحول. اضيفت نسب وزنية مختلفة (0.005, 0.01, 0.015 and 0.02) من الجسيمات النانوية اوكسيد الفضة , اوكسيد الالمونيوم واوكسيد النيبيوم إلى لخليط البوليمري (PVP-PVA). تمت دراسة تأثير تراكيز الجسيمات النانوية (Ag_2O, Al_2O_3 and NbO_2) على الخصائص التركيبية ,البصرية والتوصيلية الكهربائية المتناوبة للخليط البوليمري (PVP-PVA). درست التطبيقات البيئية البيولوجية للمتراكبات النانوية التي تضمنت النشاط المضاد للبكتريا.

ويظهر طيف FTIR ازاحة في موقع القمة وكذلك تغيير في الشكل والشدة ، مقارنة مع الأفلام النقية (PVP-PVA)، وهذا يشير إلى الاهتزازات المقابلة للبوليمرات والجسيمات النانوية اوكسيد الفضة, اوكسيد الالمونيوم واوكسيد النيبيوم. ولوحظ أن هناك نقص في النفاذية بزيادة تراكيز الجسيمات النانوية اوكسيد الفضة, اوكسيد الالمونيوم واوكسيد النيبيوم.

لقد أظهرت صور المجهر الضوئي وصور مجهر الماسح الالكتروني أن اوكسيد الفضة, اوكسيد الالمونيوم واوكسيد النيبيوم النانوي يتوزع بشكل متجانس في الخليط البوليمري.

بينت النتائج التجريبية للخواص البصرية للمتراكبات النانوية زيادة الامتصاصية، معامل الامتصاص، معامل الخمود، معامل الانكسار، ثوابت العزل الحقيقي والخيالي, والتوصيلية البصرية للخليط البوليمري (PVP-PVA) بزيادة تراكيز الجسيمات النانوية بينما النفاذية وفجوة الطاقة يقلان بزيادة تراكيز الجسيمات النانوية(Ag_2O, Al_2O_3 and NbO_2). المتراكبات النانوية تمتلك امتصاصية عالية في المنطقة فوق البنفسجية.

وكذلك درست الخواص الكهربائية المتناوبة للمتراكبات النانوية في درجة حرارة الغرفة في مدى تردد يتراوح من (100Hz-5MHz). بينت النتائج التجريبية زيادة ثابت العزل الكهربائي, فقدان العزلي والتوصيلية الكهربائية المتناوبة مع زيادة تركيز الجسيمات النانوية (Ag_2O, Al_2O_3 and NbO_2). ان ثابت العزل الكهربائي وفقدان العزل الكهربائي للمتراكبات النانوية يقلان بزيادة تردد المجال الكهربائي المسلط, وان التوصيلية الكهربائية المتناوبة تزداد بزيادة التردد.

أظهرت نتائج التطبيقات للمتراكبات النانوية المحضرة ($PVP-PVA-Ag_2O-NbO_2$) ($PVP-PVA-Al_2O_3-NbO_2$) كمضادات لبكتريا موجبة غرام (*المكورات العنقودية الذهبية المكورات المعوية*) وسالبة غرام (*الاشريشيا القولونية و الكلبسيلة الرئوية*). بينت النتائج أن منطقة التثبيط ازدادت بزيادة تراكيز الجسيمات النانوية (Ag_2O, Al_2O_3 and NbO_2).

Summary

The present work includes preparation of (PVP-PVA-Ag_2O-NbO_2) and (PVP-PVA-Al_2O_3-NbO_2) nanocomposites by using solution casting method. The (PVP-PVA) base composites is prepared with concentration (50 wt.%) of polyvinyl pyrrolidinone and (50 wt.%) of polyvinyl alcohol. The different weight percentages are (0.005, 0.01, 0.015 and 0.02) of silver oxide, aluminum oxide and niobium oxide nanoparticles are added to (PVP-PVA) base blend. The effect of (Ag_2O, Al_2O_3 and NbO_2) nanoparticles concentration on the structural, optical and the A.C electrical properties of (PVP-PVA) base composites is studied. The environmental biological applications of nanocomposites are investigated for antibacterial activity applications.

FTIR spectra show shift in peak position, change in shape and intensity compare with pure films of (PVP-PVA), this indicates to the corresponding vibrations of two polymers and silver oxide, aluminum oxide and niobium oxide nanoparticles. It is noted that there is a decrease in transmittance with increasing the concentrations of silver oxide, aluminum oxide and niobium oxide nanoparticles.

Optical microscope and scanning electron microscope images indicate that the silver oxide, aluminum oxide and niobium oxide nanoparticles additives distribution were homogeneous in the blend.

The experimental results of optical properties for nanocomposites showed that the absorbance, absorption coefficient, extinction coefficient, refractive index, real and imaginary dielectric constants, and optical conductivity of (PVP-PVA) base composites were increased with increase the (Ag_2O, Al_2O_3 and NbO_2) nanoparticles concentrations, while the transmittance and energy band gap were decreased with increase the

(Ag_2O, Al_2O_3 and NbO_2) nanoparticles concentrations. The nanocomposites have high absorbance in the UV-region.

Also, the A.C electrical properties of nanocomposites were studied in the frequency ranging (100Hz-5MHz) at room temperature. The experimental results showed that the dielectric constant and dielectric loss of nanocomposites was decreased with increasing the frequency of the applied electric field and increased with increasing the concentrations of (Ag_2O, Al_2O_3 and NbO_2) nanoparticles, while A.C electrical Summary II conductivity rises with increasing the frequency and (Ag_2O, Al_2O_3 and NbO_2) nanoparticles concentrations.

The antibacterial activity of (PVP-PVA-Ag_2O-NbO_2) and (PVP-PVA-Al_2O_3-NbO_2) nanocomposites against gram positive bacteria (*S. aureus and E. faecalis*) and gram negative bacteria (*E. coli and K. pneumonia*). Was investigate. The results showed that strong activity are the inhibition zone was increased with the increases of (Ag_2O, Al_2O_3 and NbO_2) nanoparticles concentrations.

Contents

List of Symbols

Symbol	Description
Tg	Glass transition
Tm	Melting temperature
A	Absorbance
T	Transmittance
I_A	Absorbed light intensity
I_T	Transmitted intensity beam
I_o	Incident intensity of light
α	Absorption coefficient
t	Thickness of the sample
h	Planck's constant
υ	Frequency
E_g^{opt}	Optical energy gap
R	Reflectance
n	Refractive Index
c	Light speed in vacuum
v	Velocity of the light in specimen
n^*	Complex refractive index
k	Extinction coefficient
λ	Wavelength of photon
ε_1	Real dielectric constant
ε_2	Imaginary dielectric constant
σ	Optical conductivity

έ	The dielectric constant
C_p	The parallel capacitance
C_o	The vacuum capacitor
ε″	The dielectric loss
D	The dispersion factor
$\sigma_{A.C}$	The A.C conductivity
W	The angular frequency

Symbol	*Description*
PVP	Polyvinyl pyrrolidone
PVA	Polyvinyl alcohol
Ag_2O	Silver oxide
NbO_2	Niobium oxide
Al_2O_3	Aluminum oxide
V.B.	Valens band
C.B.	conductive band
S. aureus	Staphylococcus aureus
E. coli	Escherichia coli
E. faecalis	Enterococcus faecalis
K. pnenmoniae	Klebsiella pneumoniae
FTIR	Fourier Transform Infrared Radiation
UV	Ultraviolet spectrum

List of Figures

List of Tables

Chapter One

Introduction and Literature Review

1.1 Introduction

Nanotechnology refers to a field of science and technology applications whose special and unique properties could be attributed to their large surface areas and small sizes [1]. Nanotechnology is a new discipline of science that is interested in materials that are small in size (1-100) nanometer [2].

Nanomaterials can be classified according to dimensions into; three dimensions as nanoparticles and nanoshells, two dimensions as nanotube nanofibers, and nanowire, one dimensions as thin films and layers, as well as zero-dimensional nanomaterials as nanospheres and nanoclusters. Generally, the studies are showing extensive interest towards metal oxide nanomaterials because of their potential use in wide range of applications like antibacterial activity [3].

Nanotechnology is an emerging interdisciplinary technology that has been booming in many areas during the recent decade, including materials science, mechanics, electronics, optics and medicine [4].

The applications of nanotechnology has only been increasing in the recent years, including the highest potential application is in the field of materials that its followed by electronics and medicine application. Some of the potential applications of nanotechnology are as follows: Filters for cost-effective desalinization of water. Micro sensors and diagnostics for more effective treatment antibacterial dressings and coatings [5].

Antibiotics are one of the most important discoveries in the history of medicine, responsible for saving millions of lives by making formerly deadly infections curable. Antibiotic reliability is the foundation for

modern medicine and has facilitated the development of numerous, formerly impossible, medical procedures. Almost every aspect of what we refer to as contemporary medicine, including all surgical procedures, treatment for burns and wounds. All of this was made feasible because to the discovery of antibiotic drugs. On the other hand, academics and medical experts are still having trouble finding a solution to the expanding problem of antibiotic resistance, which is particularly widespread in healthcare settings. It is imperative that quick action be taken to solve this issue since it poses a risk to the fundamental basis upon which modern medicine was established [6].

Bacteria develop resistance to antibacterial drugs through a variety of mechanisms that require a fresh approach to develop new bactericidal. The search for new antimicrobial agents or modifications in already existing ones to improve their antimicrobial activity becomes indispensable. Nanotechnology provides a good platform to alter physico-chemical properties of different materials compared to their bulk counterpart that can be harnessed for bio applications. Nano medicine an offshoot of nanotechnology has taken a stride in diagnosis, monitoring, drug delivery and control of diseases [7].

1.2 Polymer

Polymers consist of large organic molecules (macromolecules) of repeating small structural units (monomers) connected together in a process called polymerization. Each molecule is composed of thousands of atoms connected by covalent chemical bonds [8,9].

polymers consist of huge, combined molecules. In the solid state, polymers are comprised of crystalline and noncrystalline regions. Crystalline polymers consist of 90% of crystalline regions, while the non-crystalline polymers are almost entirely non crystalline [10].

Polymers with a unique composition have semiconductor capabilities, but most commercial polymers are insulators since polymers are simply formed. Polymeric materials may be produced and processed into various forms depending on the purpose, such as thin films [11,12].

Polymers are classified as natural and artificial, with natural polymers such as proteins, starches, cellulose, and rubber, either the industrial they have a lot of properties and uses the molecules in the polymer are a large compared with molecules hydrocarbon (where it is the foundation of the organic material), because of their size they are often referred to as macromolecules [13,14].

Polymers are utilized in the electronic device business because they have numerous qualities, such as low cost, ease of setup, high resistance, and flexibility, in addition to the mechanical properties [15].

Polymeric materials have pervaded every aspect of our lives and in every field. It's difficult to imagine today's world without human-made polymeric materials, with all of its wealth and convenience. Polymer science is new, exciting, and simple to work with in a variety of applications. Despite these important qualities, the polymer has poor mechanical properties due to defects in the structure [16,17]. As a result, researchers have been working to create new methods and approaches for developing polymers of high quality such as electrical, physical, thermal and mechanical that might be useful with a diverse array of uses [18,19].

One of the best and successful ways that have been applied is nanotechnology, where polymer nanocomposite has been involved more and gets more consideration by researchers, engineers, and the industrial sector to bring the high performance of the new nanocomposite with better properties [20,21]. Many variables influence enhancement, including nanofillers employed, interface interaction, component quality, and so on [22]. Where the nanofillers effect on the material properties.

Assuming that the interaction takes place between the dispersed particles and the matrix, Recently, the carbon family has widely been considered as the most significant nanofiller because of its ability to tunable and improve the properties of the materials [23,24].

In recent decades polymers has advanced rapidly. Scientists are now working on polymers of the highest quality that may be utilized in a variety of applications and polymer research is fast evolving in numerous exciting ways [25,26]. It also made inroads into a wide range of sectors and applications, including photovoltaic cells and optoelectronics, as well as the medical field [27,28].

1.3. Polymer Blend

The polymer blends have been one of the primary areas in polymer science and technology over the past several decades. Polymer blend is defined as the combination of two or more dissimilar polymers by physical mixing with/without chemical interaction between them [29,30].

The Polymer blends include both crystalline and amorphous polymers [31]. Blending of two or more types of polymer is a useful technique for preparing and developing materials with properties superior to those of individual constituents [32]. There are many reasons why polymer blending is considered as one of the most important areas in polymer research and development, among these reasons, that polymer blends offer a fast and cheap way to obtain new polymeric materials. These materials generally exhibit a range of features which depend upon the properties of their components, and polymer blends offer versatile industrial applications through enhancement of properties and economic benefits [33,34].

There are three major factors, morphology, miscibility, and compatibility, which mainly decide the performance of the polymer

blends. Numerous efforts have been undertaken to understand these three factors in polymer blend systems [35,36].

Materials are made up of two or more blending's that are overlapped and have a physical or chemical difference in the distribution or arrangement. This procedure of blending materials with varied mechanical properties allows us to create new materials with qualities that differ from the individual features of each component [37].

1.4 Nanocomposites

Nanocomposites are multiphase materials, where one of the components has nanoscale additives [38]. According to matrix materials, nanocomposites can be classified as polymer matrix nanocomposites (PMNC), metal matrix nanocomposites (MMNC) and ceramic matrix nanocomposites (CMNC) [39,40].

The addition of inorganic nanoparticles into a polymer matrix will change both properties from inorganic nanoparticles and polymer to be enhanced and hence advanced new functions can be generated to the nanocomposites [41].

The combination of organic polymer and inorganic nanoparticles will be offered materials with improved mechanical, electrical, optical, magnetic, thermal and many other specific properties. Thus, their effect on composite properties is either enhanced or the same impact is achieved at the lower concentrations of the filler [42].

The nanocomposites applications are quite promising in the fields of microelectronic packaging, medicine, optical integrated circuits, drug delivery, sensors, packaging materials, coatings and adhesives….etc. [43]. These advanced nanocomposites have many advantages such as low cost production and the possibility of device fabrication on large scale and flexible substrates [44].

Nanocomposite polymer consists of three major substances are the matrix, reinforcement, and the interfacial region as illustrate in Figure (1.1). The last is in charge of incorporation between the matrix and nanofiller [45].

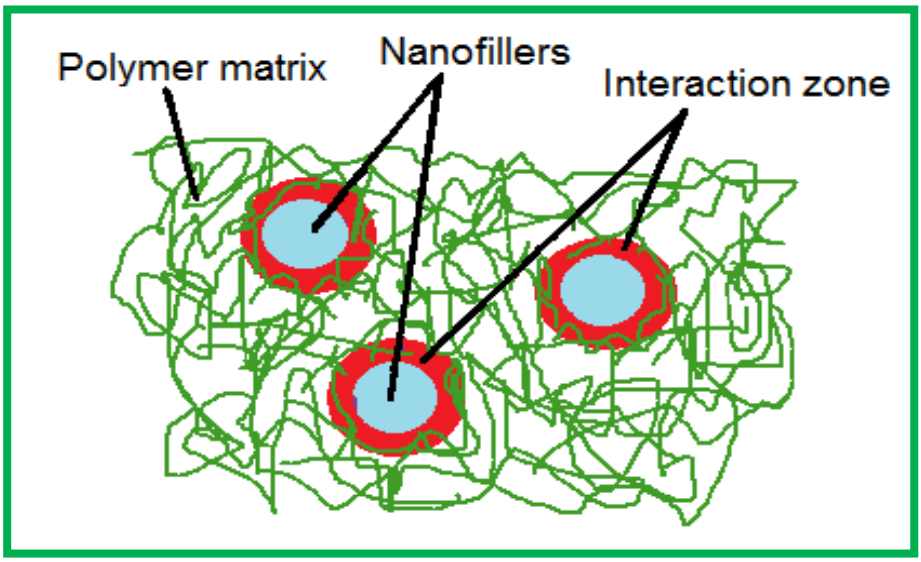

Figure (1.1): The component of nanocomposites [45].

1.5 Nanomedicine

Nanomedicine is the medical application of nanotechnology, and it is a relatively new field of science and technology for treatment, monitoring, control of diseases and diagnosis [46]. Nanomedicine ranges from the medical applications of nanomaterials and biological devices, to nanoelectronic biosensors [47].

Nanomaterials can be useful for both in vivo and in vitro biomedical research and applications. Thus, the integration of nanomaterials with biology has led to the development of diagnostic devices, analytical tools, physical therapy applications, and drug delivery [48,49].

Nanomedicine seeks to deliver a valuable set of research tools and clinically useful devices in the near future. The national nanotechnology initiative expects new commercial applications in the pharmaceutical

industry that may include advanced drug delivery systems and in vivo imaging [50].

1.6 The Properties of the Used Materials

1.6.1 Polyvinyl pyrrolidone (PVP)

Polyvinyl pyrrolidone (PVP) is a synthetic biodegradable polymer and it has excellent characteristics like high dielectric constant, good solubility in water and many organic solvents, chemical stability, having high mechanical strength, moderate electrical conductivity and it is low cost. Furthermore, the amorphous nature of PVP has low scattering loss, which is more useful for optical applications. Polyvinyl pyrrolidone is chosen because it is having good mechanical, electrical, optical characteristics [51,52].

Due to the (PVP) ability to form a film and to adhere well, it can be used as a coating or as an addition to coatings [53]. PVP is safe to use and has a high molecular weight, which can range anywhere from (40,000 to 360,000 $g.mol^{-1}$) [54]. The PVP functional group is responsible for polyvinyl pyrrolidones relatively high melting temperature, which is around 570 degrees Kelvin. It possesses a high T_g=428K value [55].

The aqueous solutions of (PVP) are used in pharmaceutical industry and medicine, optical and electrical applications, adhesives, cosmetics, coatings and environmental applications [56,57].

Polyvinyl pyrrolidone (PVP) is a water soluble polymer with good bio-stability. It is chemically stable, has low toxicity and is biocompatible. Hence, it is useful in a variety of applications such as cosmetics, tissue engineering, and biomedical engineering [58].

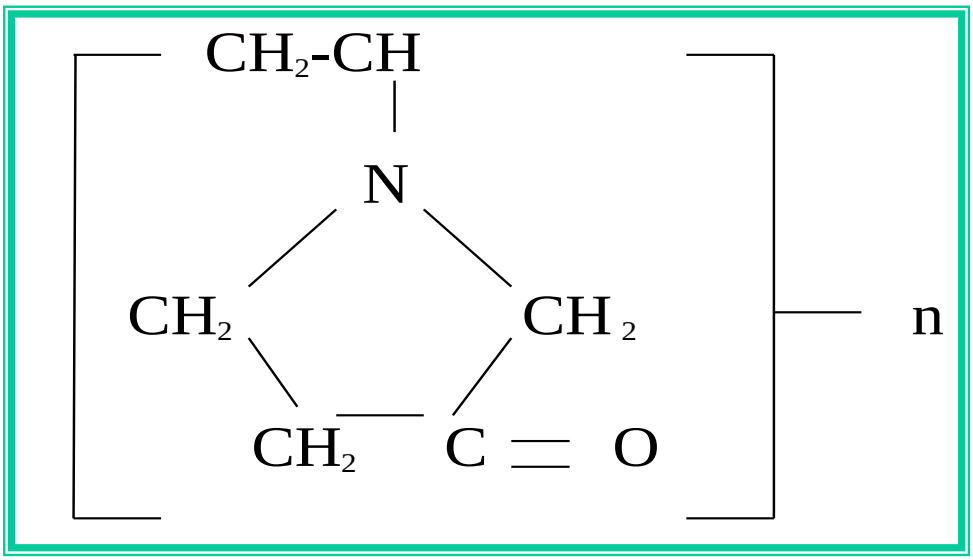

Figure (1.2): The chemical structure of polyvinyl pyrrolidone [59].

1.6.2 Polyvinyl alcohol (PVA)

Polyvinyl alcohol (PVA) has unique properties such as biodegradable, good chemical stability, eco-friendly, good charge storage capacity, high abrasion resistance, elongation, tensile strength, flexibility, thermal stability and low manufacturing cost. PVA a water soluble synthetic polymer which have less toxicity and possess excellent wound dressing bio reactor properties [60, 61]. PVA is distinguished by its semi-crystalline character, which may be defined as the material's physical characteristics are enhanced by the presence of both amorphous and crystalline patches, which create interfacial effects. Tg= 85 C^{o}, Tm= 230 C^{o}, and density 1.3g/cm^{3} are the properties of PVA [62].

It swiftly decomposes when exposed to high heat. Polymers, salts, nanocomposites, and ions are commonly added to PVA in order to alter and improve its performance [63]. PVA is basically a electrical insulator, but it becomes conductive in nature while doping with some conductive inorganic fillers. PVA is extensively used as polymer matrix for the synthesis of different composite by cost deficient technique [64].

PVA is an important polymer, because of its unique physical and chemical properties. It is used industrially for adhesives, in biomedical materials as drug-delivery system and membranes. PVA can also be used in medical applications such as artificial blood vessels, artificial intestines, and contact lenses. It had been noted as a medical material due to its compatibility to the living body [65,66].

Since PVA may be easily prepared, biodegradable, chemically resistant and mechanically strong, it has been used in a wide variety of biomaterial applications [67]. Composites have good potential for various industrial fields because of their excellent properties such as high hardness, high melting point, low density, high thermal conductivity, good chemical stability [68].

PVA is distinguished from other polymers by a number of favorable features, including its strength, resistance to corrosion, and high temperature stability. These OH groups facilitate the hydrogen bonding that forms effective polymer mixtures [69].

PVA is used in this investigation as model polymers. with very good properties, especially good resistance to harsh cutting conditions and stable to acid and alkalis. It is used in various applications such as lenses, internal and external lighting of cars [70, 71].

PVA is used extensively in the manufacturing of non-toxic, harmless, and living tissues, amongst other things, as a thermoplastic polymer [72]. PVA could also be chemically bonded to nanoparticles, in addition to the possibility of physical entanglement [73]. It finds widespread application in the paper and textile manufacturing industries, as well as in the production of oxygen-resistant membranes and the coating of photographic film [74].

PVA have unique polymers have many significant functional groups that increase their ability to compatible with other materials, nanofillers and polymers, etc, that make them attractive materials for scientists, engineering, and researchers [75,76]. PVA are investigated with a range of other materials, polymers, and filers, etc. to overcome their weakness or developed their properties for several or specific applications [77]. Figure (1.3) shows structure of PVA.

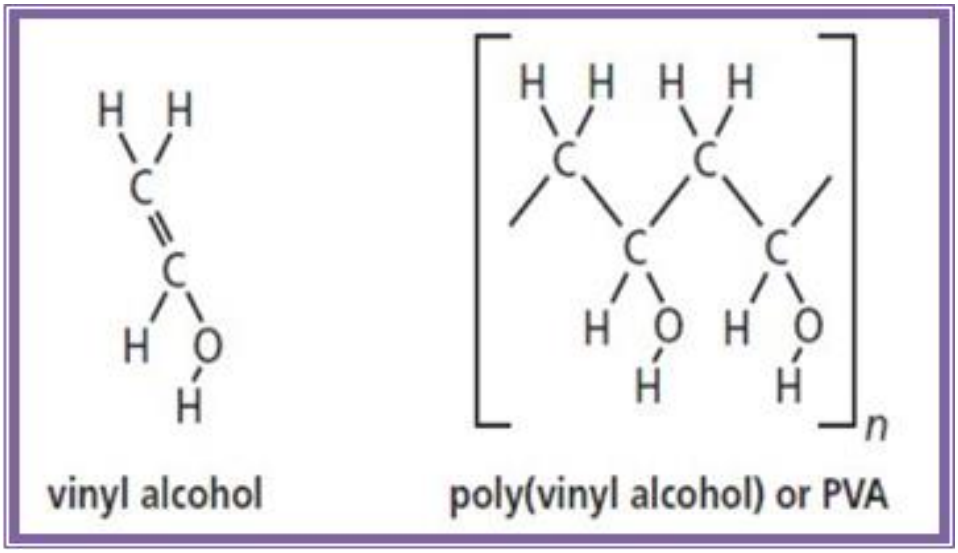

Figure (1.3): The chemical structure of polyvinyl alcohol (PVA) [78].

1.6.3 Silver oxide Nanoparticles (Ag_2O NP_S)

Silver nanoparticles are nanoparticles of silver of between (1-100) nm in size. While frequently described as being 'silver' some are composed of a large percentage of silver oxide due to their large ratio of surface-to-bulk silver atoms [79].

Because of the beneficial optical, conductive, and antibacterial properties that silver nanoparticles possess, they are used in a wide range of technologies and can be found in a variety of consumer goods thanks to their incorporation into such technologies. Silver nanoparticles can be found in a variety of consumer products, such as antibacterial toothpaste and antibacterial skin cream [80,81].

1. Optical Applications: Silver oxide nanoparticles are used to efficiently harvest light and for enhanced optical spectroscopies.
2. Conductive Applications: Silver oxide nanoparticles are used in conductive inks and integrated into composites to enhance thermal and electrical conductivity.
3. Antibacterial Applications: Silver oxide nanoparticles are incorporated in apparel, footwear, paints, wound dressings, appliances, cosmetics, and plastics for their antibacterial properties.

There are numerous uses for silver nanoparticles in various fields such as catalysis, optoelectronics, detection, diagnostics, antimicrobials and the treatment of various diseases and ailments. Silver nanoparticles have been used as an anti-cancer therapy in numerous studies, and all of them have been favorable. Silver nanoparticles anti-cancer activity, on the other hand, should open up new avenues in medicine [82,83].

Silver nanoparticles may be useful in biomedical research (Ag). The anti-microbial properties of nano-silver are superior to those of bulk silver because of the latter's lower toxicity and higher extinction coefficient. Silver nanomaterials have been discovered to have a wide range of applications in everyday consumer life. These applications include nanosilver infused storage containers, nanosilver coated surfaces of medical devices to prevent hospital-related infections, bandages, footwear, and many more home goods that claim to be anti-microbial [84]. Because of its particular capacity to fight infectious diseases and prevent the growth of bacteria, silver nanoparticles have become a prominent component in many health products. As antimicrobial silver compounds have been employed in different biomedical goods and applications, several researchers have started to evaluate the usage of silver nanoparticles as anti-cancer [85]. Figure (1.4) shows structure of

Ag_2O, and the important characteristics of the NbO_2 nanoparticles can be summarized in table (1.1).

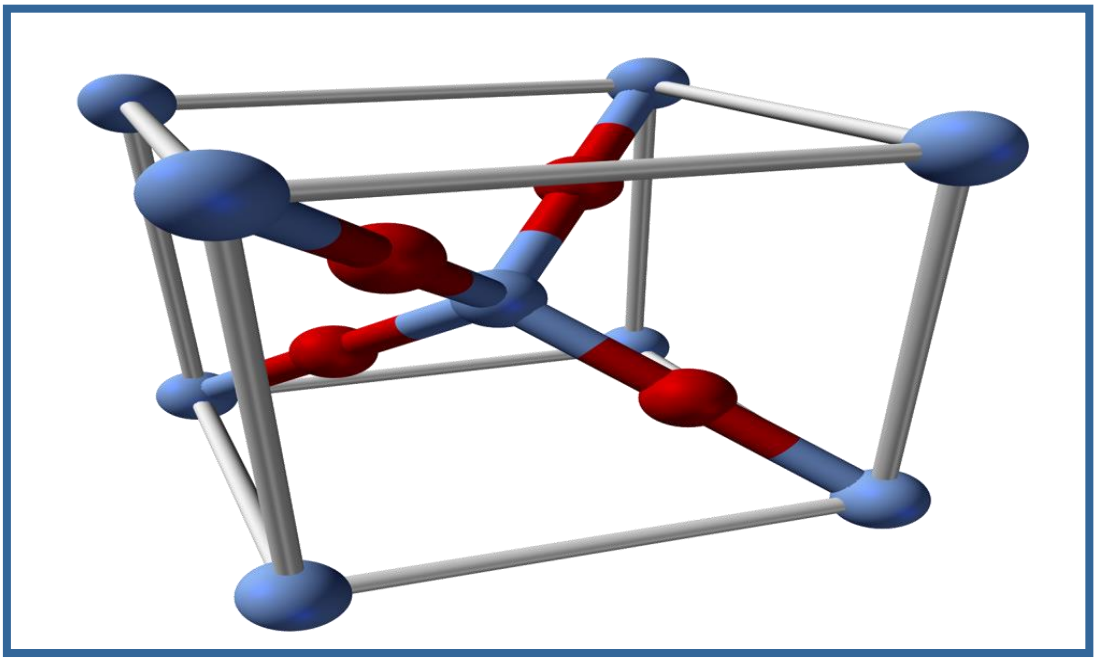

Figure (1.4): The lattice structure of Ag_2O [86].

Table (1.1) Characteristics of the Silver oxide nanoparticles [86].

Characteristic	Silver oxide
Molecular weight	101.96 g/mol
Chemical formula	Ag_2O
Density	7.14 g/cm^3
Melting Point	300 C^o
Solubility in water	Insoluble
Appearance	Black
Crystal structure	Cubic

1.6.4 Niobium oxide Nanoparticles (NbO_2 NPs)

Niobium oxides are crucial and strategically high materials of technology. Niobium oxides bring about several diverse and remarkable properties, ranging from its solid appearance in nature, to its, melting point of 1512 C°, its density and molecular weight of 4.47 g/cm^3 and 265.81 respectively. All these to a large extent, make it a flexible group of material. Precisely, niobium oxides have shown enormous potentials in numerous applications of technology which include, transparent conductive oxides, solid electrolytic capacitors, dye-sensitized solar cells, sensing materials, catalytic processes and as biocompatible coatings. Niobium oxide became promising electrochromic materials for device applications, in part, because of its excellent chemical stability and corrosion resistance in both acid and base media [87].

Niobium oxides which are semiconductors are inclusive of, but not limited to, niobium dioxide (niobium (IV) oxide) NbO_2, niobium monoxide (niobium (II) oxide) NbO, niobium pentoxide (niobium (V) oxide) Nb_2O_5, as there are other different oxides of the metal. Each of these oxides of niobium have distinct electrical characteristics which ranges from metallic conducting NbO to semiconducting NbO_2 with value of 3.9, and then insulating Nb_2O_5, which thermodynamically, is the most stable oxide, with the smallest available energy formation. However, the existence of NbO and NbO_2 in a film, would influence the general properties of the Nb_2O_5 films [88]. Figure (1.5) shows structure of NbO_2, and the important characteristics of the NbO_2 nanoparticles can be summarized in table (1.2) [89].

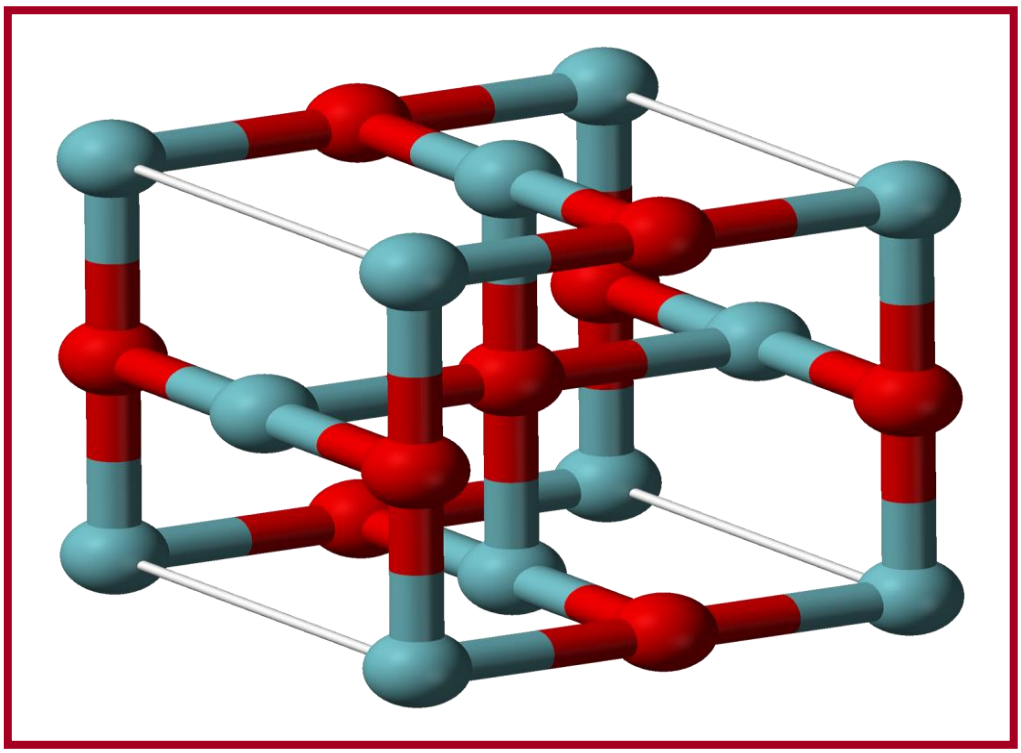

Figure (1.5): The lattice structure of NbO_2 [89].

Table (1.2) Characteristics of the Niobium oxide nanoparticles [89].

Characteristic	Niobium oxides
Molecular weight	124.91 g/mol
Chemical formula	Ag_2O
Density	5.9 g/cm^3
Melting Point	2188 K
Solubility in water	Insoluble
Appearance	bluish black solid
Crystal structure	Tetragonal

1.6.5 Aluminum oxide Nanoparticles (Al_2O_3 NPs)

Aluminum oxide (Al_2O_3) nanoparticles are class of metal oxide nanoparticles that have diverse biomedical applications owing to their exceptional physicochemical and structural features such as resistance towards wear, chemicals, mechanical stresses as well as their favorable optical properties and a porous vast surface area. Other reasons for widespread applications of Aluminum oxide nanoparticles are their low cost of preparation and easy handling. Therefore, owing to the economic importance, the recent achievements and possible health risks associated with the biomedical applications of Aluminum oxide nanoparticles are overviewed in this work [90].

Aluminum oxide nanoparticles, belong to the family of metal oxide nanomaterials, these cost-effective nanomaterials possess high surface area as well as mechanical strength; and they have exceptional chemical stability towards high temperatures and harsh conditions such as abrasive environment [91]. Figure (1.6) shows structure of Al_2O_3, and the important characteristics of the Al_2O_3 nanoparticles can be summarized in table (1.3) [92].

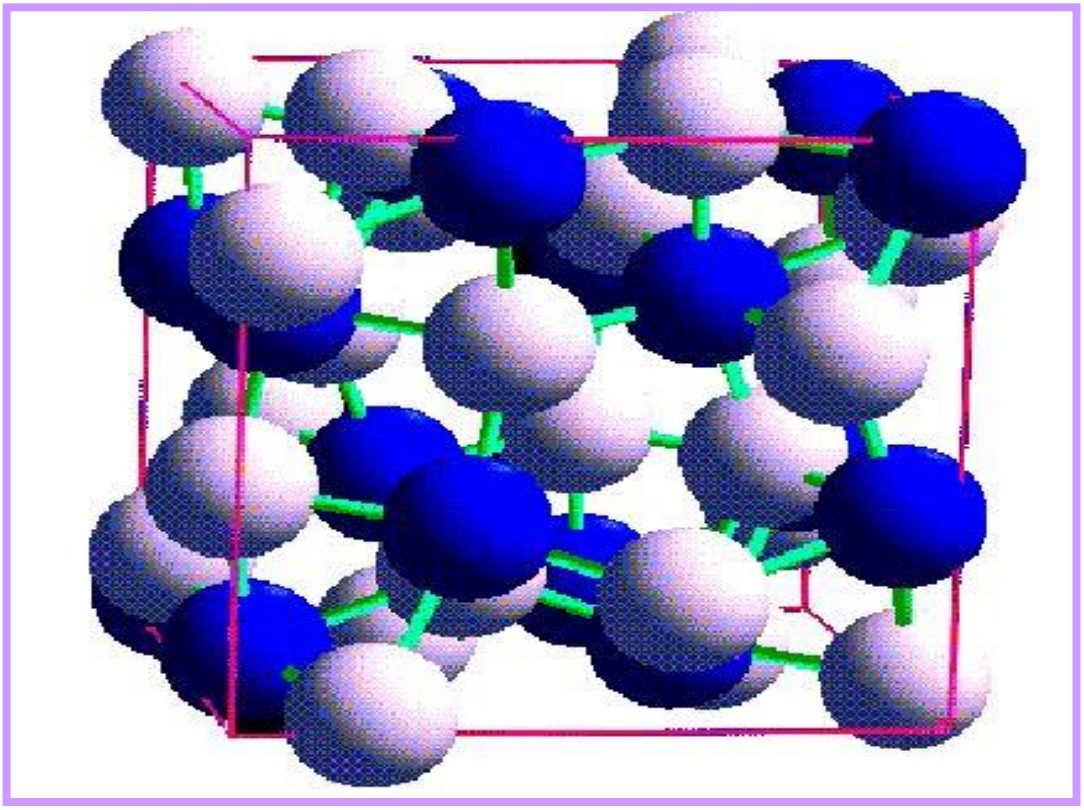

Figure (1.6): The lattice structure of Al_2O_3 [92].

Table (1.1) Characteristics of the Aluminum oxide nanoparticles [92]

Characteristic	Aluminum oxide
Molecular weight	101.96 g/mol
Chemical formula	Al_2O_3
Density	3.987 g/cm^3
Melting Point	2.072 C^0
Boiling Point	2.977 C^0
Solubility in water	Insoluble
Electrical conductivity	Insulator
Crystal structure	Trigonal

1.7 Literature Review

There are many previous studies dealt with the topic bio-nanocomposites, and their applications:

Y. Zhao *et al.* [93] in (2012) studied the optical properties of (silver/polyvinyl alcohol/carboxymethyl-chitosan nanofibers) and its application. Results showed that the absorbance increase and the value of optical energy gap decrease with the increase of the weight percentages of silver nanoparticles. As well as, the antibacterial abilities of silver nanoparticles/polyvinyl alcohol/carboxymethyl-chitosan nanofibers against gram-negative *Escherichia coli* were explored by bacterial growth inhibition halos and bactericidal kinetic testing. The inhibition halo surrounding silver nanoparticles that contained fibers can be clearly observed. However, the polyvinyl alcohol/carboxymethyl-chitosan nanofibers without silver nanoparticles did not show inhibition zone. With the increase of silver nanoparticles content, the area of inhibition zone expanded.

W. H. Eisa *et al.* [94] in (2012), studied the structural and optical properties of (polyvinyl alcohol/polyvinyl pyrrolidone/silver) nanocomposites. The results showed that the absorbance increases with the increasing of the weight percentages of silver nanoparticles.

M. H. Al-Humairi *et al.* [95] in (2013), studied the optical properties of (polyvinyl alcohol/silver) and (polyvinyl alcohol/titanium oxide) nanocomposites. Results showed that the absorbance, absorption coefficient, extinction coefficient, refractive index and dielectric constant (real, imaginary), while the energy gap are decreases with increases in nanoparticles concentrations.

H. N. Chandrakala *et. al.* [96] in (2013), employed the (polyvinyl alcohol- sodium zirconate) composites by using solution casting method with different concentrations of (sodium zirconate) nanoparticle. The

effect of (sodium zirconate) nanoparticle on structural and electrical on PVA matrix were investigated. They indicated that (FT-IR) analysis showed the interaction between (sodium zirconate) nanoparticles and (polyvinyl alcohol) matrix, (SEM) images are displayed uniform distribution of (sodium zirconate) nanoparticles through the (polyvinyl alcohol) matrix. A.C conductivity of (polyvinyl alcohol/sodium zirconate) nanocomposites are increased with increasing additive of the (sodium zirconate) and frequency, but the dielectric constant and dielectric loss increased with increasing additive of the (sodium zirconate) and decreased with increasing frequency.

M. Ghanipour *et al.* [97] in (2013), studied the optical behavior of undoped and silver nanoparticles doped polyvinyl alcohol films. Results showed that the absorbance increase and the value of energy gap decrease with the increase of the weight percentages of silver nanoparticles.

R. Augustine *et. al.* [98] in (2014), studied the polycaprolactone /zinc oxide nanocomposite membranes as biomaterials with antibacterial properties. Results showed that the fabricated material showed an overall good antimicrobial activity against both *Escherichia coli* and *Staphylococcus aureus*, which suggests the ability of the fabricated material to prevent bacterial proliferation at the implantation site.

S. azizi *et. al.* [99] in (2014), studied blend of the (polyvinyl alcohol/chitosan) with various additive of (zinc oxide/silver) nanoparticles. Zinc oxide and silver nanoparticles are strengthened by cellulose nanocrystals (Cellulose nanocrystals). SEM tests exhibited that the (cellulose nanocrystals/zinc oxide-silver nanoparticles) distribution is homogeneously in the blend of (polyvinyl alcohol/Chitosan). Ultraviolet and visible light are displayed good absorbed by additive (zinc oxide/silver nanoparticles) into (polyvinyl alcohol/chitosan) blend. So, the (polyvinyl alcohol/ chitosan/cellulose nanocrystals/zinc oxide/silver

nanoparticles) nanocomposites films showed excellent antimicrobial properties. Killing both Gram-negative *Salmonella choleraesuis* and Gram-positive *Staphylococcus aureus*

H. Hakim *et al*. [100] in (2015), studied the effect of aluminum oxide nanoparticles on the optical properties of (polyvinyl pyrrolidone-polyethylene glycol) blend. Results showed that the nanocomposites of (polyvinyl pyrrolidone- polyethylene glycol - aluminum oxide) have high absorbance in the UV region and decrease in the Vis-region; the transition was found to be indirect type, the energy band gap decrease with the increase of the concentration of aluminum oxide nanoparticles. The addition of aluminum oxide to the (polyvinyl pyrrolidone-polyethylene glycol) blend causes shift the optical energy gab from (3.1 eV) to (2.4 eV).The values of the refractive index (n) of the nanocomposites increase exponentially with increasing of photon energy. The real and imaginary dielectric constant show the exponential increase with increasing of the incident photon energy. The optical constants of (polyvinyl pyrrolidone-polyethylene glycol) blend increase with the increase of the concentration of aluminum oxide nanoparticles.

R. G. Kadhim *et al.* [101] in (2015), studied the electrical and structural properties of (Poly(methyl methacrylate)/titanium oxide) nanocomposites were prepared by using casting method. Results showed that the dielectric constant, dielectric loss, and the A.C electrical conductivity for (Poly(methyl methacrylate)/titanium oxide) nanocomposites are increasing with the increasing of concentrations of the sliver nanoparticles. The dielectric constant and the dielectric loss of the (Poly(methyl methacrylate)/titanium oxide) nanocomposites is decreasing with the increase of frequency of the applied electric field, but the A.C electrical conductivity increasing with the increase of the frequency.

R. T. Abdulwahid *et. al* [102] in (2016), studied the structural and optical properties of polyvinyl alcohol: lead oxide based solid polymer nanocomposites. They found that the absorbance, absorption coefficient and refractive index of polyvinyl alcohol are increased with increase the concentration of lead oxide nanoparticles, the percentages of increase the refractive index is from (1.15 to 1.42). The energy band gap is reduced from (6.32-4.33) eV with increase the concentration of nanoparticles.

M. Karpuraranjith *et al.* [103] in (2017), studied the prepared the (cesium/zinc oxide-polyvinyl pyrrolidone) nanocomposites by using precipitation method. The antibacterial activity of chitosan, (polyvinyl pyrrolidone-zinc oxide) and (cesium/zinc oxide-polyvinyl pyrrolidone) nanocomposites tested against gram positive bacteria *Staphylococcus aureus* and gram negative bacteria *Escherichia coli*. The results observed that the bacterial inhibition of gram positive bacteria has higher effect than gram negative bacteria.

M. E. Diken *et al.* [104] in (2018), The manufacture and characterization of poly(acrylicacid)/organo-modified nanohydroxyapatite nanocomposites were examined, with a particular emphasis placed on the thermal, optical, and biocompatibility properties of the materials. The findings of the investigation showed that the organo-modified nanohydroxyapatite particles were dispersed in the nanoscale into the poly (acrylicacid) matrix and that they were uniformly distributed within the film. This was observed with the scanning electron microscope (SEM). The organo-modified nano hydroxyapatite content had an increasing effect on the glass transition temperature of poly (acrylicacid). Experiments using ultraviolet (UV) absorbance demonstrated that poly (acrylicacid) possessed a stronger ultraviolet (UV) transmission than its nanocomposites.

R. M. Tripathi *et al*. [105] in (2018), studied the antibacterial activity of (poly vinyl alcohol-silver) nanocomposite film for food packaging material. Results showed that the antibacterial activity of the nanocomposite film was investigated against *Salmonella typhimurium* by means of disk diffusion method. poly vinyl alcohol-silver nanocomposite film shows excellent antibacterial activity against *Salmonella typhimurium*.

I. A. Hamad *et al*. [106] in (2019), studied the structural and optical properties for nanostructure (silver oxide/silicone & Psi) films for photodetector applications . Results showed that the silver oxide is an important p-type (in chasm to most oxides which were n-type), with a high conductivity semiconductor. From the optical absorbance data, the energy gap value of the silver oxide thin films was 1.93 eV.

A. Hazim *et al.* [107] in (2019), prepared of novel (Polymethyl methacrylate)/zirconium dioxide/silver oxide) nanocomposites and studying their structural, electronic, optical properties as antibacterial for dental industries. Results showed that the optical properties for Polymethyl methacrylate/zirconium dioxide/silver oxide) nanocomposites absorbance, refractive index absorption coefficient, extinction coefficient, real and imaginary parts of dielectric constants and optical conductivity of Polymethyl methacrylate/zirconium dioxide) nanocomposites increase while the transmittance and energy band gap decrease with increase in silver nanoparticles concentrations. The results of antibacterial properties showed that the Polymethyl methacrylate/zirconium dioxide/silver oxide) nanocomposites have good antibacterial activity for positive and negative gram organisms bacteria.

R. M. Mohammed *et al.* [108] in (2020), effect of antimony oxide nanoparticles on structural, optical and A.C electrical properties of (polyethylene oxide/polyvinyl alcohol) blend for antibacterial

applications. Results showed that the absorbance, absorption coefficient, extinction coefficient, refractive index, dielectric constant (real and imaginary) and optical conductivity of (polyethylene oxide/polyvinyl alcohol) blend are increased while the transmittance and energy band gap are decreased with increasing of the antimony oxide nanoparticles concentrations. The results of antibacterial activity showed that the inhibition zone diameter increases with increase in antimony oxide nanoparticles concentrations.

A. Hashim *et al.* [109] in (2021), Determination of optical parameters of polymer blend/nanoceramics for electronics applications. Results showed that the absorbance, absorption coefficient, extinction coefficient, refractive index, dielectric constant (real, imaginary) and optical conductivity of (Poly(vinyl alcohol)/Polyethylene glycol) blend are increased while the transmittance and energy band gap are decreased with increasing of the zirconium dioxide content increase nanoparticles concentrations.

M. H. Meteab *et al.* [110] in (2022), controlling the structural and dielectric characteristics of Polystyrene-Polycarbonate/Cobalt (III) oxide-Silicon carbide hybrid nanocomposites for nano electronics applications. The FTIR results showed that there are no chemical interactions between the polymer matrix and (Cobalt (III) oxide/ Silicon carbide) nanoparticles. The Field Emission Scanning Electron Microscope (SEM) and optical microscope (OM) confirmed that the (Cobalt (III) oxide-Silicon carbide) nanoparticles were distributed uniformly throughout the Polystyrene /Polycarbonate blend. The dielectric properties were examined at frequency range from(100 Hz to 5 $\times 10^6$ Hz). The results of dielectric characteristics indicated that the dielectric constant and dielectric loss of (Polystyrene -Polycarbonate /Cobalt (III) oxide- Silicon carbide) nanocomposites were decreased with

increasing of the frequency while it increased when the concentration of (Cobalt (III) oxide- Silicon carbide) nanoparticles increases. The A.C conductivity of (Polystyrene -Polycarbonate/Cobalt (III) oxide- Silicon carbide) nanocomposite rises with the increase in frequency and concentration of (Cobalt (III) oxide- Silicon carbide) nanoparticles. The dielectric constant and electrical conductivity of Polystyrene/ Polycarbonate blend were improved about 19.9% and 33.3% respectively.

1.8 The Objective of Research

The main objectives of this research are listed as following:

1. Preparation and study the optical, electrical and structural properties of (PVP-PVA-Ag_2O-NbO_2) and (PVP-PVA-Al_2O_3-NbO_2) nanocomposites.
2. Estimate the antibacterial activity of (PVP-PVA-Ag_2O-NbO_2) and (PVP-PVA-Al_2O_3-NbO_2) nanocomposites against different bacteria.

Chapter Two

Theoretical Part

2.1 Introduction

This chapter provides a theoretical introduction to nanocomposites optical characteristics and A.C electrical conductivity, as well as the rules that are utilized to interpret the results. Nanocomposites are becoming more popular due to advancements in the materials optical, electrical, and mechanical characteristics. Because of their appealing electrical/ electronic characteristics and high refractive index, nanoparticles in particular represent sophisticated technological materials [111].

Nanocomposites of organic and inorganic materials can benefit from both organic polymers (dielectric, ductility, flexibility) and inorganic materials (high thermal stability, strength, high refractive index, hardness) properties, and so offer a wide range of applications [112].

2.2 Optical Properties

Optical absorption spectra may be used to investigate electronic transitions as well as provide insight into the energy gap and band structure of crystalline and amorphous materials. This approach works on the concept that a photon with an energy level higher than the band gap energy will be absorbed. In optical instruments, absorption and transmission in the ultraviolet, visible, and infrared region critical [113,114].

Because of its applications in integrated optics, such as optical data storage and optical information, the hunt for optical characteristics has expanded in recent years [115,116].

2.2.1 The Absorbance (A) and Transmittance (T)

Absorbance can be defined as the ratio between absorbed light intensity (I_A) by material and the incident intensity of light (I_o) [117]:

$$A = \frac{I_a}{I_o} \quad \text{..... (2-1)}$$

Transmittance (T) is given by ratio of the intensity of the transmitting rays (I_T) through the film to the intensity of the incident rays (I_o) on it as follows [118]:

$$T = \frac{I_T}{I_o} \quad \text{..... (2-2)}$$

We can also find a transmittance as a function of wavelength through the exponential relationship for both absorbance and transmittance which [119]:

$$A = \log\left(\frac{1}{T}\right) \quad \text{..... (2-3)}$$

2.2.2 Absorption Coefficient (α)

The absorption coefficient provides useful information such as the optical energy band gap. The following equation may be used to calculate the absorption coefficient α (ν) from the optical absorption spectrum [120]:

$$\alpha(\nu) = 2.303\frac{A}{t} \quad \text{..... (2-4)}$$

The sample thickness is (t), and the absorbance is (A).

The following equation can be used to describe direct and indirect transitions [121]:

$$\alpha h\nu = B(h\nu - E_g^{OPt})^r \quad \text{..... (2-5)}$$

Where, ν is the frequency, B is a constant, h is Planck's constant, E_g^{opt} is the energy band gap and r can take the values 2, 3, 1/2 or 3/2 for transitions designated as indirect allowed, indirect forbidden, direct allowed and direct forbidden, respectively as shown in Figure (2.1). The calculation of values of optical energy band gap includes the plotting of $(\alpha h\nu)^{1/r}$ against hν [122].

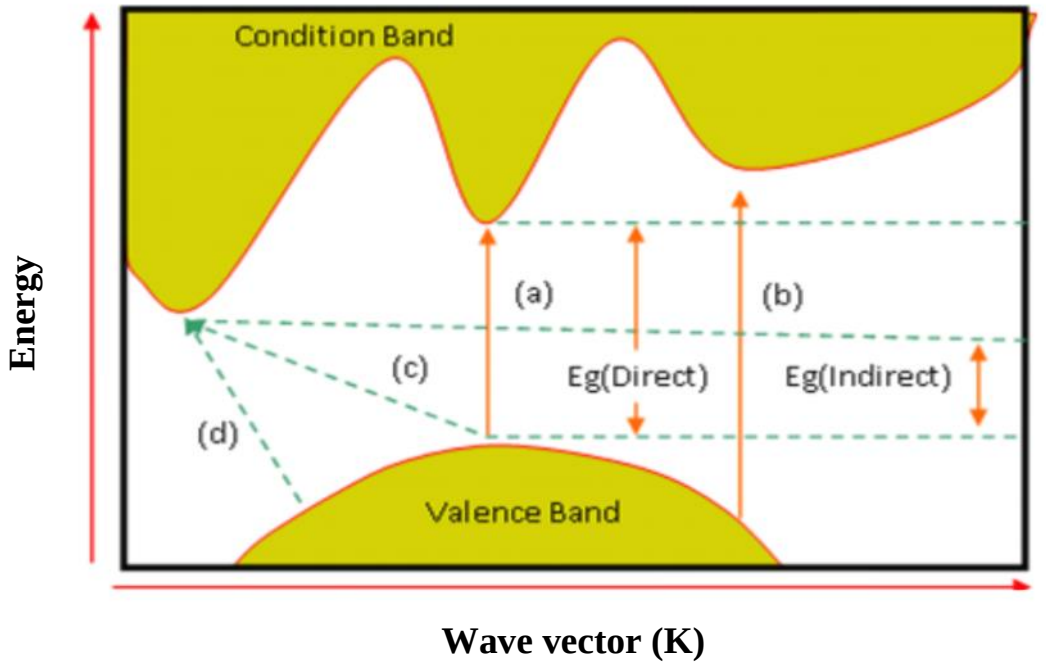

Figure (2.1): The transition process [123].

(a) allowed direct transition. **(c) allowed indirect transition.**

(b) forbidden direct transition. **(d) forbidden indirect transition.**

The reflectance can be obtained from absorption and transmission spectra in accordance with the law of conservation of energy by the following relation [124]:

$$A+R+T=1 \quad \ldots\ldots\ldots\ldots\ldots\ldots\ldots \quad (2\text{-}6)$$

2.2.3 Fundamental Absorption Edge

The fundamental absorption edge can be defined as the rapid increasing in absorbance when absorbed energy radiation is almost equal to the band energy gap; therefore, the fundamental absorption edge represents the less difference in the energy between up point in valance band to bottom point in conduction band [125].

2.2.4 Absorption Regions

There are three different types of absorption areas:

A) High absorption Region

This region is shown in Figure (2.2). (A), it is represent the nature of electron transitions is direct. The magnitude of absorption coefficient is greater than or equals to 10^4 cm^{-1} [126].

B) Exponential Region

This region is shown as in Figure (2.2) (B), it is represent the transition between extended levels in valence band (V.B) to localize levels in conduction band (C.B). Also from localize levels in top valence band to extended levels in bottom conduction band. The magnitude of absorption coefficient between ($1<\alpha<10^4$) cm^{-1} [126].

C) Low absorption Region

The absorption coefficient (α) in this region is very small, it is about ($\alpha<1 cm^{-1}$). the electron transitions in this region attribute to density as a result of structure defects, as shown in Figure (2.2), (C) [126].

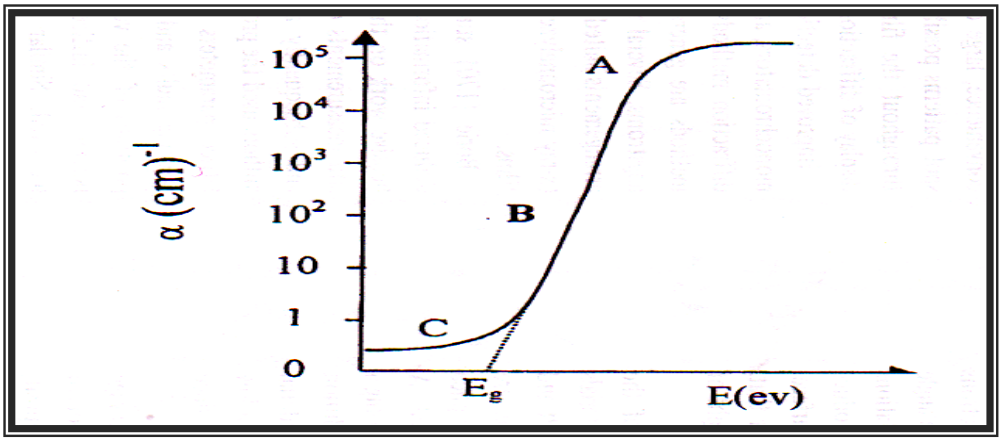

Figure (2.2): Variation in the absorption edge as a function of the absorption area [126].

2.2.5 Optical Constants

2.2.5.1 The Refractive Index and Extinction Coefficient

Refractive index (n) can be estimated by determining the ratio of the velocity of light in a vacuum (c) to the velocity of light within a specimen (v) [127]:

$$n=\frac{c}{v} \quad \text{..... (2-7)}$$

The real refractive index component is denoted by the letter n, and the imaginary refractive index component is marked by the letter k. The complex refractive index is denoted by the symbol n*.

$$n^*=n-ik \quad \text{..... (2-8)}$$

The energy loss of electromagnetic radiation through that medium is measured by the extinction coefficient of a particular substance [128]:

$$K=\frac{\alpha\lambda}{4\pi} \quad \text{..... (2-9)}$$

Where (K) denotes the extinction coefficient and (λ) the incoming light wavelength.

The equation calculates the refractive index (n) [129]:

$$n=\frac{1+\sqrt{R}}{1-\sqrt{R}} \quad \text{..... (2-10)}$$

Where R is the reflectance.

2.2.5.2 The Dielectric Constant and Optical Conductivity

The following equations are used to compute the real and imaginary components of the dielectric constant (ε_1 and ε_2) [130]:

$$\varepsilon_1 = (n^2 - K^2) \quad \text{..... (2-11)}$$

$$\varepsilon_2 = (2nk) \quad \text{..... (2-12)}$$

The following equation was used to compute the optical (σ) conductivity [131]:

$$\sigma = \frac{\alpha nc}{4\pi} \quad \text{..... (2-13)}$$

The speed of light is defined as c.

2.3 The A.C Electrical Properties

The A.C electrical properties determined by calculating the parallel capacity (Cp) and the factor of dissipated via using LCR Hi TESTER (Japan) meter. The dielectric properties were Calculated in a frequency range of (100Hz - 5MHz). The dielectric constant ($\acute{\varepsilon}$) is determined with the aid of [132]:

$$\acute{\varepsilon} = \frac{\varepsilon_p}{\varepsilon_o} \quad \text{..... (2-14)}$$

Where: C_o is vacuum capacitor and C_p is parallel capacitance.

The dielectric loss (ε'') is given by [133]:

$$\varepsilon'' = \acute{\varepsilon}\, D \quad \text{..... (2-15)}$$

Where D is dispersion factor.

The A.C conductivity ($\sigma_{A.C}$) was determined by the following relation [134].

$$\sigma_{A.C} = w\, \varepsilon''\, \varepsilon_0 \quad \text{..... (2-16)}$$

W: The angular frequency representation.

ε_0 : the vacuum permittivity.

2.4 The Difference Between Gram-positive and Gram-Negative Bacteria

Gram-positive and Gram-negative are two distinct types of bacteria. Scientists categorize these types based on their structures and their appearance after Gram staining. Gram staining is a process of dyeing bacteria and then viewing them beneath a microscope.

2.4.1 *Staphylococcus*

Staphylococcus aureus (*S. aureus*) is a gram positive and commensal bacterium that colonizes 30% of healthy individuals from different body parts . The organism causes infections by owing different virulent genes that encode different virulent factors such as toxins and enzymes [135].

Staphylococcal infection are caused by *S. aureus* bacteria. These types of germs are commonly found on the skin or in the nose of many healthy people. Most of the time, these bacteria cause no problems or cause relatively minor skin infections [136,137]. But Staphylococcal infections can turn deadly if the bacteria invade deeper into the body, entering the bloodstream, joints, bones, lungs or heart [138,138].

Treatment usually involves antibiotics and cleaning of the infected area. However, some staph infections no longer respond, or become resistant to common antibiotics [139]. To treat antibiotic-resistant staph infections, health care providers may need to use antibiotics that can cause more side effects. Further, the virulence of S. aureus has risen with existence of antibiotics resistance strains such as Methicillin resistant *S. aureus* (MRSA) and Vancomycin resistance *S. aureus* (VRSA) [140]. The basic structure of *Staphylococcus aureus* was illustrated in the figure (2.3) [141].

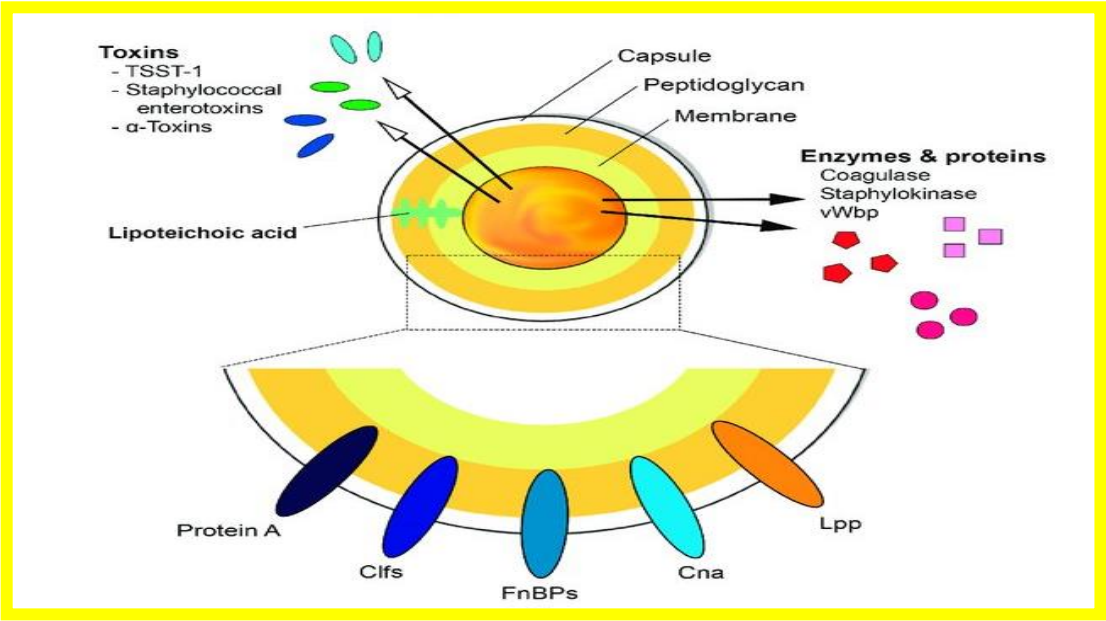

Figure (2.3): Schematic diagram illustrating the basic structure of *Staphylococcus aureus* [141].

2.4.2 *Escherichia Coli*

Escherichia coli (*E. coli*), a member of the Enterobacteriaceae family and the Enterobacterales order, is a Gram-negative bacillus found mainly in the human gut microbiota, but that may also be found in other sites [142].

Escherichia coli bacteria normally live in the intestines of people and animals. Most *E. coli* are harmless and actually are an important part of a healthy human intestinal tract. However, some *E. coli* are pathogenic, meaning they can cause illness, either diarrhea or illness outside of the intestinal tract. The types of *E. coli* that can cause diarrhea can be transmitted through contaminated water or food, or through contact with animals or persons [143,144].

Most strains are usually harmless. A few strains cause diarrhea/bloody diarrhea, vomiting and stomach pains and cramps. One strain can lead to kidney failure if not properly managed. Eating contaminated food is the most common way to get an *E. coli* infection [145, 146].

Escherichia coli have strain-specific O lipopolysaccharide antigens on their cell wall (at least 188 O antigens are currently recognized) and flagella or H antigens if present (at least 53 H types are recognized) [147]. There are also numerous different capsular polysaccharide (K) antigens. Escherichia coli are serotyped based on the combination of O, H, and K antigens, although generally only the O and H types are listed, for example, *E. coli* O157:H7. Serotyping of *E. coli*, together with genome, virulence, and phage typing, is a useful [148].

Antimicrobial resistance (AMR) is one of the leading causes of death (estimated five million associated deaths annually) globally [149]. In recent years, AMR has made therapeutic drugs ineffective against bacterial infections [150]. The increasing levels of AMR are accompanied by limited reserves of antimicrobial drugs to tackle them. This endangers the sustainability of effective public health responses to infectious diseases with resistant organisms. Increased patient morbidity, mortality, health-care-related costs, and treatment failure are key repercussions of this situation [151]. The basic structure of *Escherichia coli* was illustrated in the figure (2.4) [152].

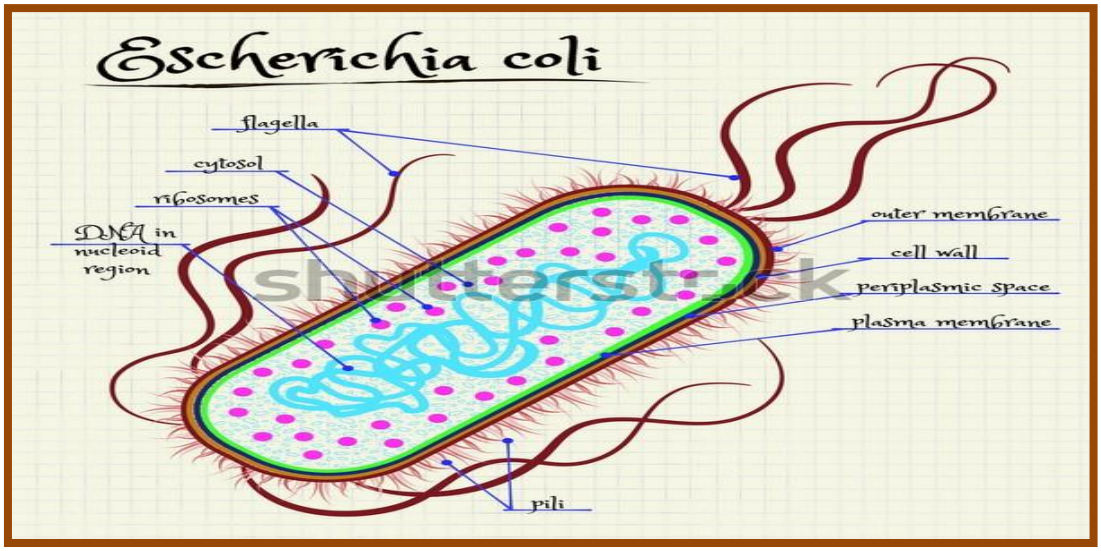

Figure (2.4): Schematic diagram illustrating the basic structure of *Escherichia coli* [152].

2.4.3 *Klebsiella Pneumonia*

Klebsiella pneumoniae (*K. pneumoniae*) is a Gram-negative, rod-shaped ubiquitous bacterium that inhabits soil, water, and sewage ecosystems. It is also found on various human body sites and organ systems, including skin, nose, throat, and intestinal tract, as part of the natural microflora [153].

K. pneumoniae is a prominent member of the *K. pneumoniae* species complex that consists of seven species that include *K. pneumoniae, Klebsiella quasipneumoniae subsp. quasipneumoniae, Klebsiella quasipneumoniae subsp. similipneumoniae, tropica, Klebsiella quasivariicola,* and *Klebsiella africana* [154]. The first four species are commonly associated with human infections such as pneumonia, urinary tract infections, soft tissue and wound infections, septicemia, and pyogenic liver abscesses [155].

The World Health Organization (WHO) declared antimicrobial resistance (AMR) as one of the top 10 most serious global public health threats facing humanity [156]. The WHO lists K. pneumoniae as one of the AMR bacteria of concern due to its demonstrated proclivity for developing antimicrobial resistance to many classes of antibiotics such as penicillins, cephalosporins, and quinolones, which are typically used to treat *K. pneumoniae* infections. This resistance is due to both chromosomal-encoded and plasmid-encoded genes [157].

In recent years, most *K. pneumoniae* infections are caused by strains termed "classic" *K. pneumoniae* (cKp). These strains persist in hospital environments and cause infections in debilitated patients. (cKp) strains appear to be distinct from hypervirulent *K. pneumoniae* (hvKp), a variant that was first described in the Asian Pacific Rim to cause community-acquired, invasive and metastatic infections, including liver abscess, endophthalmitis, meningitis and septic arthritis in diabetics and immunocompetent young individuals. The emergence and spread of new multidrug-resistant (MDR) clones and the international dissemination of hvKp strains have renewed interest in *K. pneumoniae* [158]. The basic structure of *K. pneumoniae* was illustrated in the figure (2.5) [159].

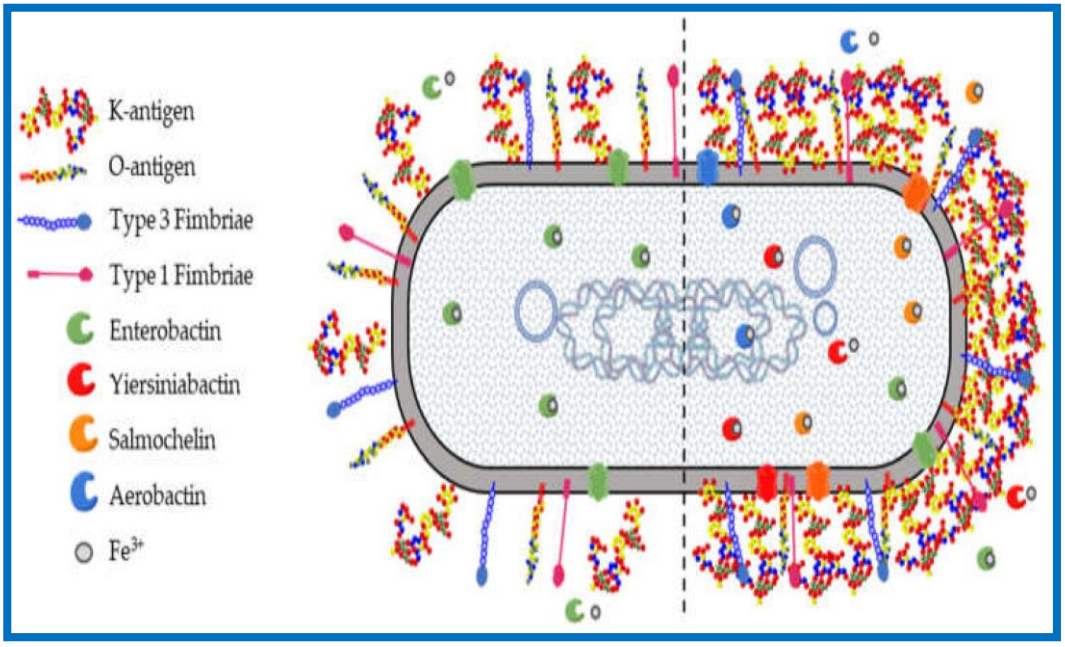

Figure (2.5): Schematic diagram illustrating the basic structure of *K. pneumoniae* [159].

2.4.4 *Enterococcus Faecalis*

Enterococcus faecalis (*E. faecalis*) is a Gram-positive, commensal bacterium inhabiting the gastrointestinal tracts of humans. Like other

species in the genus *Enterococcus*, *E. faecalis* is found in healthy humans and can be used as a probiotic [160].

The role of *E. faecalis* in root canal infections also remains unclear. It had been thought that *E. faecalis* not only possesses various virulence factors but also is able to share these virulence traits among species to further contribute to its survival and ability to cause infection [161]. On the other hand, its ability to survive and persist as a pathogen in root canals makes it a more important virulence factor [162].

Recently, molecular methods have been used to investigate the microbiota of endodontic infections, and the list of putative pathogens involved with failed endodontic therapy has expanded to include even as-yet-uncultivated bacteria [163,164]. However, in addition to detecting new putative pathogens, molecular biology studies have confirmed the status of *E. faecalis* as the most frequently found species in previously filled root canals that have failed [165,166]. The basic structure of *E. faecalis* was illustrated in the figure (2.6) [167].

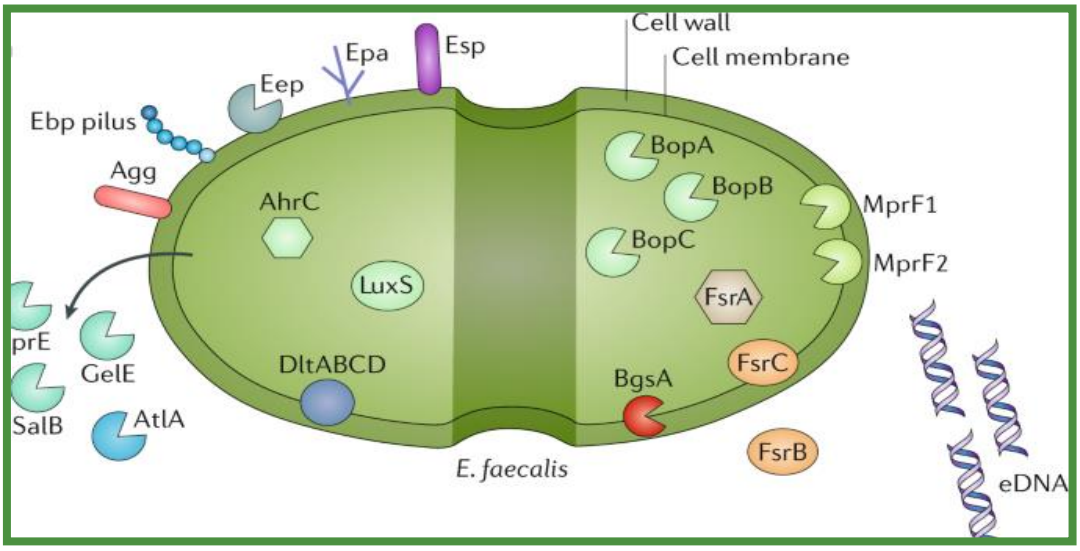

Figure (2.6): Schematic diagram illustrating the basic structure of *E. faecalis* [167].

2.5 Antibacterial Activity

Infectious illnesses, in general, pose a severe danger to public health across the world, particularly when antibiotic-resistant bacterial strains evolve. As a result, there is a strong motivation to create novel bactericidal agents [168]. Both gram-positive and gram-negative bacterial strains are regarded to be a substantial public health concern in general. Antibiotics have long been used to treat illnesses in both the community and the hospital [169,170].

Nanobiotechnology developments, notably the capacity to create metal oxide nanoparticles of specified size and form, are anticipated to lead to the creation of novel antibacterial agents. The particle size has a significant impact on the functional activities of nanoparticles. Nanoparticles have gotten a lot of interest lately because of their unusual physical, chemical, and biological features in a variety of sectors, including medicine [171-173].

The widespread application of antibiotics for the purpose of preventing and treating bacterial infections has contributed to the proliferation of bacteria that are resistant to antibiotics, which has stimulated the research and development of novel antibacterial agents. Nanoparticles are comparable in size to biological macromolecules, although being far smaller than human cells. Nano treatment techniques are being developed as a way to improve medical treatments [174,175].

Chapter Three

Experimental Part

3.1 Introduction

This chapter covers the stages of sample preparation for (PVP-PVA-Ag_2O-NbO_2) and (PVP-PVA-Al_2O_3-NbO_2) nanocomposites, as well as the stages of sample testing and measurement, which include the following: optical microscopic, Infrared radiation transformed using the Fourier transform, a scanning electron microscope, optical measurements, A.C electrical conductivity measurements, and antibacterial activity application measurements.

3.2 The Materials Used in This Work

3.2.1 Polymers

This work makes use of two different polymers:

A) Polyvinyl pyrrolidone (PVP):

It was available in powder form and had a high purity level in Panveac Spain company (99.8 %) in parity.

B) Polyvinyl alcohol (PVA):

It was available in powder form and had a high purity level in Panveac Spain company (99.8 %) in parity.

3.2.2 Nanoparticles

A) Silver oxide nanoparticles (Ag_2O):

utilized in the form of a powder with a particle diameter of 66 nm, manufactured by Sigma-Aldrich and having a high purity (99.9 %) in parity.

B) Aluminum oxide nanoparticles (Al_2O_3):

utilized in the form of a powder with a particle diameter of 66 nm, manufactured by EPRUI USA company and having a high purity (99.9 %) in parity.

C) Niobium oxide nanoparticles (NbO_2):

utilized in the form of a powder with a particle diameter of 66 nm, manufactured by Sigma-Aldrich and having a high purity (99.9 %) in parity.

3.3 Preparation of (PVP-PVA-Ag_2O-NbO_2) and (PVP-PVA-Al_2O_3-NbO_2) Nanocomposites

The nanocomposites were made by dissolving one gram of polyvinyl pyrrolidone (50 wt.%) and polyvinyl alcohol (50 wt.%) in 30 ml distilled water using a magnetic stirrer. After that, the polymers were mixed for one hour at 50 C° temperature to achieve a more uniform solution. Nanoparticles made of (silver oxide and niobium oxide) were added to the polymer blend solution at concentrations that are as follows: (0.005, 0.01, 0.015 and 0.02 wt.%) to get the first nanocomposites(PVP-PVA-Ag_2O-NbO_2), as well as nanoparticles consist of (aluminum oxide and niobium oxide) were added to the polymer blend solution at concentrations that are as follows: (0.005, 0.01, 0.015 and 0.02 wt.%) to get the second nanocomposites (PVP-PVA-Al_2O_3-NbO_2).

The nanocomposites samples of (PVP-PVA-Ag_2O-NbO_2) and (PVP-PVA-Al_2O_3-NbO_2) were created by utilizing the casting procedure, and after that, the solution was transferred to a clean petri dish with a diameter of 10 centimeters. The samples were then allowed to air dry at room temperature for one week, after which the dried film was readily peeled off using tweezers clamped. A digital micrometer was utilized in order to obtain accurate readings of the samples wall thickness, and the range of thickness have been measured about (100-110) μm. Figure (3.1) illustrate the flow chart of the experimental work that was done.

Table (3.1): Weight percentages for nanocomposites (PVP-PVA-Ag_2O-NbO_2)

PVP wt.%	PVA wt.%	Ag_2O wt.%	NbO_2 wt.%	Weight of Sample
0.5	0.5	0	0	1gm
0.4975	0.4975	0.0025	0.0025	
0.495	0.495	0.005	0.005	
0.4925	0.4925	0.0075	0.0075	
0.49	0.49	0.01	0.01	

Table (3.2): Weight percentages for nanocomposites (PVP-PVA-Al_2O_3-NbO_2)

PVP wt.%	PVA wt.%	Al_2O_3 wt.%	NbO_2 wt.%	Weight of Sample
0.5	0.5	0	0	1 gm
0.4975	0.4975	0.0025	0.0025	
0.495	0.495	0.005	0.005	
0.4925	0.4925	0.0075	0.0075	
0.49	0.49	0.01	0.01	

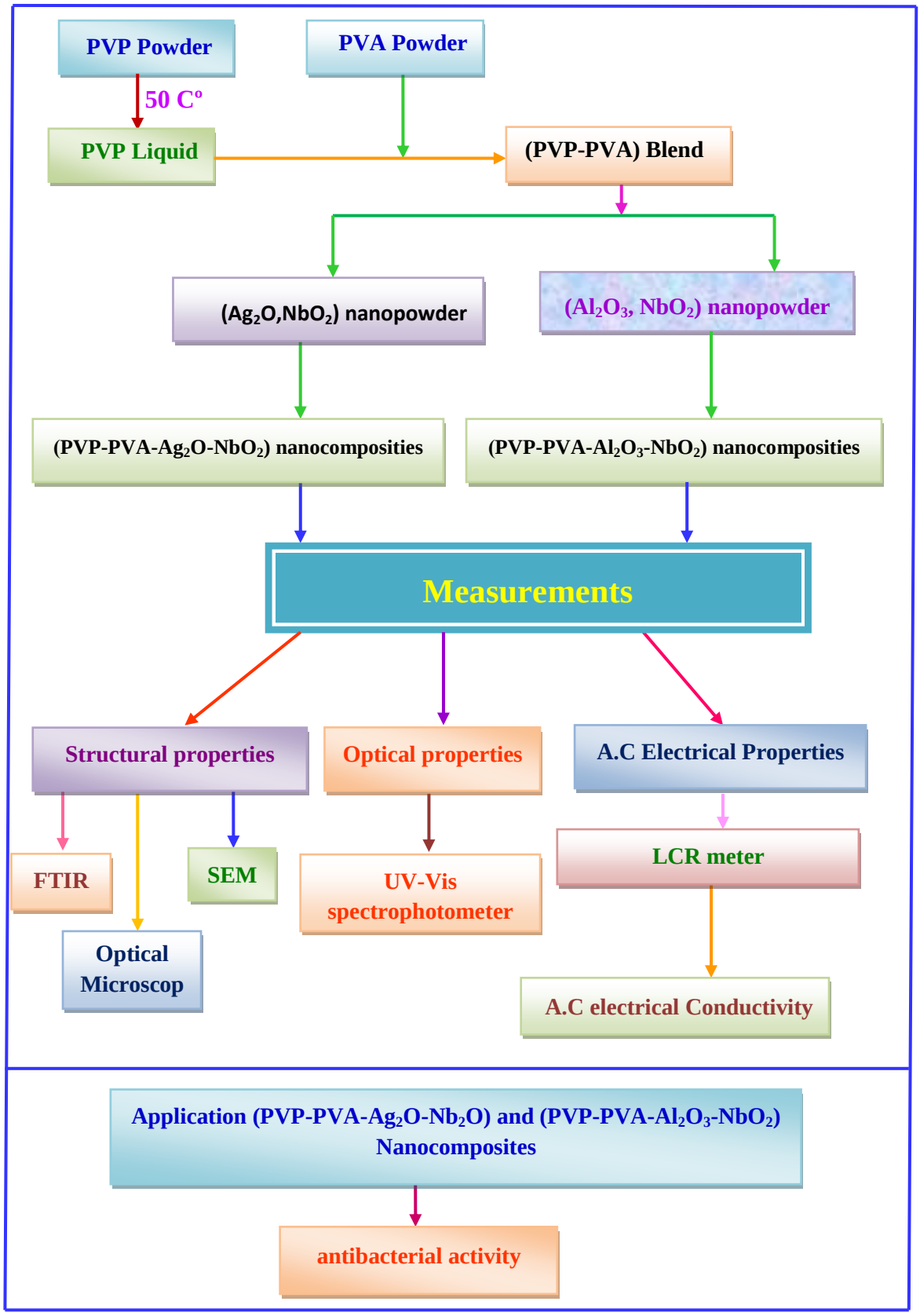

Figure (3.1): Scheme of experimental work.

3.4 Measurement of Structural Properties for Nanocomposites

3.4.1 Melting Point Measurement Instrument

The melting points of all basic materials have been measured by using digital melting point tester type (Stuart SMP 30), made in Germany and that found in College of Science-Babylon University, as shown in Figure (3.2).

Figure (3.2): Melting point tester.

3.4.2 FTIR Spectrometer

FTIR was used to record the FTIR spectra of nanocomposites made of (PVP-PVA-Ag_2O-NbO_2) and (PVP-PVA-Al_2O_3-NbO_2) (Bruker company, German origin, type vertex -70). in University of Babylon, College of Education for pure sciences. Figure (3.3): Fourier transform infrared spectrometer for wavenumbers between (1000 and 4000) cm^{-1} (3.2).

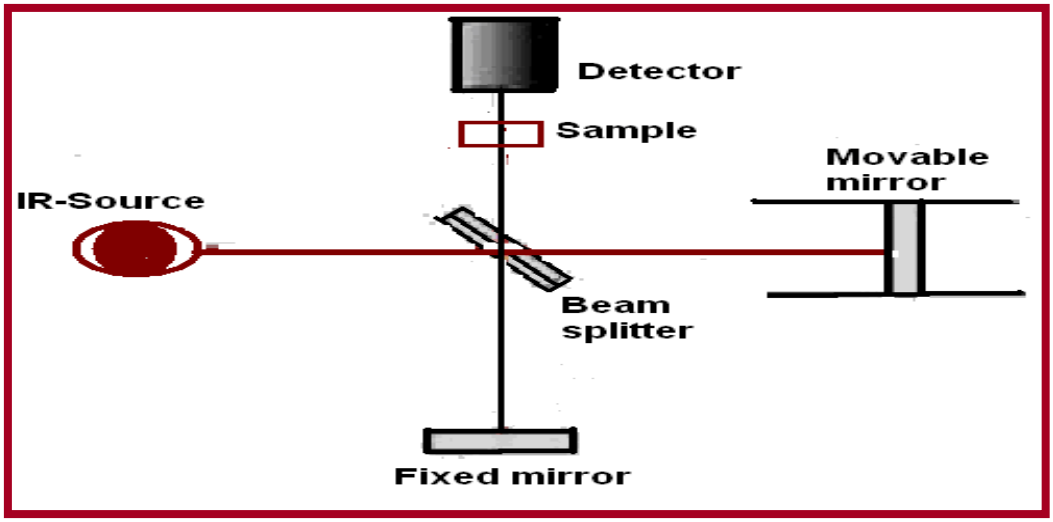

Figure (3.3): Schematic representation of FTIR spectrometer.

3.4.3 Optical Microscope

The (PVP-PVA-Ag_2O-NbO_2) and (PVP-PVA-Al_2O_3-NbO_2) nanocomposites samples are examined by using the optical microscope (supplied from Olympus name (ToupView) type (Nikon-73346)) in University of Babylon, College of Education for pure sciences with magnification (10x).

3.4.4 Scanning Electron Microscope

The surface morphology of (PVP-PVA-Ag_2O-NbO_2) and (PVP-PVA-Al_2O_3-NbO_2) nanocomposites made in concentration (0.005, 0.01, 0.015 and 0.02 wt.%) of (Ag_2O, NbO_2) and (Al_2O_3, NbO_2) respectively was examined by employing a microscope that uses scanning electrons (company, German origin, type vertex5600 LV SEM) in Iran, University of Technology, Department of Applied Sciences, as shown in the Figure (3.4).

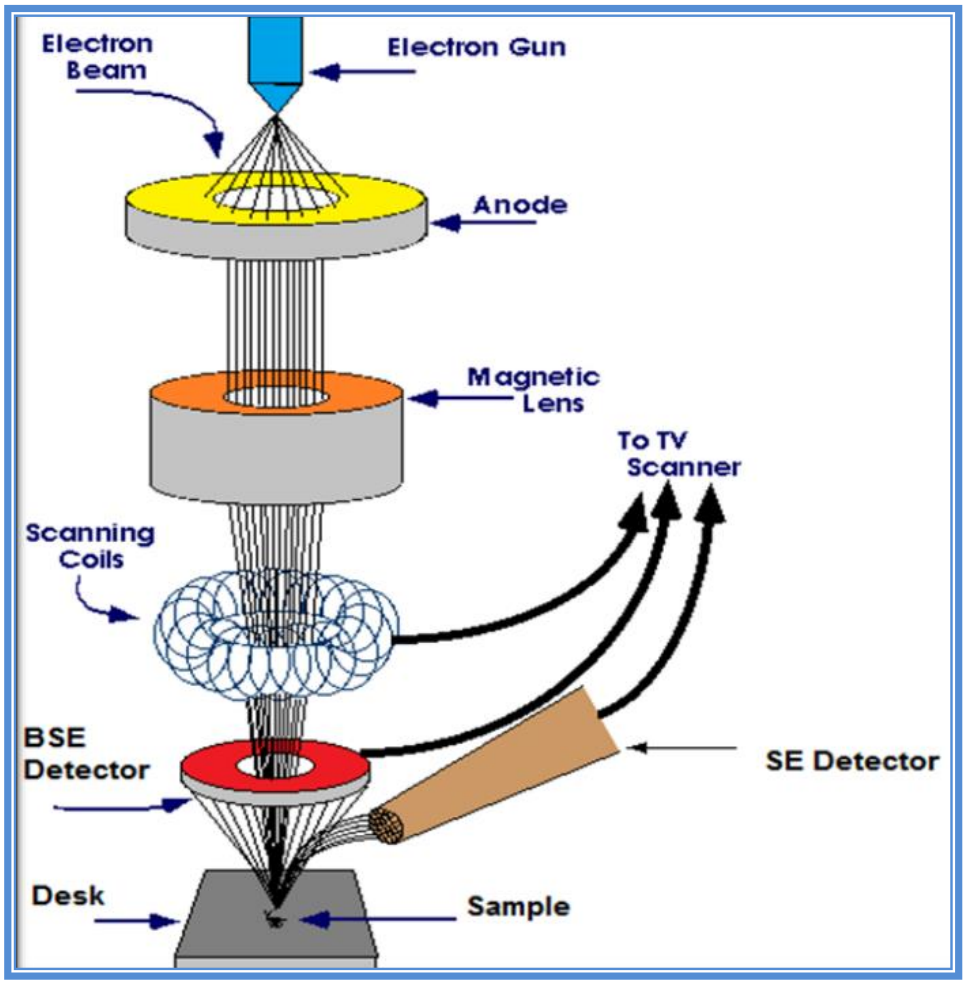

Figure (3.4): A graphical representation of how the SEM.

3.5 Optical Properties Measurements

The optical properties (PVP-PVA-Ag_2O-NbO_2) and (PVP-PVA-Al_2O_3-NbO_2) nanocomposites are measured by using spectrophotometer (shimadzu,UV-1800^{0}A) in wavelength (220-820) nm.

3.6 Measurements of A.C Electrical Properties

In this work, the A.C electrical properties of (PVP-PVA-Ag_2O-NbO_2) and (PVP-PVA-AL_2O_3-NbO_2) nanocomposites have been measured by measuring the capacity (C_p) and loss angle tangent (D) as a function of frequency of the electric field by using LCR meter type (HIOKI 3532-50 LCR HI TESTER)with different frequencies from (100Hz-5MHz) at room temperature as shown in Figure (3.5).

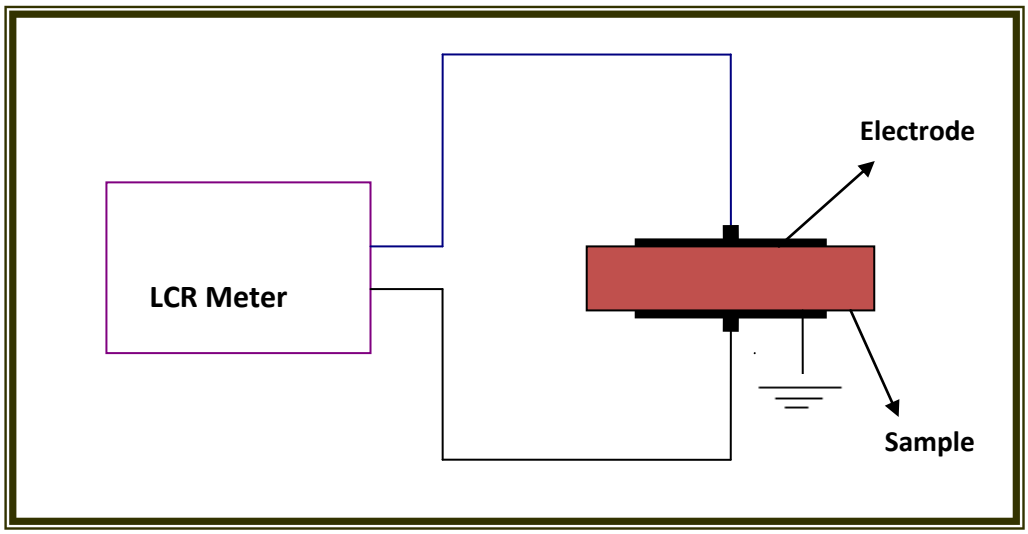

Figure (3.5): Schematic diagram for A.C electrical properties measurement.

3.7 Antibacterial Activity Application Measurements of Nanocomposites

Antimicrobial activity of the (PVP-PVA-Ag_2O-NbO_2) and (PVP-PVA-Al_2O_3-NbO_2) nanocomposites tested samples were determined using a disc diffusion method. The antibacterial activity was done by using gram positive organism (Staphylococcus aureus and Enterococcus faecalis) and gram negative organism (Escherichia coli and Klebsiella pneumoniae).

Bacteria (Staphylococcus aureus, Enterococcus faecalis, Escherichia coli and Klebsiella pneumoniae) were cultured in Muller-Hinton Medium. The solution of the (PVP-PVA-Ag_2O-NbO_2) and (PVP-PVA-Al_2O_3-NbO_2) nanocomposites were placed in the wells and incubated at 37 Cº for 24 hours. The inhibition zone diameter was measured, in University of Kufa, College of sciences.

Chapter Four

Results and Discussion

4.1 Introduction

This chapter includes the results and discussion of structural, optical and A.C electrical measurements for (PVP-PVA-Ag_2O-NbO_2) and (PVP-PVA-Al_2O_3-NbO_2) nanocomposites. As affected with adding filler of Silver oxide, Aluminum oxide and Niobium oxide nanoparticles on structural, A.C electrical and optical characterize for (PVP-PVA) blend. Antibacterial activity applications of (PVP-PVA-Ag_2O-NbO_2) and (PVP-PVA-Al_2O_3-NbO_2) nanocomposites are also estimated.

4.2 The Structural Properties

The structural properties of nanocomposites are studied using three techniques: fourier transform infrared radiation, optical microscope and scanning electron microscope.

4.2.1 Purity Test

The melting point (M.P.) of a basic polymer PVP and PVA polymers, was measured by using the device that is shown in Figure (3.2). This method represents one way of finding the melting point of materials. The melting point of all polymers are given in Table (4.1) which includes the experimental and theoretical values that obtained from Tables, and by comparing these two values, we verified the authenticity of materials and concluded the values of purity. All samples were prepared to melting point test as a powder. In this study, the results show that good agreement between the theoretical and experimental values as shown in Table below with some acceptance variations.

Table (4.1): The experimental and theoretical values of (M.P.).

Polymer Type	*Theoretical M.P. (C^0)*	*Experimental M.P. (C^0)*	*M.P. Range*	*Purity % ($M.P._{(Exp.)}$/ $M.P._{(Theo.)}$)×100 %*
PVP	150	149.7	1.5	99.8
PVA	230	229.7	1.5	99.8

4.2.2 Fourier Transform Infrared Radiation of Nanocomposites

Figures (4.1) and (4.2) show that the FTIR spectra of (PVP-PVA-Ag_2O-NbO_2) and (PVP-PVA-Al_2O_3-NbO_2) nanocomposites respectively. For all samples of nanocomposites are FTIR spectra showed broad bands at around (3306.73 cm^{-1}) observed because of OH groups in the polymers matrix chain. The band observed at (2938.15 cm^{-1}) is a characteristic of an asymmetry stretching mode of C-H groups. The peaks at 1661.03 cm^{-1} represent the presence free C=O groups. The band at 1422.61 cm^{-1} was attributed to the to the bending C-H groups. The band at 1288.72 cm^{-1} was attributed to the to the C-N group. The bands at (1090.87) cm^{-1} were attributed to the other bonds (C-O-C). The two strong bands observed at around 1422.61 cm^{-1} and 2938.15 cm^{-1} are attributed to the bending and stretching modes of C-H groups respectively. The (Ag_2O, NbO_2) and (Al_2O_3, NbO_2) nanoparticles are caused changes in spectral of (PVP-PVA) which include shift in some bonds and change in the intensities. The FTIR studies show that there is no interactions between (PVP-PVA) polymer matrix and (Ag_2O, NbO_2) and (Al_2O_3, NbO_2) nanoparticles. The transmittance in the figure decreases slightly with the increase of (Ag_2O, NbO_2) and (Al_2O_3, NbO_2) nanoparticles concentrations which attributed to increase the density of nanocomposites, this is consistent with the result of Srikanth *et al.* [176]. Experimental values for the wavenumber

of the absorption peaks and the corresponding bond were illustrated in the table (4.2).

Table (4.2): Experimental values for the wavenumber of the absorption peaks and the corresponding bond.

Wavenumbers (cm^{-1})	*Assignments*
3306.73	OH
2938.15	C-H Stretching
1661.03	C=O
1422.61	C-H Bending
1288.72	C-N
1090.87	C-O-C

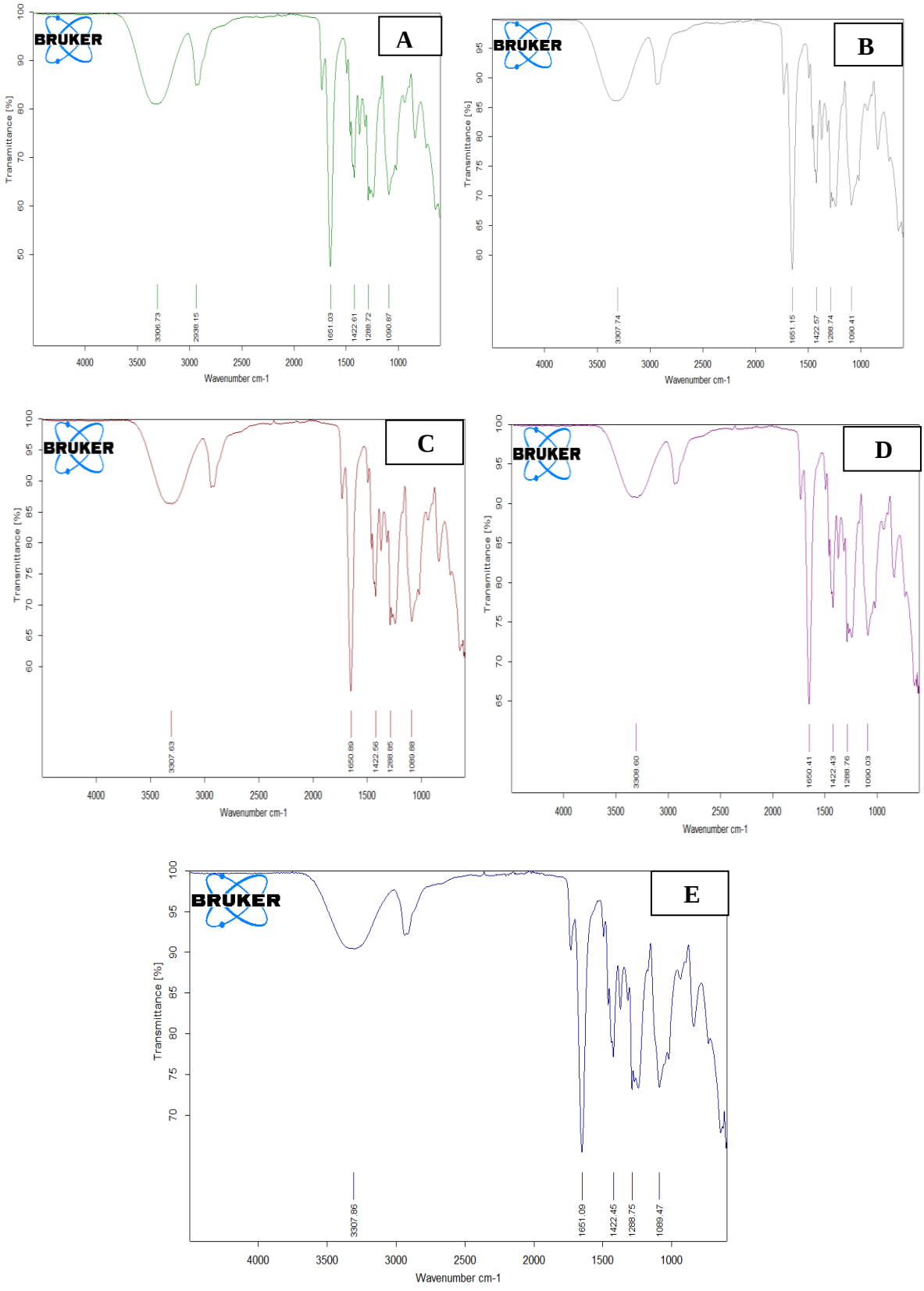

Figure (4.1): FTIR spectra for (PVP-PVA-Ag_2O-NbO_2) nanocomposites: (A)pure and (B, C, D and E) of (0.005, 0.01, 0.015 and 0.02) wt.% (Ag_2O and nanoparticles respectively.

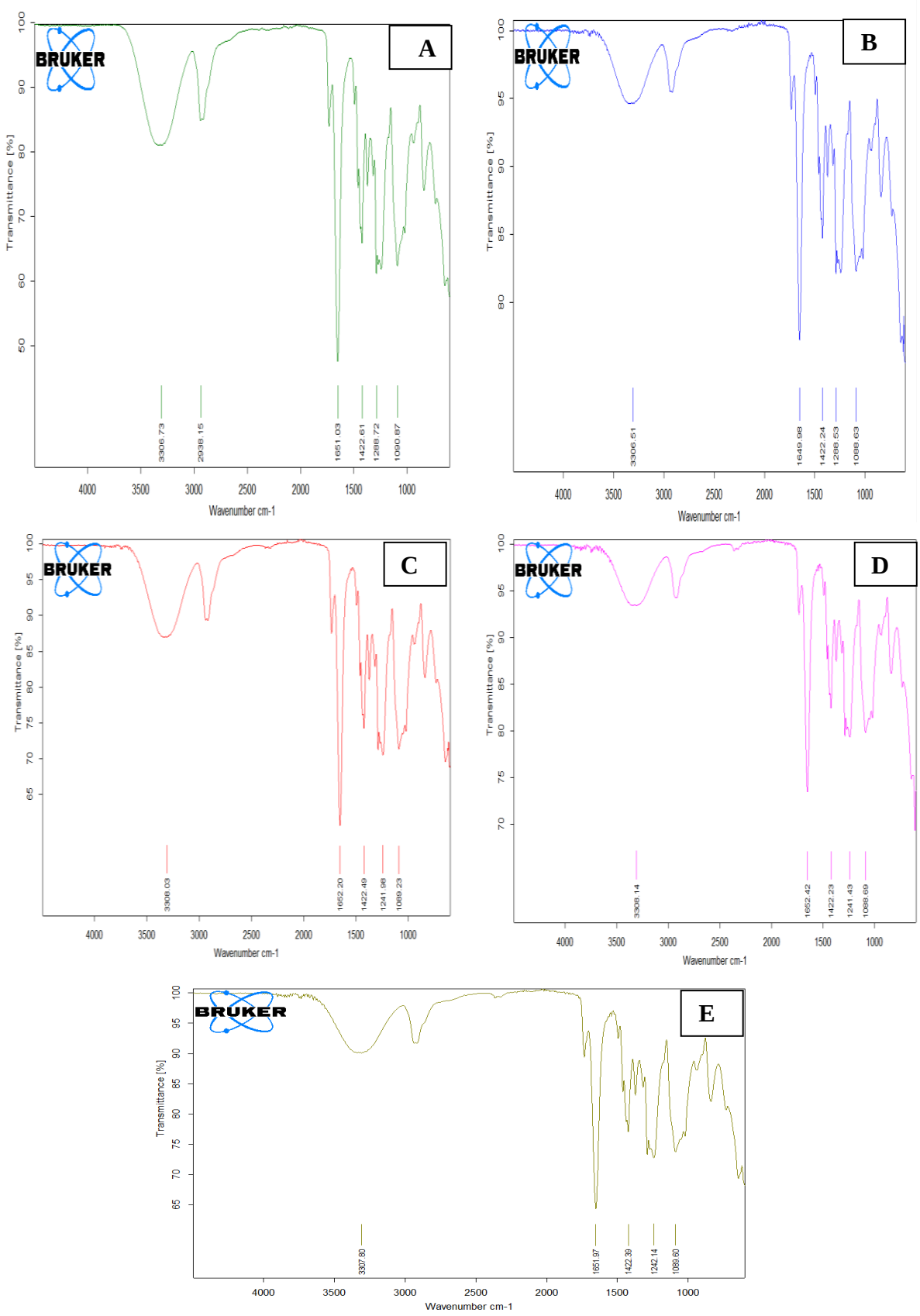

Figure (4.2): FTIR spectra for (PVP-PVA-Al_2O_3-NbO_2) nanocomposites: (A) pure and (B, C, D and E) of (0.005, 0.01, 0.015 and 0.02) wt.% (Al_2O_3 and NbO_2) nanoparticles respectively.

4.2.3 Optical Microscope

Figures (4.3) and (4.4) show that the distribution of (silver oxide, niobium oxide) and (aluminum oxide, niobium oxide) nanoparticles in (PVP-PVA) blend at magnification power (10x) respectively. The optical microscope images reveal that silver oxide, aluminum oxide and niobium oxide nanoparticles are aggregates as a cluster at low percentages as shown in these figures. Whereas at high percentages the presence of nanoparticles which is uniformly distributed inside the (PVP-PVA) blend where charge carriers are allowed to pass through the paths, this is similar with the results of Ramesh and Vijaya [177].

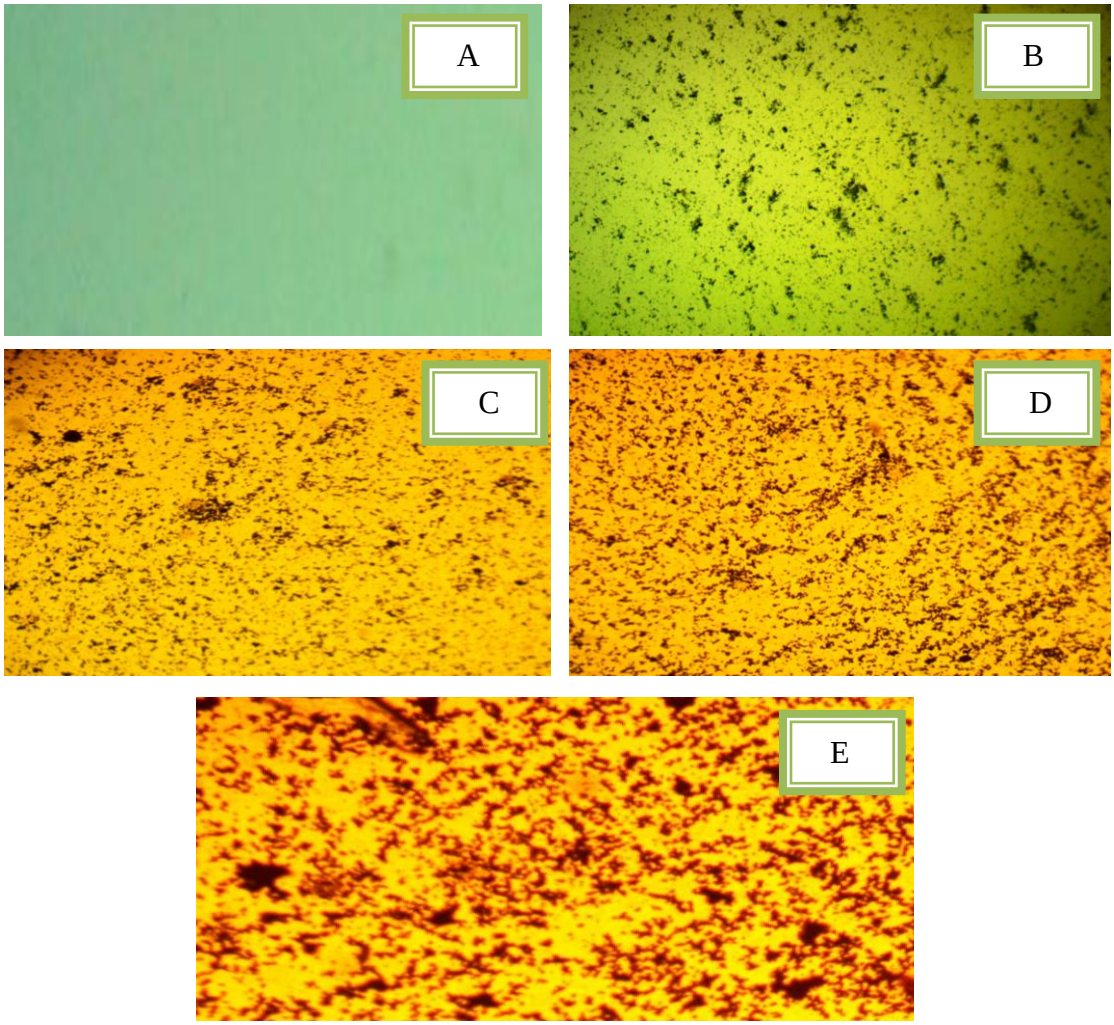

Figure (4.3): Photomicrographs for (PVP-PVA-Ag_2O-NbO_2) nanocomposites (10x) :(A) pure and (B, C, D and E) of (0.005, 0.01, 0.015 and 0.02) wt.% (Ag_2O and NbO_2) nanoparticles respectively.

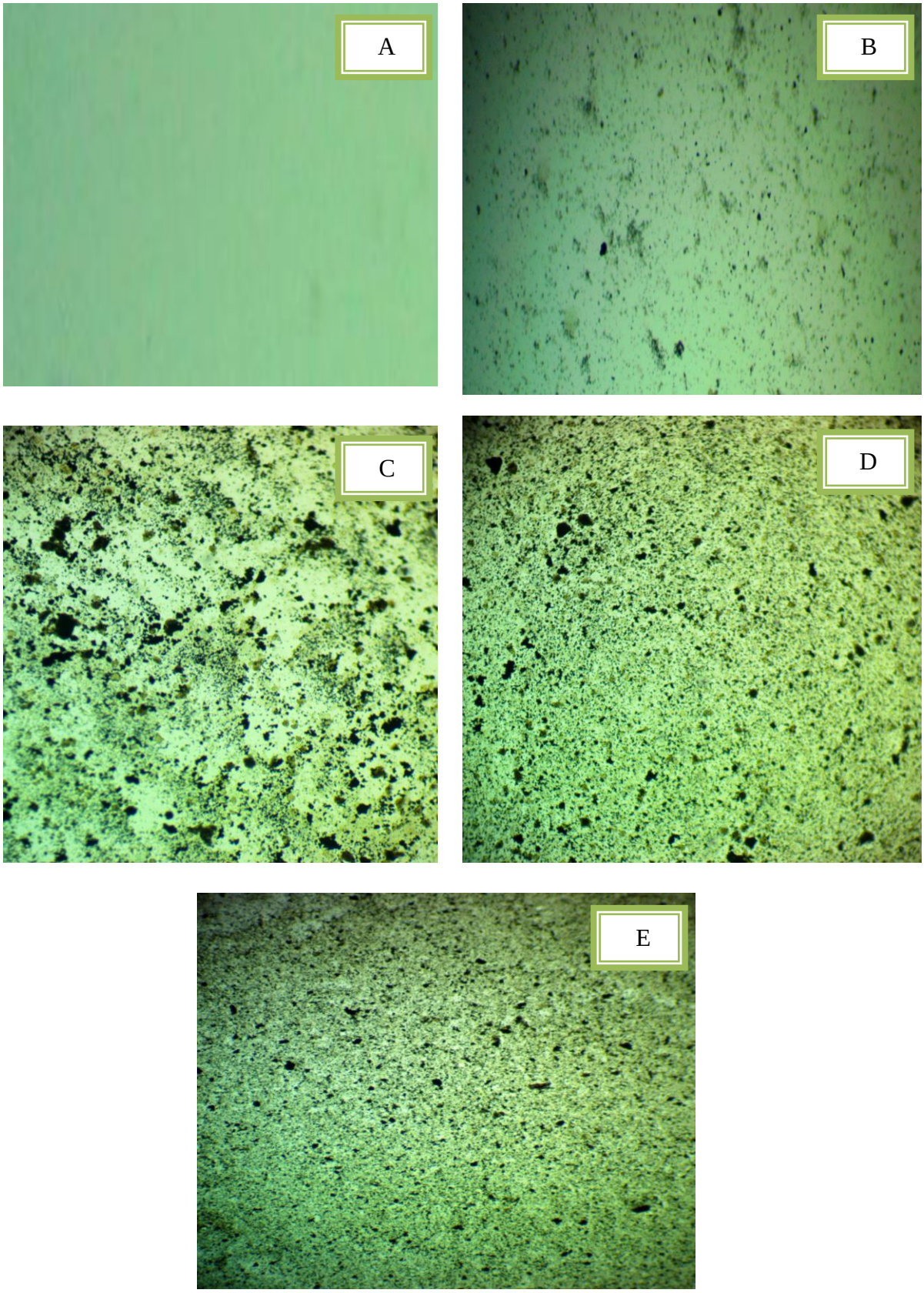

Figure (4.4): Photomicrographs for (PVP-PVA-Al_2O_3-NbO_2) nanocomposites (10x) :(A) pure and (B, C, D and E) of (0.005, 0.01, 0.015 and 0.02) wt.% (Al_2O_3 and NbO_2) nanoparticles respectively.

4.2.4 Scanning Electron Microscope (SEM)

Figures (4.5) and (4.6) shows the SEM photographs for (PVP-PVA) blend with different concentrations of (silver oxide, niobium oxide) and (aluminum oxide, niobium oxide) nanoparticles to study the morphology of nanocomposites and arrangement of nanoparticles at low and high concentrations of (Ag_2O,NbO_2) and (Al_2O_3,NbO_2) nanoparticles. Based on the FTIR assay and in comparison with the SEM assay, the formation of intermediate compounds is evident as a result of the temperature of preparation, which is formed in the form of (island) distributed on the surface of the sample, under which the nanoparticles are hidden, this gives a surface cohesion to the final compound as the weight ratio of the particles increases, diffusion law this is consistent with the result of Abdullah *et al.* [178].

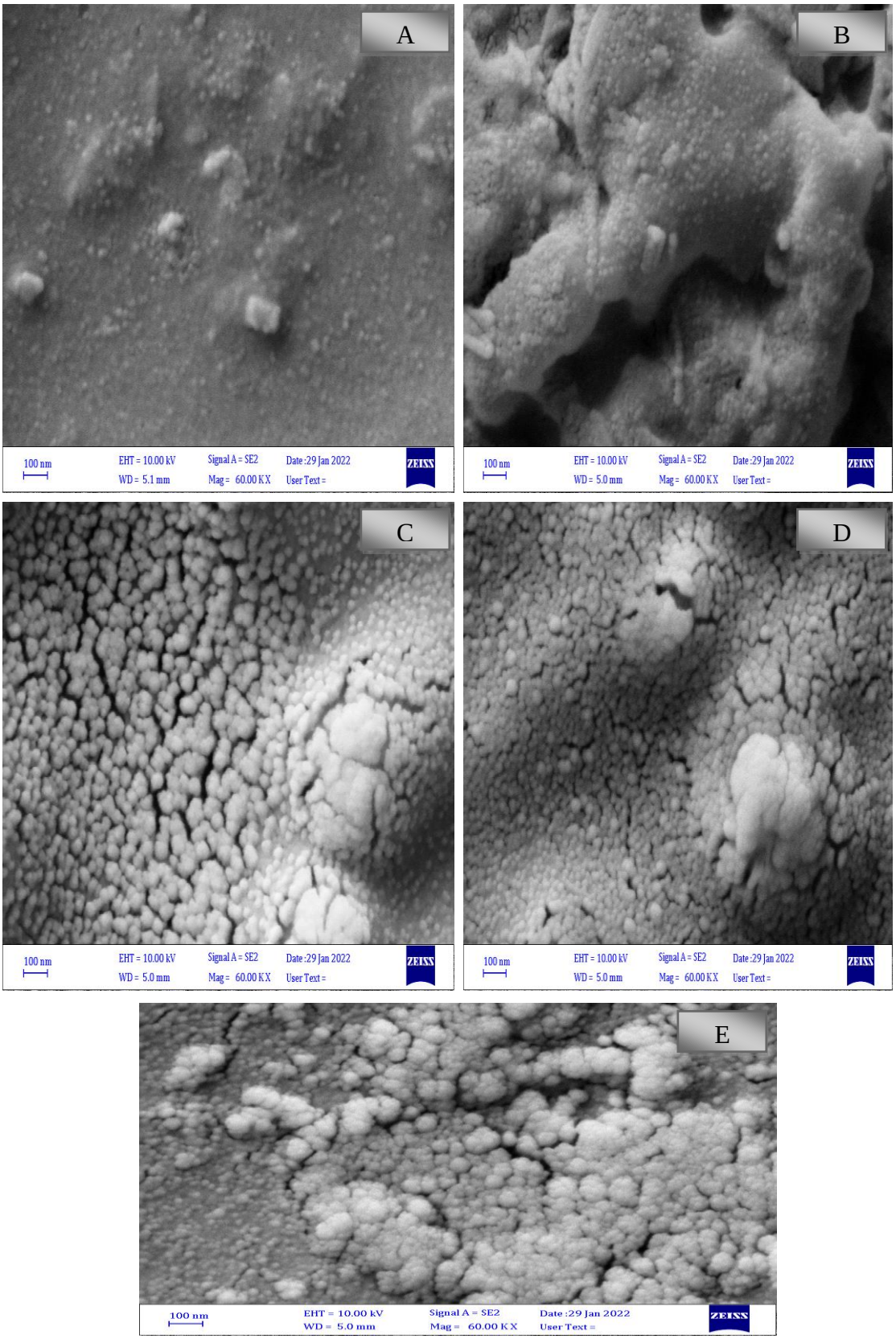

Figure (4.5): SEM images for (PVP-PVA-Ag_2O-NbO_2) nanocomposites at (100nm) : (A) pure and (B, C, D and E) of (0.005, 0.01, 0.015 and 0.02) wt. % (Ag_2O and NbO_2) nanoparticles respectively.

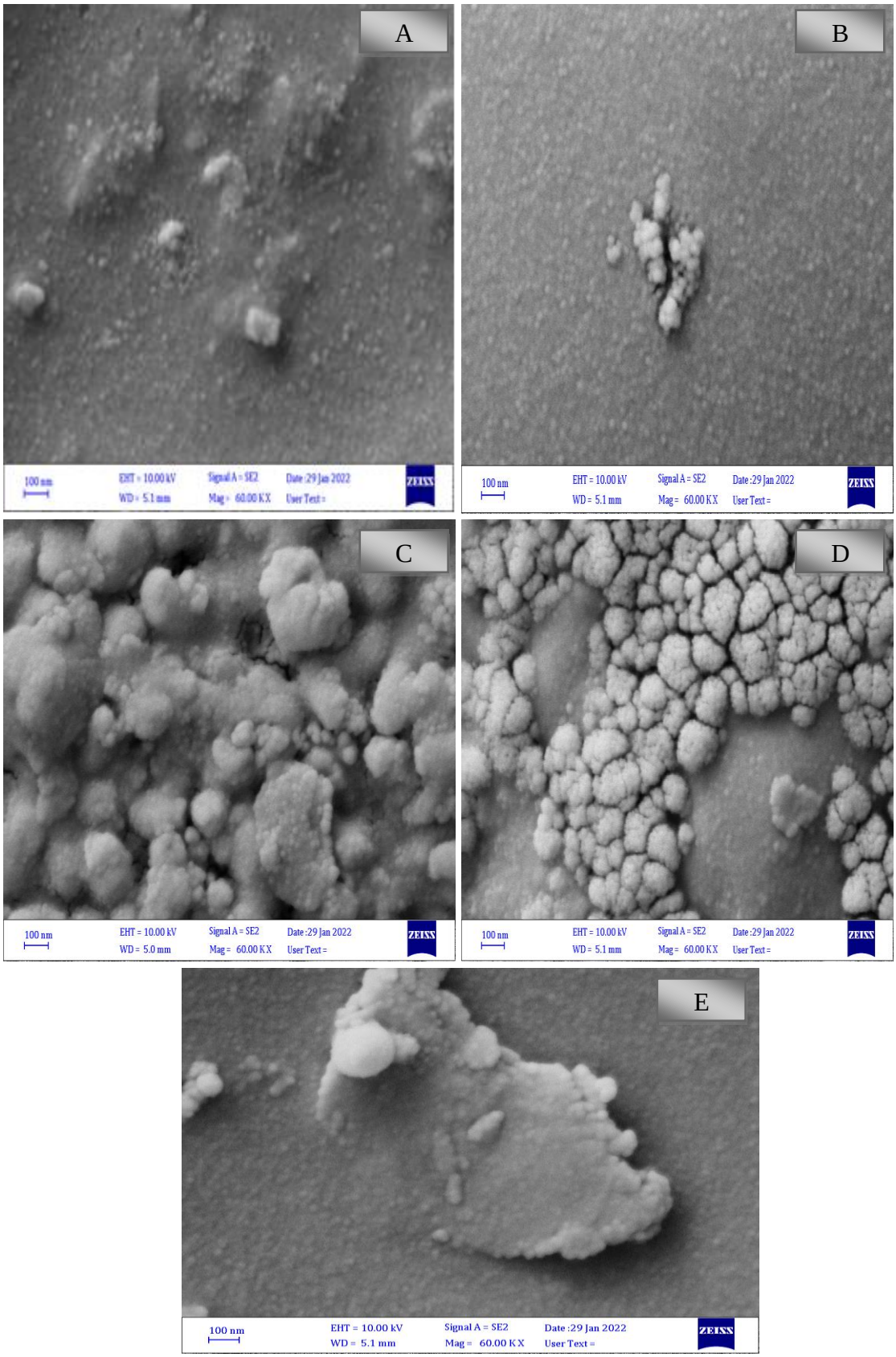

Figure (4.6): SEM images for (PVP-PVA-Al_2O_3-NbO_2) nanocomposites at (100nm): (A) pure and (B, C, D and E) of (0.005, 0.01, 0.015 and 0.02) wt. % (Al_2O_3 and NbO_2) nanoparticles respectively.

4.3 The Optical Properties

The optical properties of (PVP-PVA-Ag_2O-NbO_2) and (PVP-PVA-Al_2O_3-NbO_2) nanocomposites include: absorbance, transmittance, the absorption coefficient, energy band gap, extinction coefficient, refractive index, dielectric constants real and imaginary and optical conductivity.

The main purpose of optical properties study of (PVP-PVA-Ag_2O-NbO_2) and (PVP-PVA- Al_2O_3-NbO_2) nanocomposites to know the effect of silver oxide, aluminum oxide and niobium oxide nanoparticles additive on the optical properties of (PVP-PVA) blend and uses as antibacterial effect.

4.3.1 The Absorbance

Figures (4.7) and (4.8) show the variation of absorbance for (PVP-PVA-Ag_2O-NbO_2) and (PVP-PVA-Al_2O_3-NbO_2) nanocomposites with wavelength (λ) respectively. Figure (4.7) shows a peak at wavelength (220 nm) and this represents electronic transitions (σ-π*) and it belongs to polymers. A peak appeared when concentrations increased (0.01, 0.015 and 0.02) wt. % at wavelength (450 nm), which represents electronic transitions (n-π*). These transitions are due to the addition of Silver oxide nanoparticles. Its indicated that intensity of the peak increase with increases (Ag_2O,NbO_2) nanoparticles additive, this is because of the added (Ag_2O,NbO_2) nanoparticles have been absorbed the incident radiation by free electrons. In addition to, specific weight of (Ag_2O,NbO_2) nanoparticles compare with (PVP-PVA) blend, as a result increase in the specific weight of (PVP-PVA-Ag_2O-NbO_2) nanocomposites. But there is no changing in the location of the intensity of the peak of these nanocomposites, that's attributed no clear interaction between (PVP-PVA) blend and (Ag_2O,NbO_2) nanoparticles additive, expect of the weak band between these nanocomposites. But appear new physical properties, due to the shift in the band edges and the absorption

bands towards the higher wavelengths with different absorption intensities for different concentrations of (Ag_2O,NbO_2) nanoparticles samples. The shift in the absorption band gives an idea of the formation intermolecular hydrogen bonding existing between silver and niobium ions with the neighboring OH groups of the PVA main chain. The increase in absorption for (PVP-PVA-Ag_2O-NbO_2) nanocomposites are mainly due to the increase in (Ag_2O,NbO_2) nanoparticles.

In general the present study showed that the absorbance increases with increasing concentrations of nanoparticles, and the absorbance decreases with increasing wavelength, and this is due to the excitations of valence band electrons to the conduction band. The high absorbance of samples for nanocomposites at UV region attributed to the energy of photon enough to interact with atoms, the electron excites from a lower to higher energy level by absorbing a photon of known energy. Fundamental absorption of absorbance spectra refers from band to band or excitation transition at visible and near infrared regions, the absorbance of all samples for nanocomposites has low values, this behavior attributed to the energy of incident photons doesn’t enough energy to interact with atoms, thus the photons will be transmitted when the wavelength increases. The (PVP-PVA-Ag_2O-NbO_2) and (PVP-PVA- Al_2O_3-NbO_2) nanocomposite is better because it has an absorbance within a wide spectrum range and thus can be applied to various optical and electronic devices, this behavior consistent with the results of Phukan and Saikia [179].

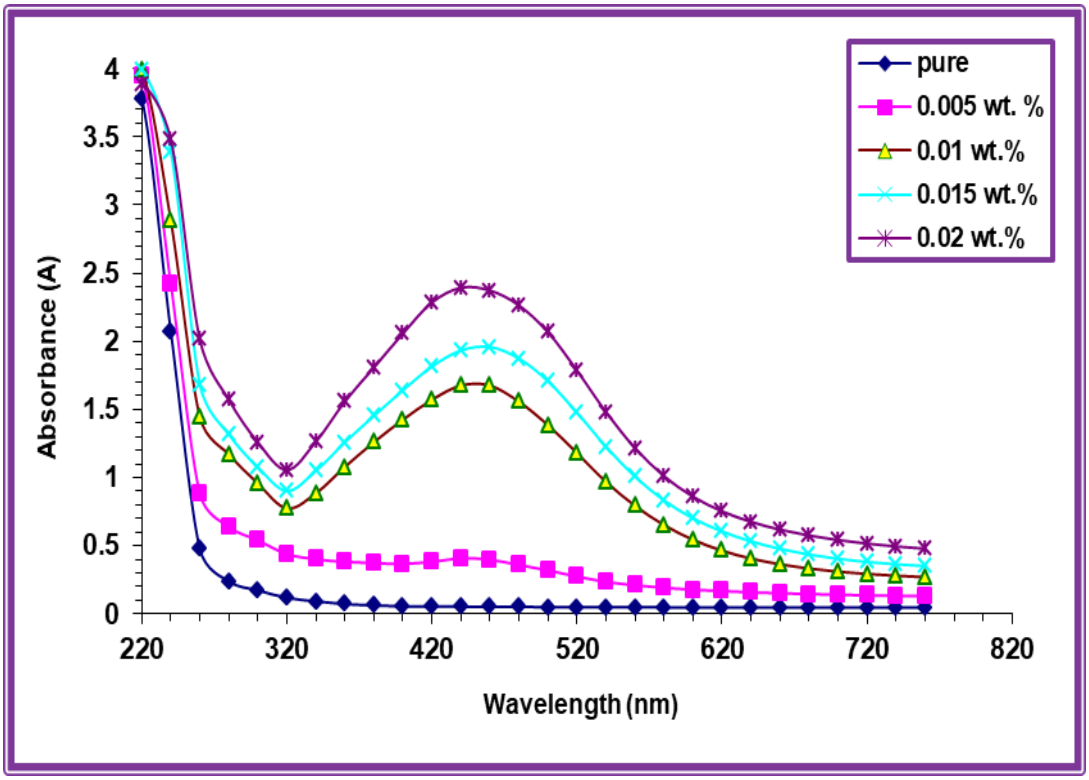

Figure (4.7): Variation of absorbance for (PVP-PVA-Ag_2O-NbO_2) nanocomposites with wavelength.

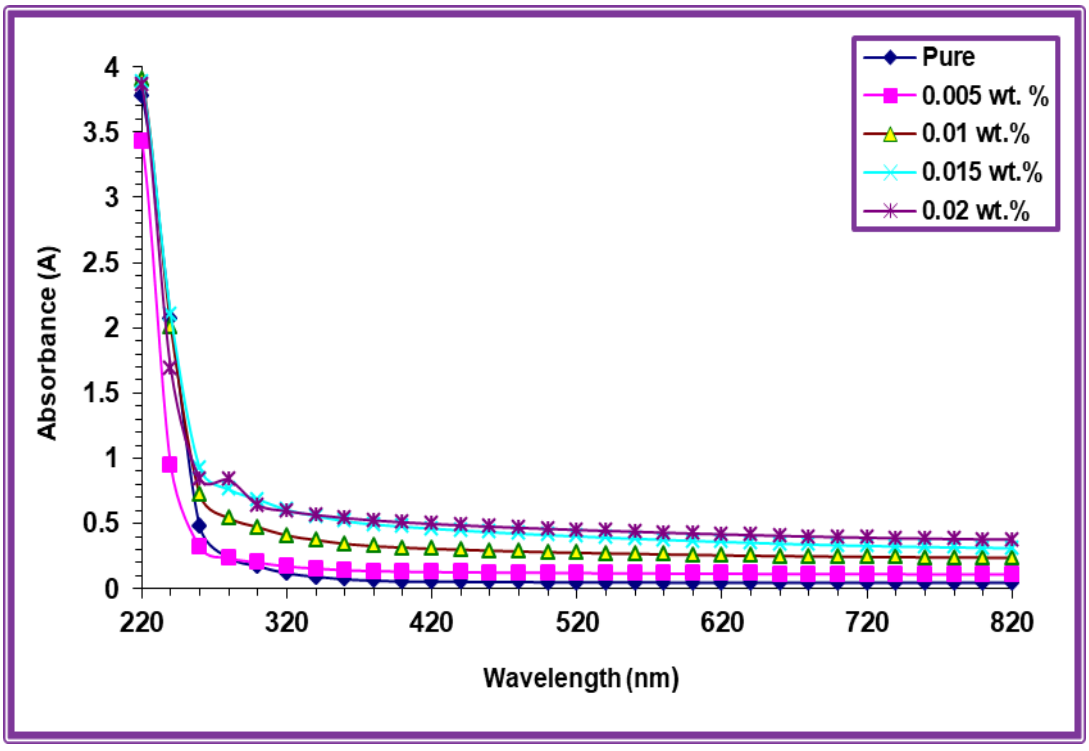

Figure (4.8): Variation of absorbance for (PVP-PVA-Al_2O_3-NbO_2) nanocomposites with wavelength.

4.3.2 The Transmittance

Figures (4.9) and (4.10) show the variation of transmittance for (PVP-PVA-Ag_2O-NbO_2) and (PVP-PVA-Al_2O_3-NbO_2) nanocomposites with wavelength (λ) respectively. Figure (4.9) shows a peak at wavelength (220 nm) and this represents electronic transitions (σ-π*) and it belongs to polymers. A peak appeared when concentrations increased (0.01, 0.015 and 0.02) wt. % at wavelength (450 nm), which represents electronic transitions (n-π*). These transitions are due to the addition of silver oxide nanoparticles.

By increase the concentrations of (Ag_2O,NbO_2) and (Al_2O_3,NbO_2) nanoparticles, the transmittance decrease of (PVP-PVA-Ag_2O-NbO_2) and (PVP-PVA-Al_2O_3-NbO_2) nanocomposites that behavior is vice versa with absorbance behavior as in Figures (4.7) and (4.8). This is mean of (Ag_2O,NbO_2) and (Al_2O_3,NbO_2) nanoparticles, enhance the (PVP-PVA-Ag_2O-NbO_2) and (PVP-PVA-Al_2O_3-NbO_2) nanocomposites absorbance. This is attributed to the fills the vacancies between polymer chains of (PVP-PVA) blend by (Ag_2O,NbO_2) and (Al_2O_3,NbO_2) nanoparticles, additive. Beside that; the free electrons of (Ag_2O,NbO_2) and (Al_2O_3,NbO_2) nanoparticles, absorbed the light incident on the samples, this leads to the free electrons crosses to the high level energy and no radiated any rays where the electrons moved to high takes free location in the energy band. Also the decreased in the transmittance may be attributed to the nature of the reflected and refracted in the samples. Its note (PVP-PVA) blend has low transmittance because of the distance between valence and conduction band is higher, where no free electrons where electrons bond with the atoms of (PVP-PVA) blends by covalent bonds, this mean these electrons need high photons to break covalent bonds and transfer to the conduction bond. The (PVP-PVA-Ag_2O-NbO_2) nanocomposite is better because it has an transmittance within a wide

spectrum range and thus can be applied to various optical and electronic devices, this is similar with the result of Feng *et al.* [180].

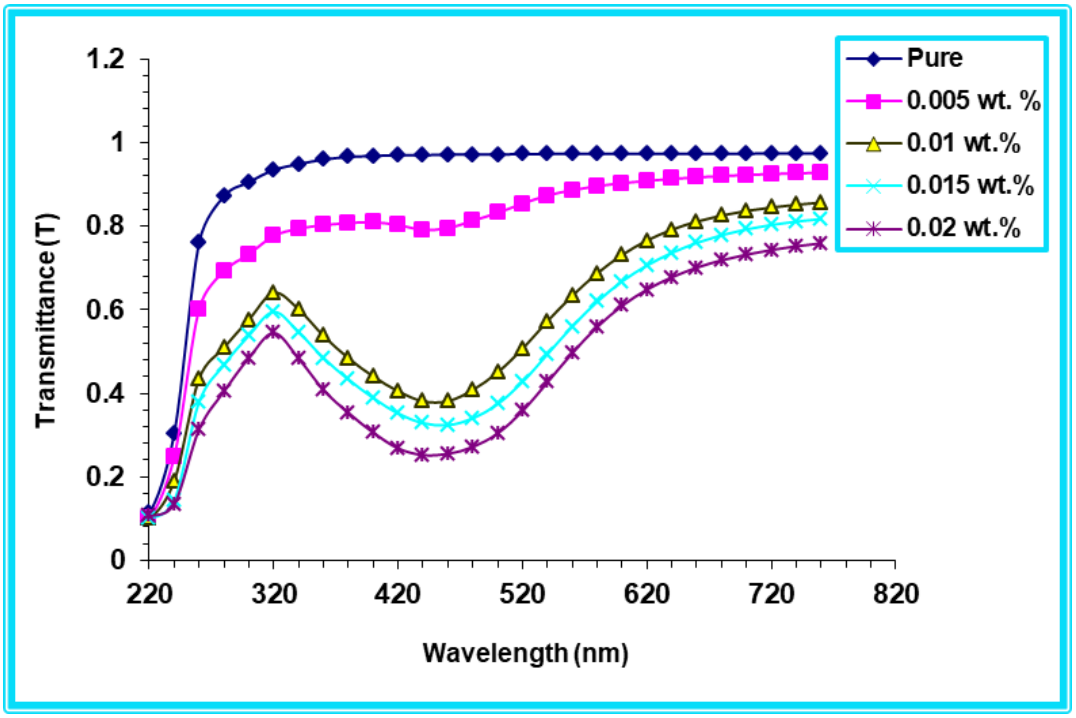

Figure (4.9): Variation of transmittance for (PVP-PVA-Ag_2O-NbO_2) nanocomposites with wavelength.

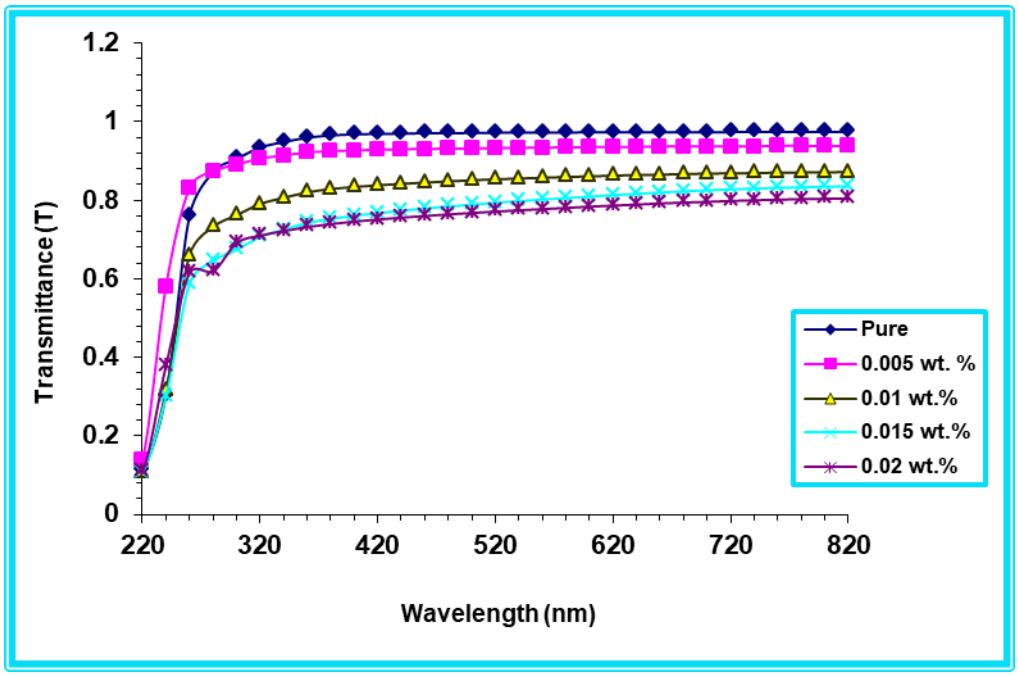

Figure (4.10): Variation of transmittance for (PVP-PVA-Al_2O_3-NbO_2) nanocomposites with wavelength.

4.3.3 The Absorption Coefficient

The absorption coefficient (α) of nanocomposites is calculated by using equation (2-4). Figures (4.11) and (4.12) shows the variation of absorption coefficient for nanocomposite as a function of photon energy of the incident light respectively. The absorption coefficient of all samples for (PVP-PVA-Ag_2O-NbO_2) and (PVP-PVA-Al_2O_3-NbO_2) nanocomposites is low at low energy, this means that the electron transition has low possibility; i.e. the energy of incident photon is not enough to transition of electron from valence band to conduction band for nanocomposites. But, at high energies the absorption coefficient of all samples for (PVP-PVA-Ag_2O-NbO_2) and (PVP-PVA-Al_2O_3-NbO_2) nanocomposites is high. This means that the electron transition has high possibility; i.e. the energy of incident photon is enough to transit the electron from the valence band to the conduction band which due to the energy of the incident photon is greater than the energy band gap. The absorption coefficient assists to know the nature of electron transition, when the values of the absorption coefficient of material are high ($\alpha>10^4$) cm^{-1}, it is expected that direct transition of electron. While, when the values of the absorption coefficient of material are low ($\alpha<10^4$) cm^{-1}, it is expected that indirect transition of electron. The values of absorption coefficient of (PVP-PVA-Ag_2O-NbO_2) and (PVP-PVA-Al_2O_3-NbO_2) nanocomposites are low ($\alpha<10^4$) cm^{-1}; the transition of electron is indirect. The absorption coefficient of (PVP-PVA-Ag_2O-NbO_2) and (PVP-PVA-Al_2O_3-NbO_2) nanocomposites increases with the increasing of the concentrations of (silver oxide, niobium oxide) and (aluminum oxide, niobium oxide) nanoparticles, this is attributed to the increasing of number of charge carriers, hence, increase the absorbance and absorption coefficient of nanocomposites, this is similar with the result of Salman *et al.* [181].

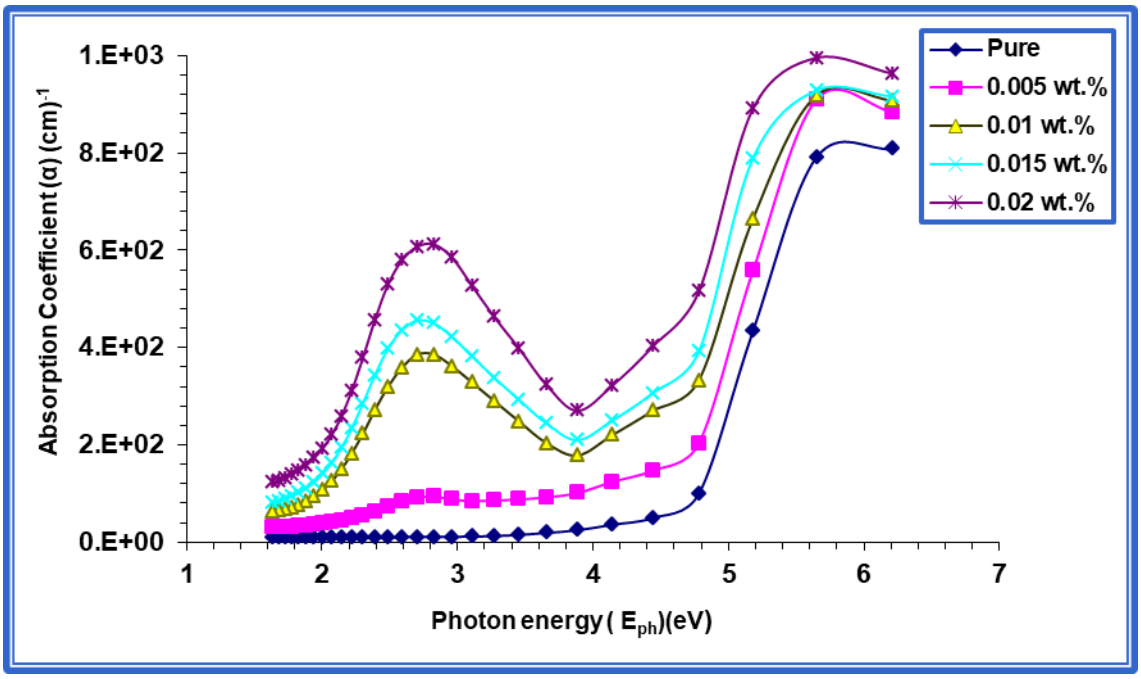

Figure (4.11): Absorption coefficient (α) for nanocomposites (PVP-PVA-Ag_2O-NbO_2) with different photon energies.

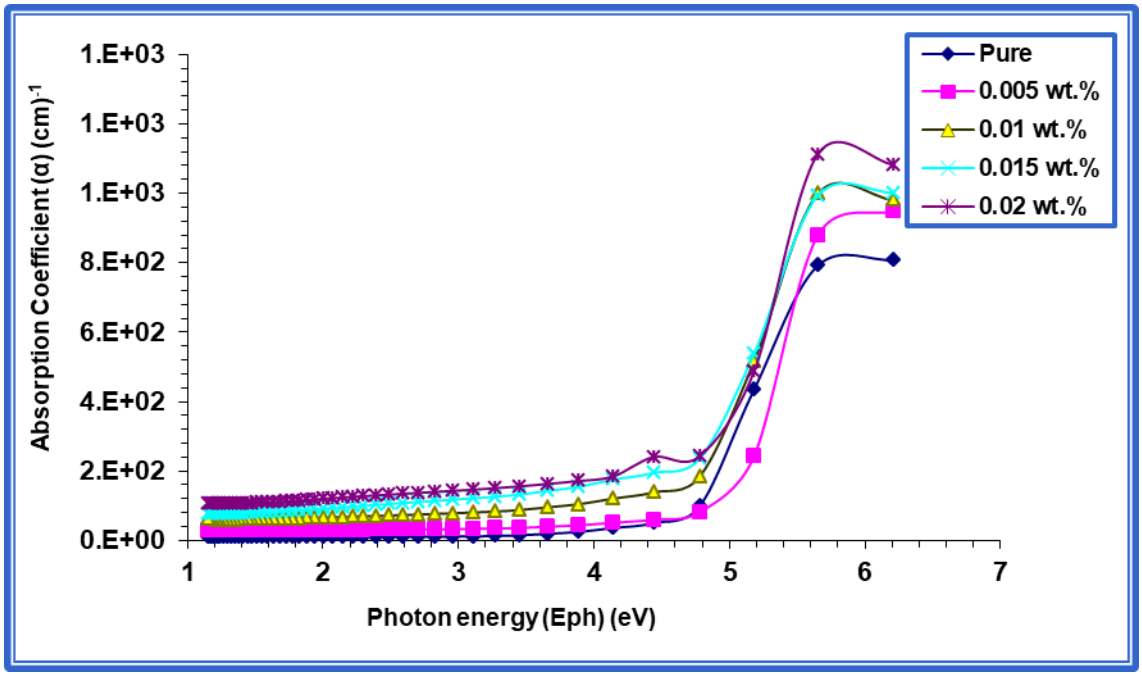

Figure (4.12): Absorption coefficient (α) for nanocomposites (PVP-PVA-Al_2O_3-NbO_2) with different photon energies.

4.3.4 The Energy Band Gap

The energy band gap of nanocomposites is calculated by using equation (2-5). The energy band gap for allowed when the value of (r =2), but when the value of (r =3) this indicates forbidden indirect transition of (PVP-PVA-Ag_2O-NbO_2) nanocomposites are shown in figures (4.13) and (4.14) respectively. The energy band gap for allowed and forbidden indirect transitions of (PVP-PVA-Al_2O_3-NbO_2) nanocomposite are shown in figures (4.15) and (4.16) respectively. The values have been getting in tables (4.3 and 4.4) its indicated that the values of indirect energy band gap(allowed and forbidden transition) of (PVP-PVA-Ag_2O-NbO_2) and (PVP-PVA-Al_2O_3-NbO_2) nanocomposites decrease with increasing (Silver oxide, Niobium oxide) and (Aluminum oxide, Niobium oxide) nanoparticles concentration, this attribute to great localize levels in the forbidden energy band gap. The energy band gap for allowed and forbidden indirect transition of (PVP-PVA-Ag_2O-NbO_2) and (PVP-PVA-Al_2O_3-NbO_2) nanocomposites are decreased with the increasing of the (Silver oxide, Niobium oxide) and (Aluminum oxide, Niobium oxide) nanoparticles concentration, this behavior is due to the creation of level in the energy gap; the transition of electron in this case is conducted in two stages that involve the transition from the valence band to the local levels in energy gap and to the conduction band in the allowed indirect transition. But in indirect forbidden transition, the transition of electrons between the tails of localize of the levels made by the additive. As a result of increasing the (silver oxide, niobium oxide) and (aluminum oxide, niobium oxide) nanoparticles concentration, this is similar with the results of Abdelghany *et al.* [182] and Hegazy *et al.* [183].

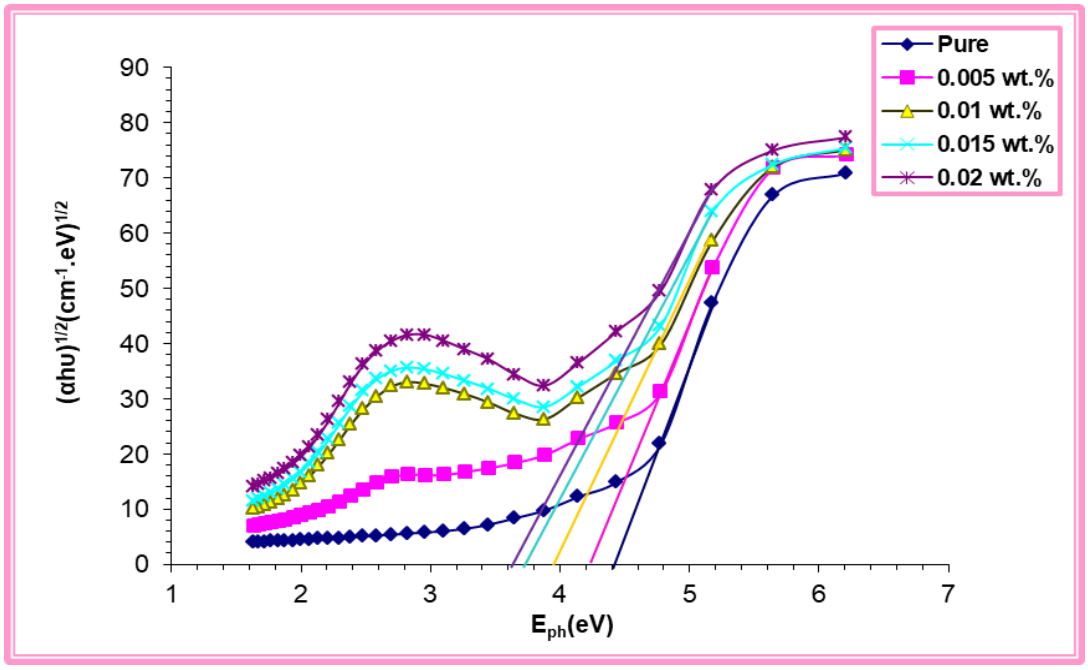

Figure (4.13): Variation of $(\alpha h\upsilon)^{1/2}$ for (PVP-PVA-Ag_2O-NbO_2) nanocomposites with photon energy.

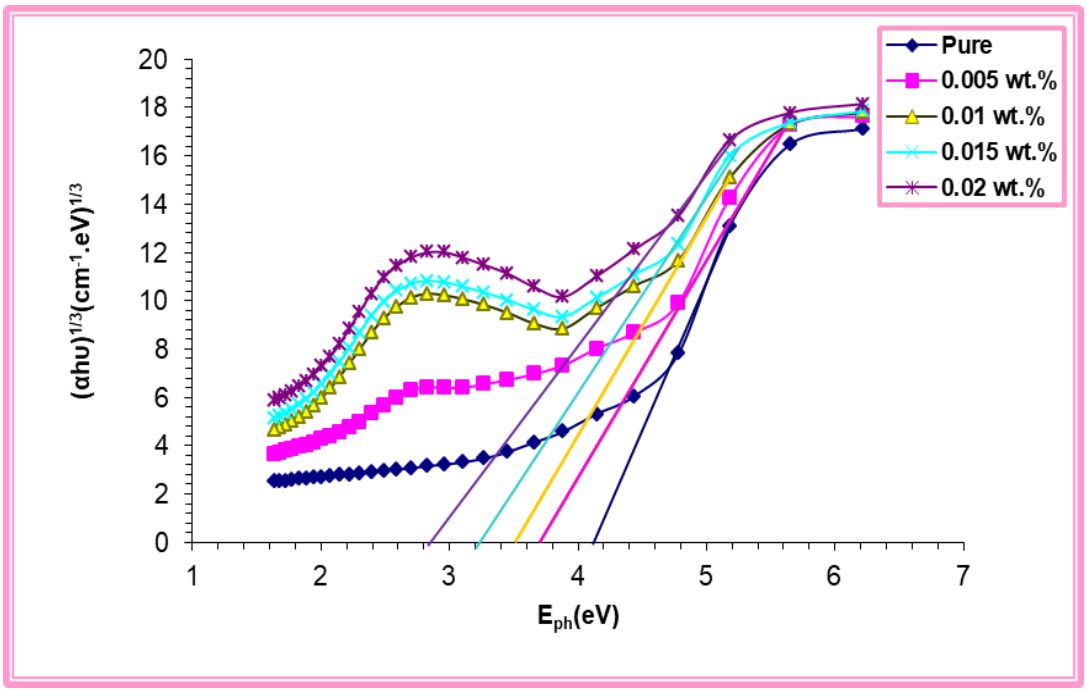

Figure (4.14): Variation of $(\alpha h\upsilon)^{1/3}$ for (PVP-PVA-Ag_2O-NbO_2) nanocomposites with photon energy

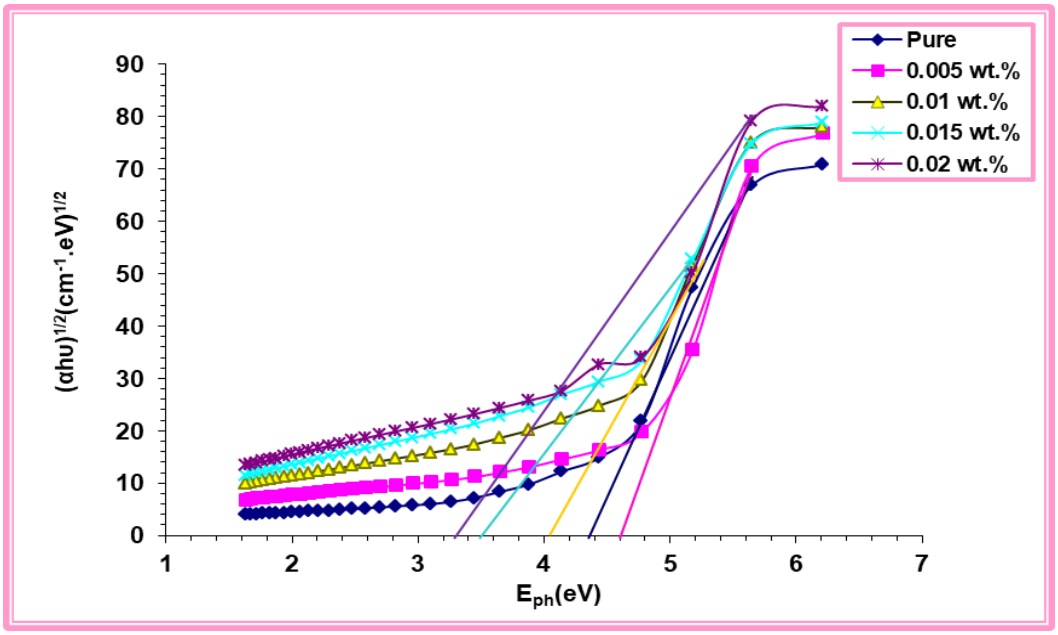

Figure (4.15): Variation of $(\alpha h\upsilon)^{1/2}$ for (PVP-PVA-Al_2O_3-NbO_2) nanocomposites with photon energy.

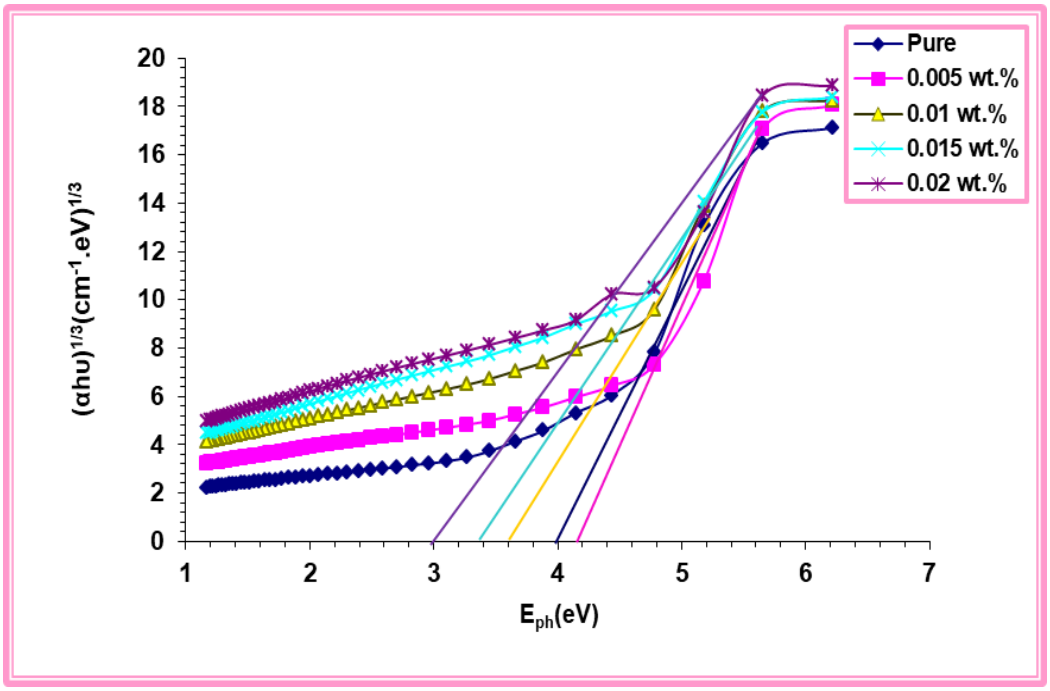

Figure (4.16): Variation of $(\alpha h\upsilon)^{1/3}$ for (PVP-PVA-Al_2O_3-NbO_2) nanocomposites with photon energy.

Table (4.3) compare between the energy band gap for allowed indirect transition and forbidden indirect transition of (PVP-PVA-Ag_2O-NbO_2) nanocomposites, where the optical energy gap values for allowed indirect transition and forbidden indirect transition decrease.

Tables (4.3): Values of energy gap for allowed and forbidden of (PVP-PVA-Ag_2O-NbO_2) nanocomposites

Wt. %	*energy band gap for allowed (ev)*	*energy band gap for forbidden (ev)*
0	4.4	4.13
0.005	4.2	3.7
0.01	3.95	3.5
0.015	3.7	3.2
0.02	3.6	2.8

Table (4.4) compare between the energy band gap for allowed indirect transition and forbidden indirect transition of (PVP-PVA-Al_2O_3-NbO_2) nanocomposites. Where the optical energy gap values for allowed indirect transition and forbidden indirect transition decrease.

Tables (4.4): Values of energy gap for allowed and forbidden of (PVP-PVA-Al_2O_3-NbO_2) nanocomposites.

Wt .%	*energy band gap for allowed (ev)*	*energy band gap for forbidden (ev)*
0	4.4	4.13
0.005	4.6	4.2
0.01	4	3.6
0.015	3.5	3.35
0.02	3.3	3

4.3.5 The Extinction Coefficient

The extinction coefficient (K) is calculated using the equation (2-9). Figures (4.17) and (4.18) show the variation of extinction coefficient for (PVP-PVA-Ag_2O-NbO_2) and (PVP-PVA-Al_2O_3-NbO_2) nanocomposites as a function of wavelength respectively. The figures shows that the extinction coefficient of (PVP-PVA-Ag_2O-NbO_2) and (PVP-PVA-Al_2O_3-NbO_2) nanocomposites increase with the increasing of the (silver oxide, niobium oxide) and (aluminum oxide, niobium oxide) nanoparticles concentration. The behavior of extinction coefficient attributes to high absorption. In addition to; loss in incident photon energy due to the interaction between the carries charge in the samples and the incident light, which leads to polarize of the medium charges. The extinction coefficient of nanocomposite has high values at UV region, this behavior attributed to high absorbance of all samples of nanocomposite. Also, extinction coefficient of nanocomposite increases with the increasing of the wavelength at visible legion and near the infrared region which attributed to the absorption coefficient of (PVP-PVA-Ag_2O-NbO_2) and (PVP-PVA-Al_2O_3-NbO_2) nanocomposites is approximately constant at visible and near infrared region, hence, the extinction coefficient increases with the increasing of the wavelength according to equation (2-9), this is similar with the result of Ghanipour and Dorranian [184], Ali [185].

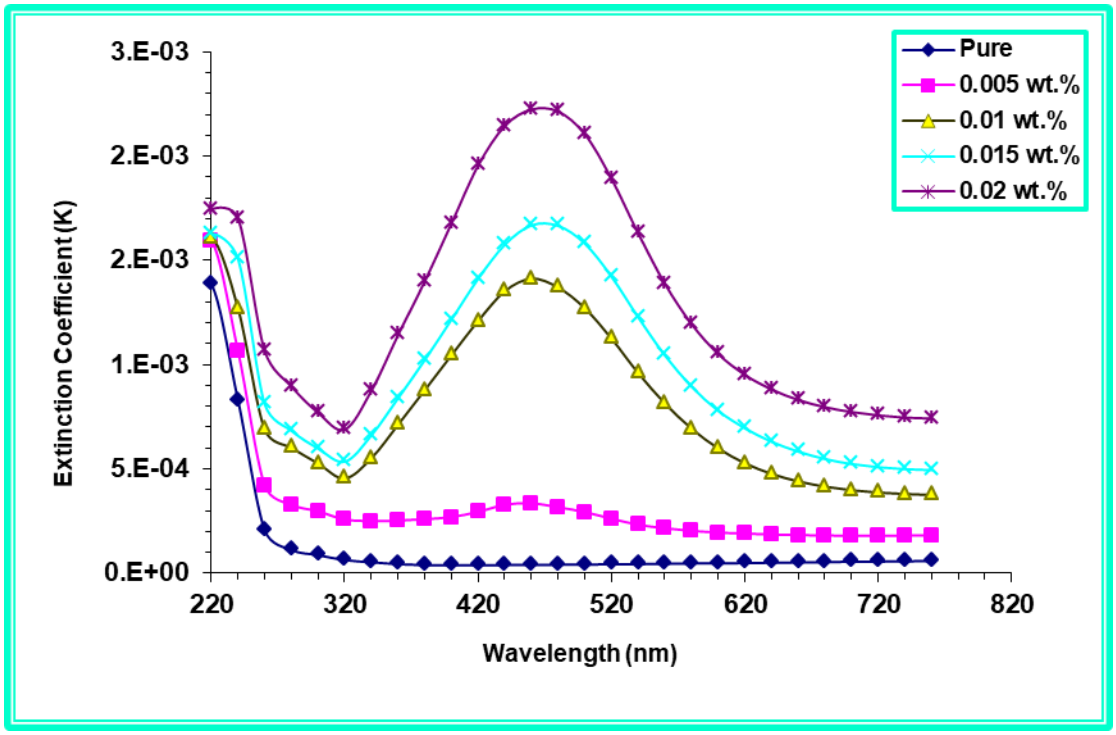

Figure (4.17): Variation of extinction coefficient for (PVP-PVA-Ag_2O-NbO_2) nanocomposites with wavelength.

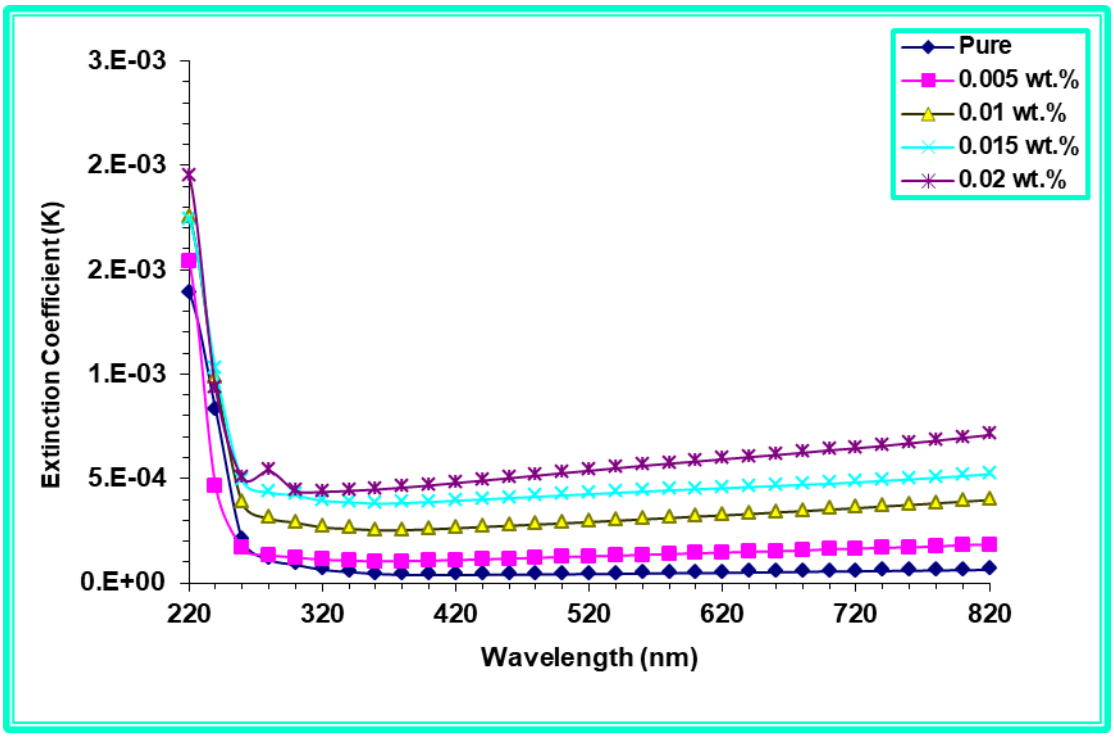

Figure (4.18): Variation of extinction coefficient for (PVP-PVA-Al_2O_3-NbO_2) nanocomposites with wavelength.

4.3.6 The Refractive Index

The refractive index is calculated by using equation (2-10). The refractive index of (PVP-PVA-Ag_2O-NbO_2) and (PVP-PVA-Al_2O_3-NbO_2) nanocomposites as a function of wavelength is shown in Figures (4.19) and (4.20) respectively. As shown in the figures, the refractive index of nanocomposites increase with increase of the of the (silver oxide, niobium oxide) and (aluminum, niobium oxide) nanoparticles concentrations, the refractive index of (PVP-PVA) blend increases due to increase the scattering of incident photon which causes to increase the reflectance. In addition to; further addition of (silver oxide, niobium oxide) and (aluminum, niobium oxide) nanoparticles causes increasing the intensity for (PVP-PVA-Ag_2O-NbO_2) and (PVP-PVA-Al_2O_3-NbO_2) nanocomposites. When the incident light interacts with (PVA-CMC) blend has further addition of (silver oxide, niobium oxide) and (aluminum, niobium oxide) nanoparticles, the reflection will be high hence the reflectivity for (PVP-PVA-Ag_2O-NbO_2) and (PVP-PVA-Al_2O_3-NbO_2) nanocomposites will be increased, this is similar to the result of Sayed and Morsi [186].

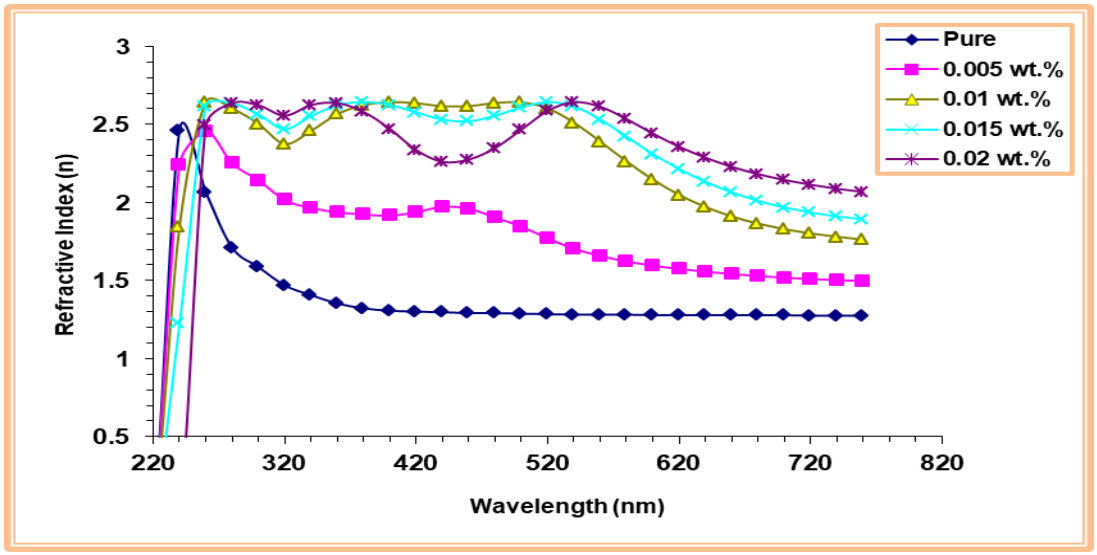

Figure (4.19): Variation of refractive index for (PVP-PVA-Ag_2O-NbO_2) nanocomposites with wavelength.

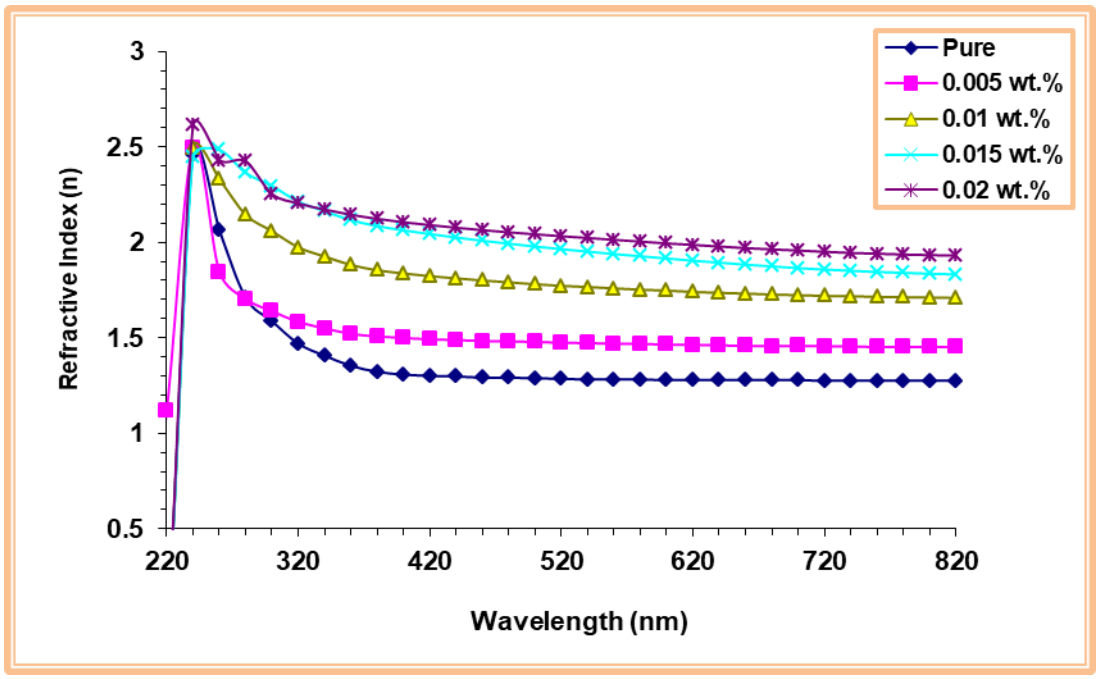

Figure (4.20): Variation of refractive index for (PVP-PVA-Al_2O_3-NbO_2) nanocomposites with wavelength.

4.3.7 The Real and Imaginary Parts of Dielectric Constant

The real and imaginary parts of dielectric constant are calculated by using equations (2-11) and (2-12) respectively. Figures (4.21) and (4.22) show the variation of the real dielectric constant with the wavelength for (PVP-PVA-Ag_2O-NbO_2) and (PVP-PVA-Al_2O_3-NbO_2) nanocomposites respectively. The effect of (Ag_2O-NbO_2) and (Al_2O_3-NbO_2) nanoparticles on the imaginary part of dielectric constant is shown in Figures (4.23) and (4.24) for (PVP-PVA-Ag_2O-NbO_2) and (PVP-PVA-Al_2O_3-NbO_2) nanocomposites respectively. The figures show that the real and imaginary parts of dielectric constant of (PVP-PVA) blend increase with the increasing of (silver oxide, niobium oxide) and (aluminum oxide, niobium oxide) nanoparticles concentration, this behavior attributed to the increasing of electrical dipoles that polarization due to contribution of nanoparticle concentration in the sample i.e., the increase in the dielectric constant of (PVP-PVA) blend represents a fractional increase in charges

within the polymers. As shown in the figures, the real and imaginary parts of dielectric constant of (PVP-PVA) blend are changed with the wavelength, this is due to the real part of dielectric constant which depends on refractive index because the effect of extinction coefficient is very small and the imaginary part of dielectric constant depends on extinction coefficient especially in the visible and near infrared regions of wavelength where the refractive index is approximately constant, while extinction coefficient increases with the increase of the wavelength, this is similar with the result of Abdullah [187], Abbas *et. al* [188].

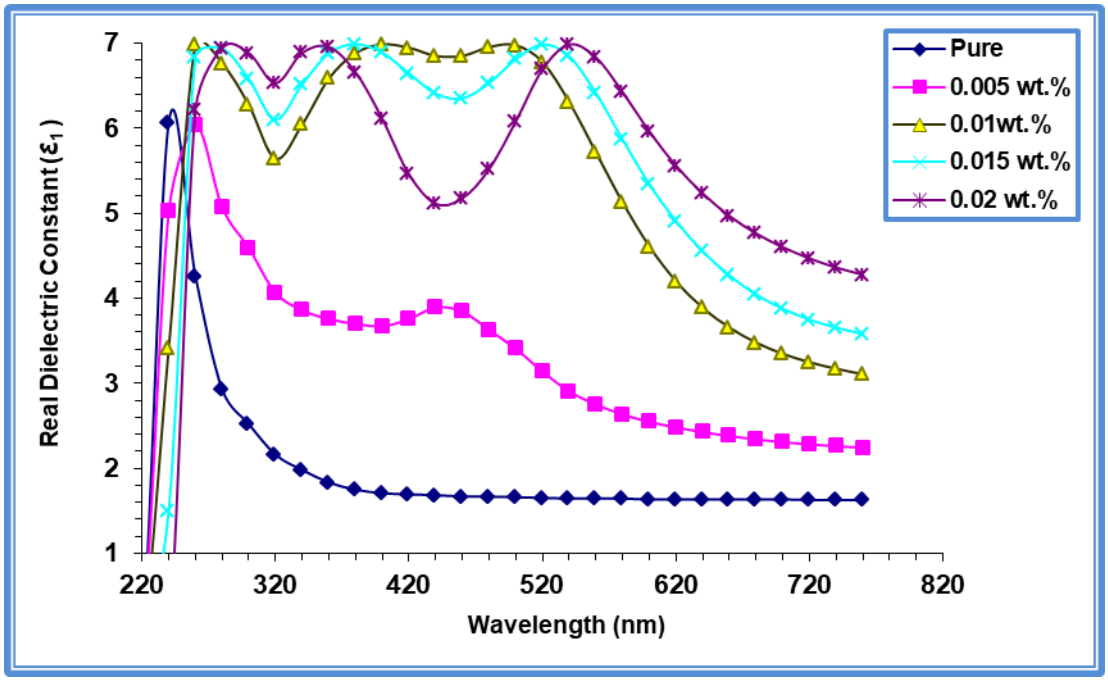

Figure (4.21): Variation in the real dielectric constant component for nanocomposites (PVP-PVA-Ag_2O-NbO_2) with wavelength.

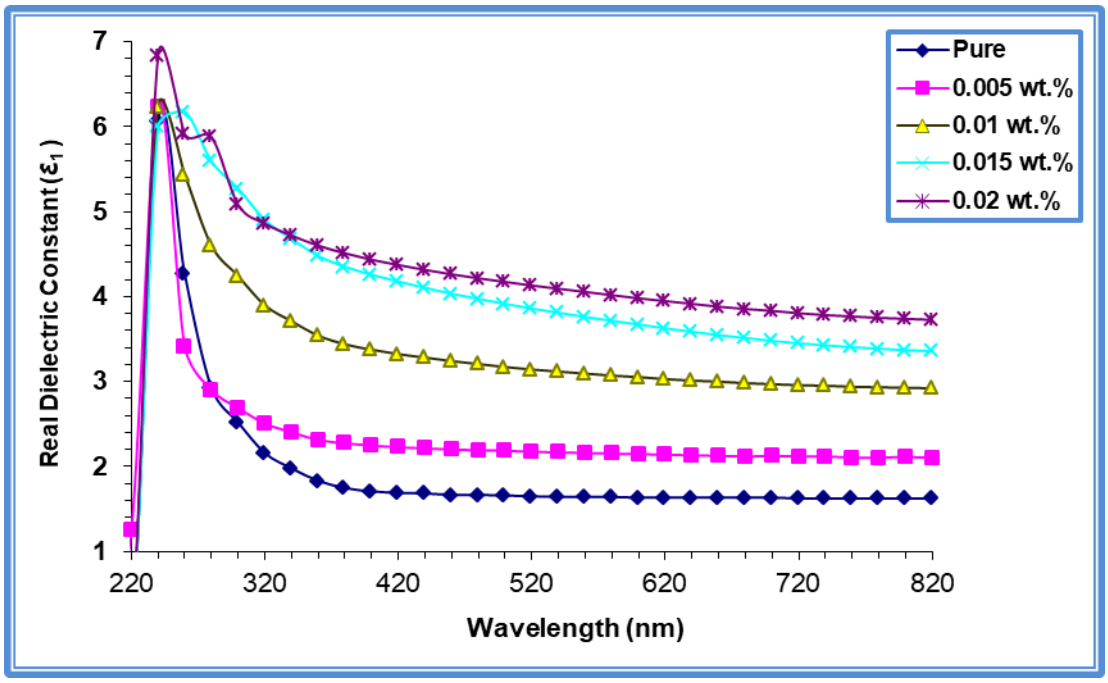

Figure (4.22): Variation in the real part of dielectric constant for nanocomposites (PVP-PVA-Al_2O_3-NbO_2) with wavelength.

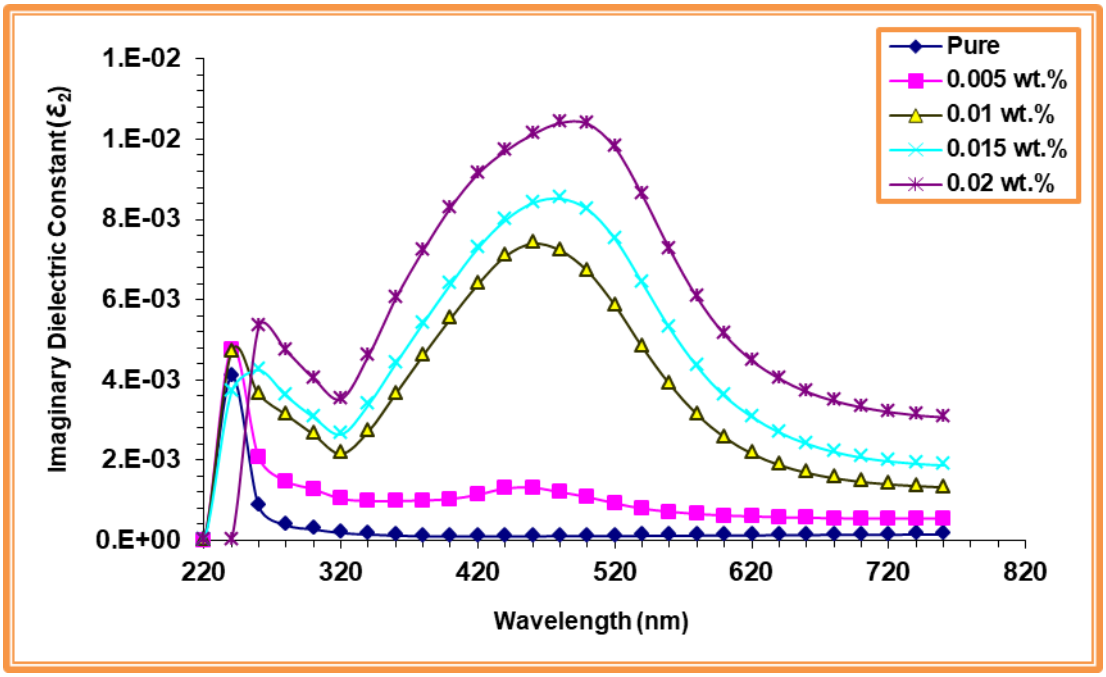

Figure (4.23): Variation in the imaginary part of dielectric constant for nanocomposites (PVP-PVA-Ag_2O-NbO_2) with wavelength.

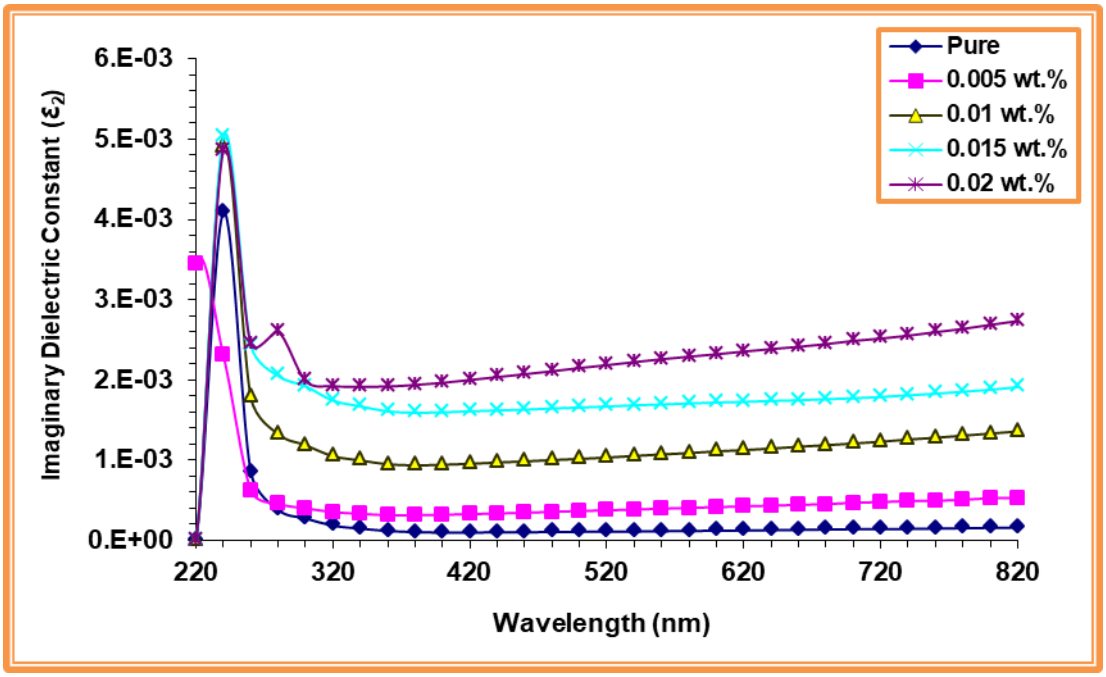

Figure (4.24): Variation in the imaginary part of dielectric constant for nanocomposites (PVP-PVA-Al_2O_3-NbO_2) with wavelength.

4.3.8 The Optical Conductivity

Figures (4.25) and (4.26) shows the variation of optical conductivity with the wavelength of nanocomposites respectively. The figure shows that the optical conductivity of all samples of nanocomposites are decreased with the increasing of the wavelength, this behavior attributed to the optical conductivity depends strongly on the wavelength of the radiation incident on the samples of (PVP-PVA-Ag_2O-NbO_2) and (PVP-PVA-Al_2O_3-NbO_2) nanocomposites, the increasing of optical conductivity at small wavelength of photon is due to high absorbance of all samples of nanocomposites in that region, hence, increasing of the charge transfer excitations. The optical conductivity spectra indicated that the samples are transmittance within the visible and near infrared regions. Also, the optical conductivity of nanocomposites is increased with the increase of (Ag_2O, NbO_2) and (Al_2O_3, NbO_2) nanoparticles concentrations, this behavior related to the creation of

localized levels in the energy gap; the increase of (Ag_2O, NbO_2) and (Al_2O_3, NbO_2) nanoparticles concentration increasing the density of localized stages in the band structure, hence, increase of the absorption coefficient consequently increasing the optical conductivity of (PVP-PVA-Ag_2O-NbO_2) and (PVP-PVA-Al_2O_3-NbO_2) nanocomposites, this is similar to the results of Venkatarayappa *et al.* [189].

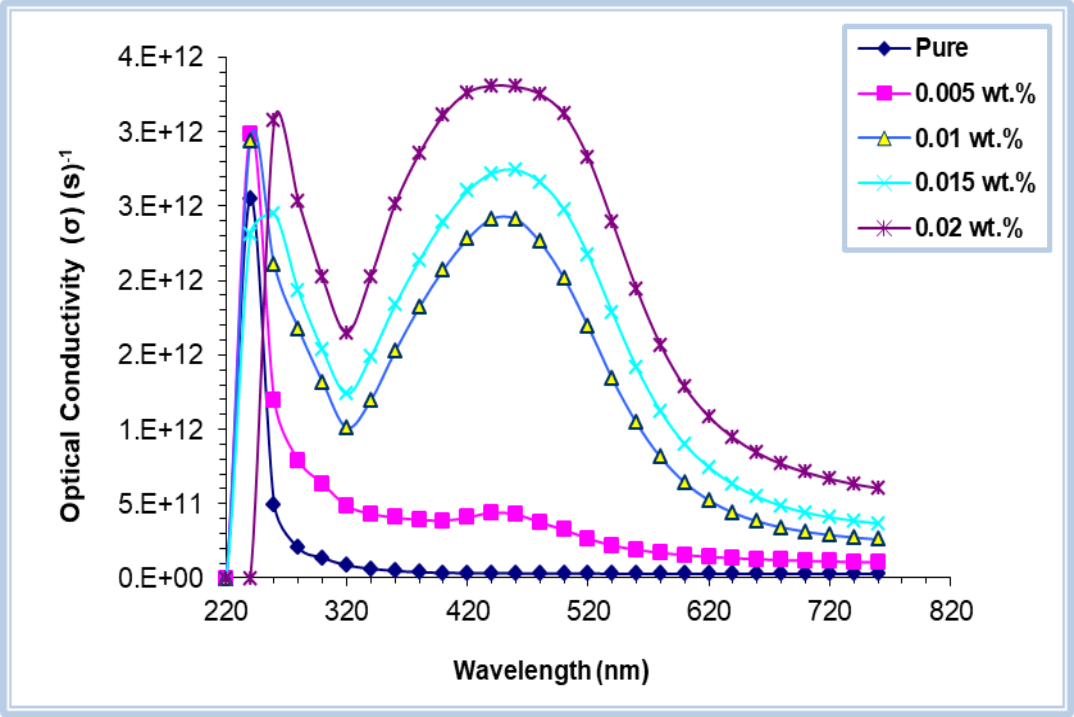

Figure (4.25): Variation of optical conductivity for (PVP-PVA-Ag_2O-NbO_2) nanocomposite with wavelength.

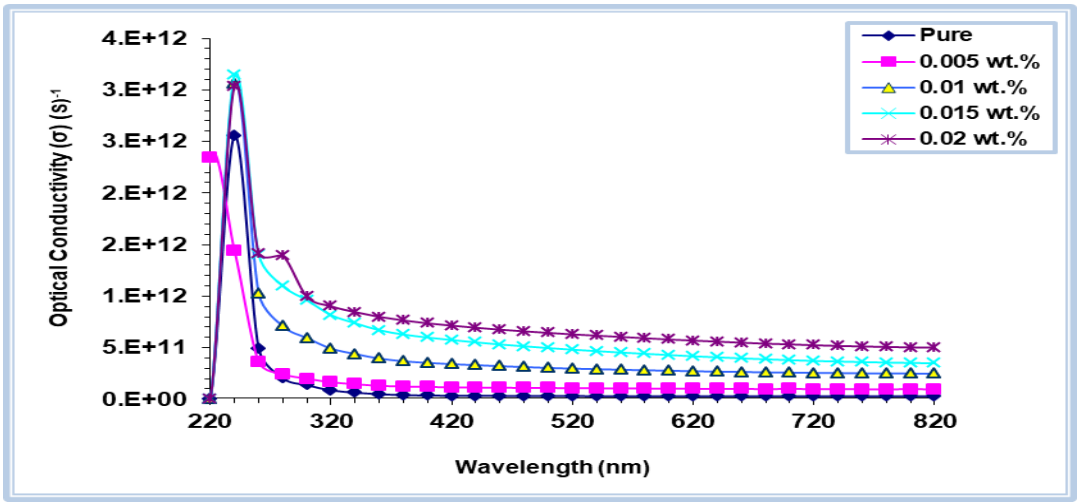

Figure (4.26): Variation of optical conductivity for (PVA-PVP-Al_2O_3-NbO_2) nanocomposite with wavelength.

4.4 The A.C Electrical Properties

The A.C electrical properties of (PVP-PVA-Ag_2O-NbO_2) and (PVP-PVA-Al_2O_3-NbO_2) nanocomposites are involved dielectric constant, dielectric loss and A.C electrical conductivity were studied in frequency range (100-5×10^6) Hz at room temperature.

4.4.1 The Dielectric Constant

Figures (4.27) and (4.28) show the variation of the dielectric constant of (PVP-PVA-Ag_2O-NbO_2) and (PVP-PVA-Al_2O_3-NbO_2) nanocomposites with frequency, respectively. As shown in the figures, the dielectric constant of all prepared nanocomposites decreases with the increase in the frequency of the applied electric field. At low frequencies (10^3 Hz), , the dielectric constant values were high. This is attributed to the decrease in the contribution of the inter polarization compared to the total polarization because the inter polarization is more important at (1 MHz). We note a decrease in the dielectric constant at high frequencies due to ionic and electronic polarization. At (4 MHz), we notice a peak in the result of the Maxwell-Wagner phenomenon. As well as we conclude from the dielectric constant that it can be applied in batteries because it has a high storage capacity. The charge carriers have difficulty orienting themselves in the field direction as a consequence of the reduction in values of the dielectric constant. At a low concentration of (Ag_2O, NbO_2) and (Al_2O_3, NbO_2) nanoparticles, the dielectric constant was weak. The dielectric constant was increased with increase in the concentrations of (Ag_2O, NbO_2) and (Al_2O_3, NbO_2) nanoparticles with an abundance of functional groups. The results showed that the concentration is best of (0.02 wt.%) have higher the dielectric constant of (PVP-PVA-Al_2O_3-NbO_2) nanocomposites, this is similar with the result of Hashim and Hadi [190].

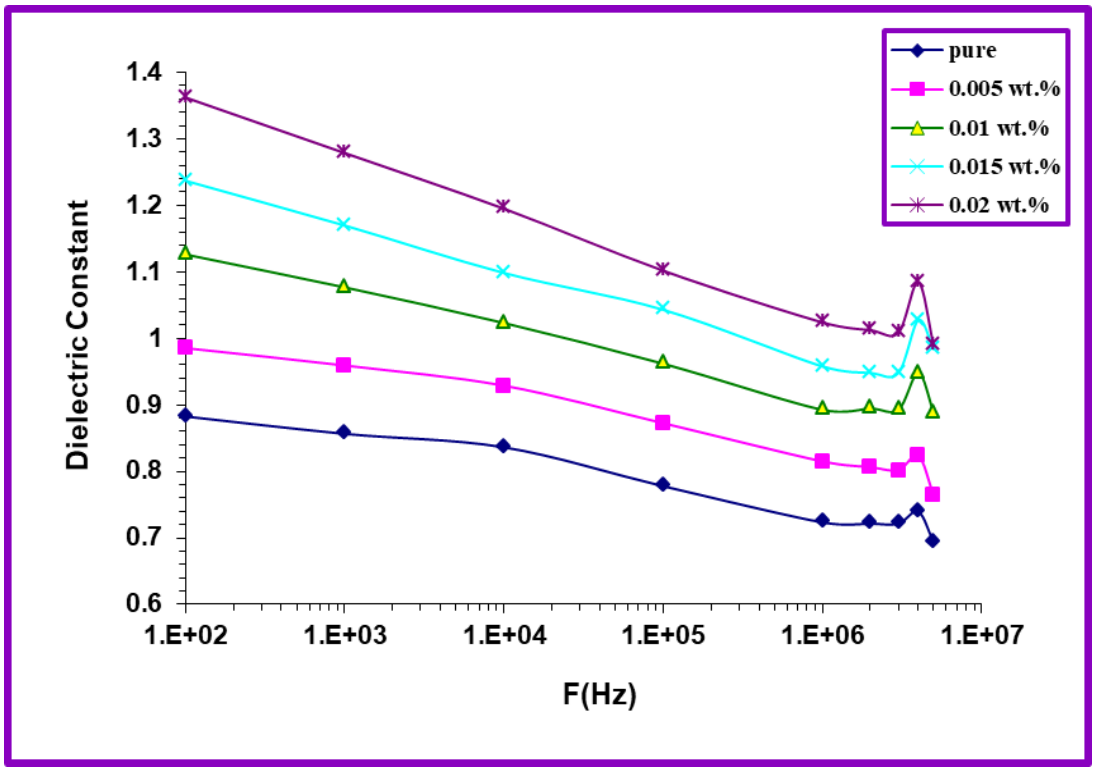

Figure (4.27): The variance in the value of the dielectric constant (ε') with the frequency of nanocomposites (PVP-PVA-Ag_2O-NbO_2) at room temperature.

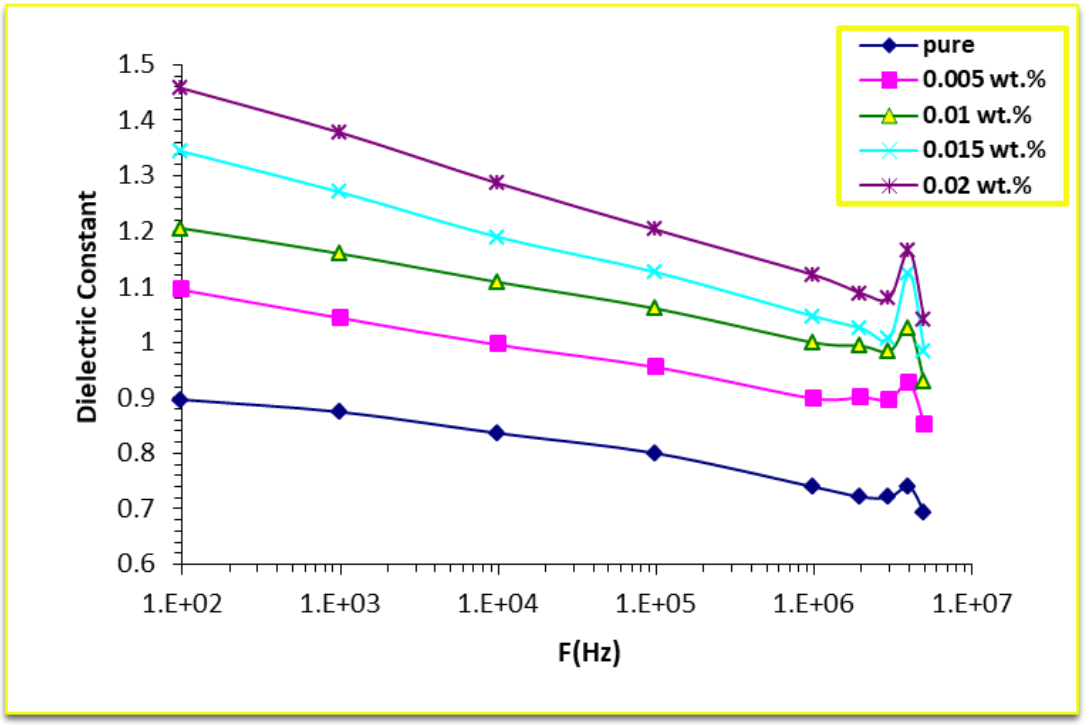

Figure (4.28): The variance in the value of the dielectric constant (ε') with the frequency of nanocomposites (PVP-PVA-Al_2O_3-NbO_2) at room temperature.

The effect of concentrations for (Ag_2O and NbO_2) and (Al_2O_3 and NbO_2) nanoparticles on dielectric constant of (PVP-PVA-Ag_2O-NbO_2) and (PVP-PVA-Al_2O_3-NbO_2) nanocomposites are shown in figures (4.29) and (4.30) respectively at 100Hz. The dielectric constant of nanocomposites can be calculated by equation (2-14). The figures show that the dielectric constant of (PVP-PVA-Ag_2O-NbO_2) and (PVP-PVA-Al_2O_3-NbO_2) nanocomposites increases with the increasing of the concentrations for (Ag_2O and NbO_2) and (Al_2O_3 and NbO_2) nanoparticles. This behavior can be explained by interfacial polarization inside nanocomposites in the applied alternating electric field and increasing of the charge carriers. The dielectric constant of (PVP-PVA-Ag_2O-NbO_2) and (PVP-PVA-Al_2O_3-NbO_2) nanocomposites at 0.02 wt.% of (Ag_2O and NbO_2) and (Al_2O_3 and NbO_2) nanoparticles concentration is higher due to the high dielectric constant value of (Ag_2O and NbO_2) and (Al_2O_3 and NbO_2) nanoparticles. When the concentration of nanoparticles increased, the capacity of the material that storing the charge was increased, so the nanocomposities can be used in electronic devices. The results showed that the concentration is best of (0.02 wt.%) have higher the dielectric constant of (PVP-PVA-Al_2O_3-NbO_2) nanocomposites, this is similar to the result of Habeeb *et al.* [191].

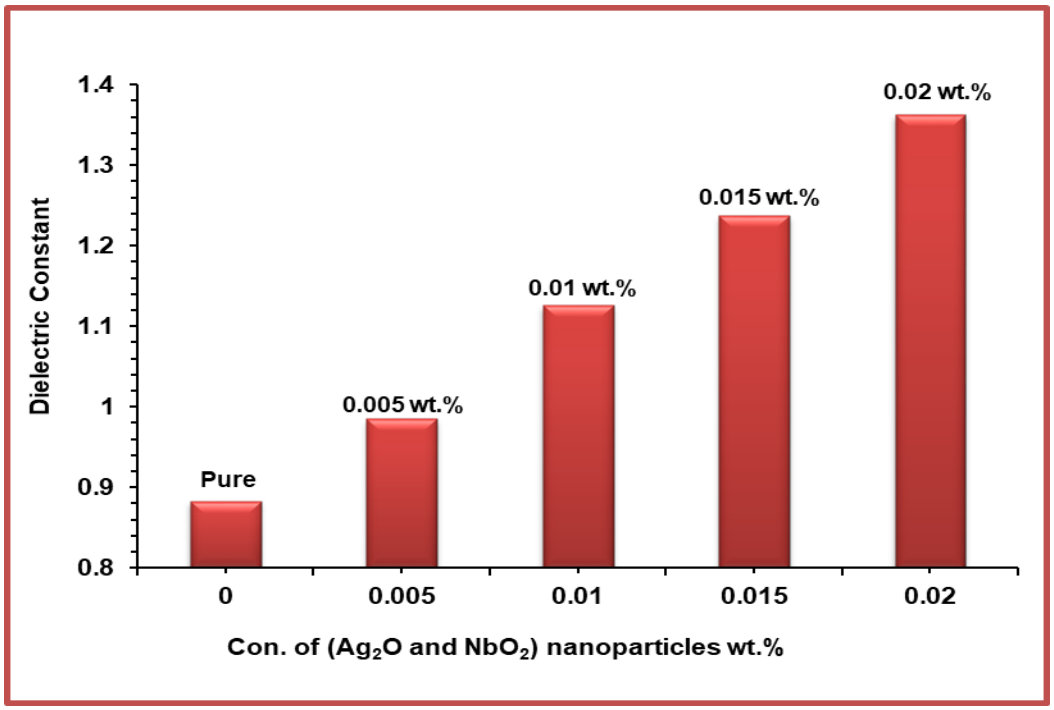

Figure (4.29): Effect of concentrations of nanoparticles (Ag_2O and NbO_2) on the dielectric constant.

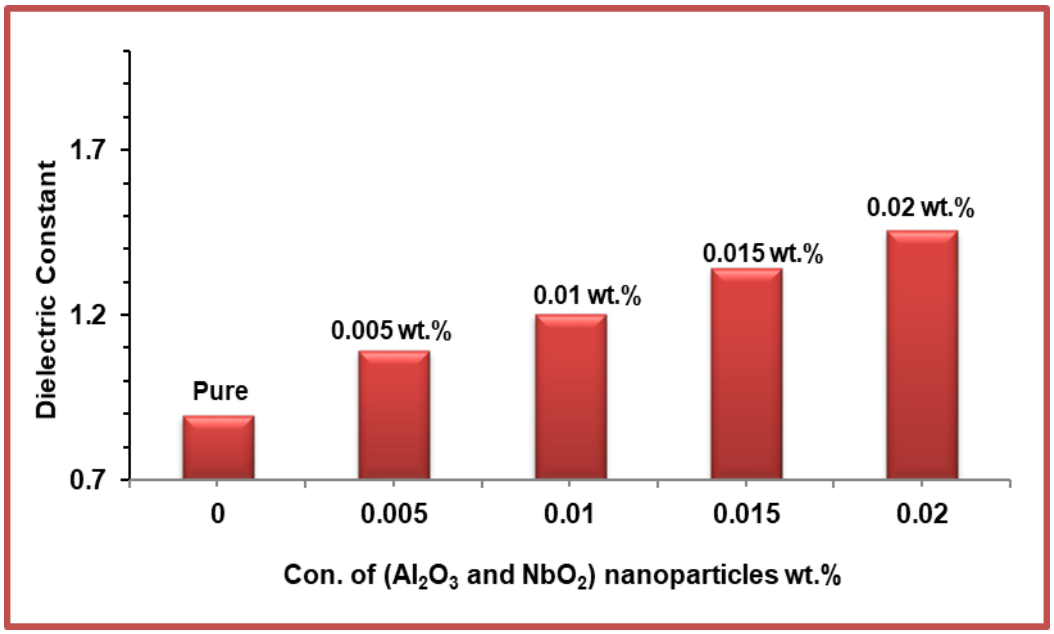

Figure (4.30): Effect of concentrations of nanoparticles (Al_2O_3 and NbO_2) on the dielectric constant.

4.4.2 The Dielectric Loss

Figures (4.31) and (4.32) respectively illustrated the dielectric loss against the frequency of (PVP-PVA), (PVP-PVA-Ag_2O-NbO_2) and (PVP-PVA-Al_2O_3-NbO_2) nanocomposites. The figures demonstrates the decreasing of dielectric loss values of nanocomposite with a rise in the frequency of applied electrical field. This activity has exhibited the reduction in the contribution of space charge polarization and the dielectric loss, also exhibited a high result of dielectric loss for the samples with low frequency, which is decreased with the increasing in the frequency. At (4 MHz), we notice a peak in the result of the Maxwell-Wagner phenomenon. Whereas, the use of (Ag_2O, NbO_2) and (Al_2O_3-NbO_2) nanoparticles significantly improves the dielectric loss of nanocomposite (PVP-PVA-Ag_2O-NbO_2) and (PVP-PVA-Al_2O_3-NbO_2) nanocomposites with increasing the loading ratio of (Ag_2O, NbO_2) and (Al_2O_3-NbO_2) nanoparticles, which is associated with an increase in the number of the charge carrier's. Through the values of dielectric loss, we observed values less than the dielectric constant, thus obtaining materials that have a high storage capacity and less loss. Based on the results, nanocomposites can be used in the manufacture of electronic devices with high storage capacities, this is similar to the result of researchers [192].

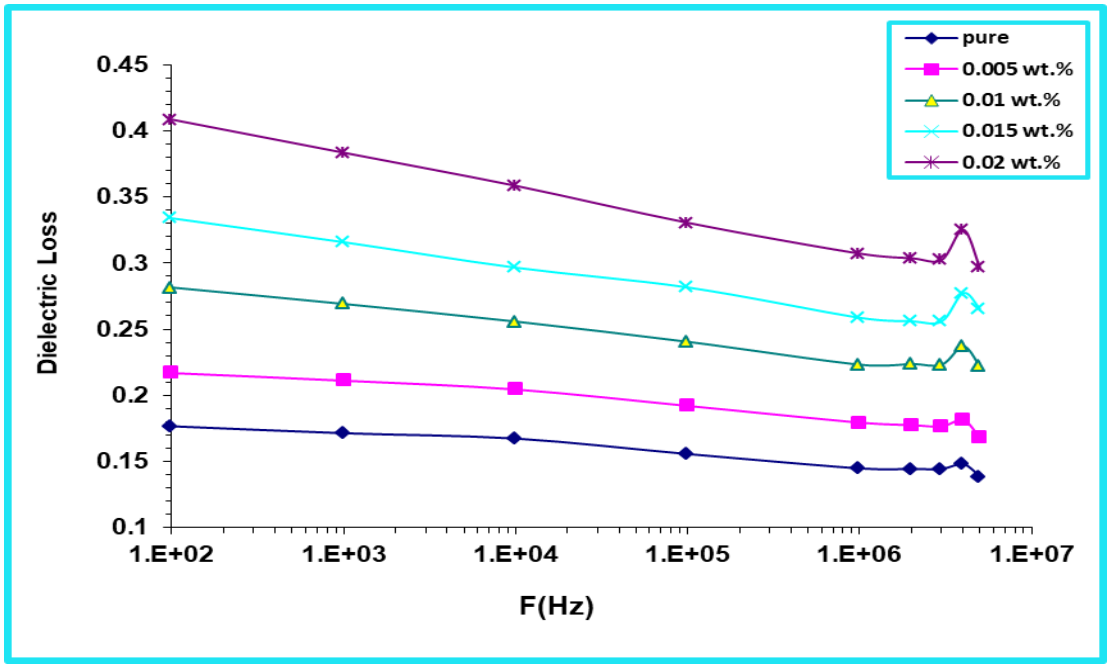

Figure (4.31): The variant of dielectric loss (ε'') with the frequency of nanocomposites (PVP-PVA-Ag_2O-NbO_2) at room temperature.

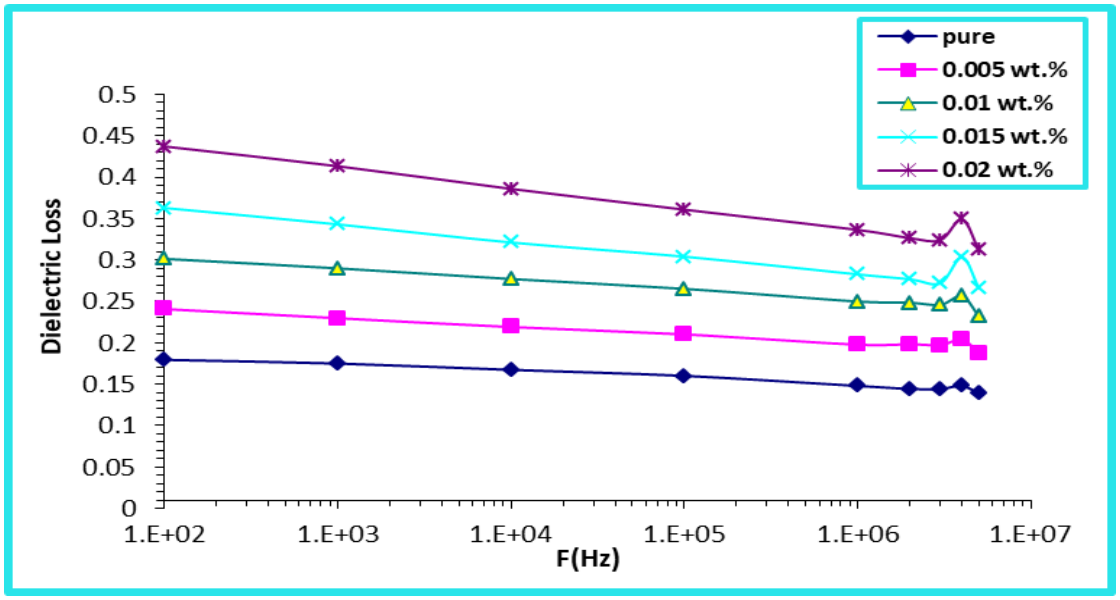

Figure (4.32): The variant of dielectric loss (ε'') with the frequency of nanocomposites (PVP-PVA-Al_2O_3-NbO_2) at room temperature.

Figures (4.33) and (4.34) show the effect of (Ag_2O and NbO_2) and (Al_2O_3 and NbO_2) nanoparticles concentrations on dielectric loss for (PVP-PVA-Ag_2O-NbO_2) and (PVP-PVA-Al_2O_3-NbO_2) nanocomposites respectively at 100Hz. The dielectric loss of nanocomposites is measured by using the equation (2-15). As shown in the figures, the value of dielectric loss of nanocomposites increases with the increase the concentrations of (Ag_2O and NbO_2) and (Al_2O_3 and NbO_2) nanoparticles. The increases of dielectric loss value of (PVP-PVA) blends, (PVP-PVA-Ag_2O-NbO_2) and (PVP-PVA-Al_2O_3-NbO_2) with increasing the concentrations of (Ag_2O and NbO_2) and (Al_2O_3 and NbO_2) nanoparticles attributed to the increases of the number of charge carriers for (PVP-PVA-Ag_2O-NbO_2) and (PVP-PVA-Al_2O_3-NbO_2) nanocomposites, , this is similar with the results of Hamzah *et al.* [193].

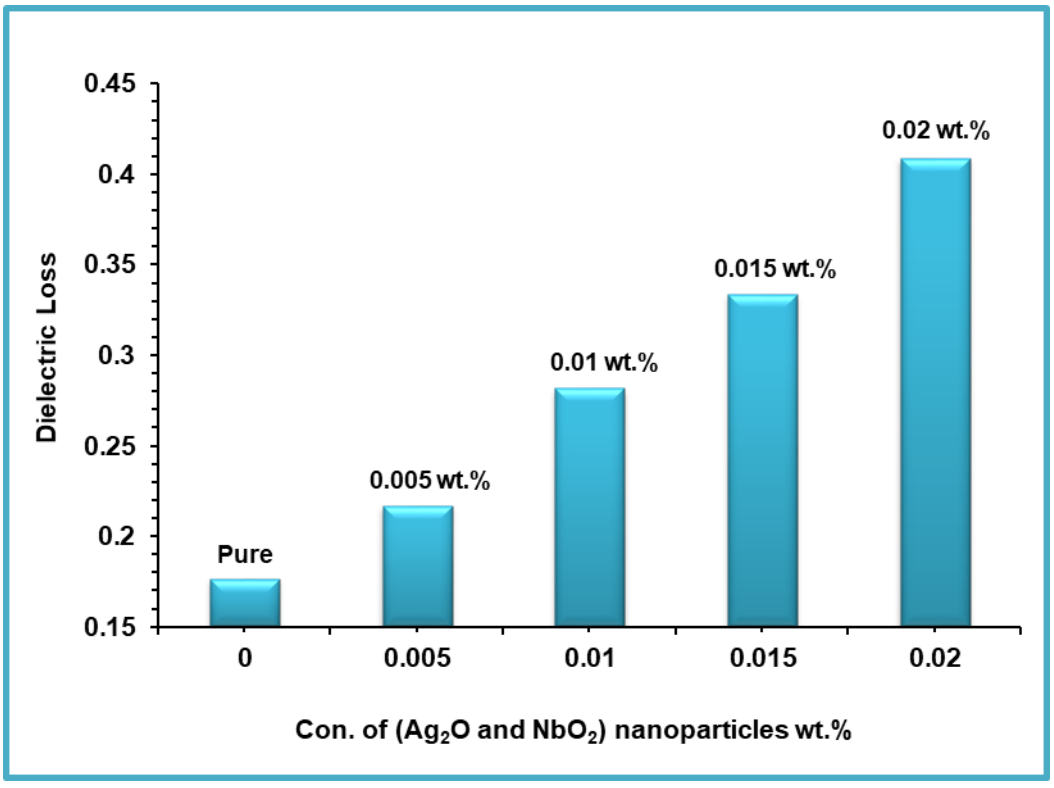

Figure (4.33): Effect the concentrations of (Ag_2O and NbO_2) NPs on dielectric loss at 100Hz.

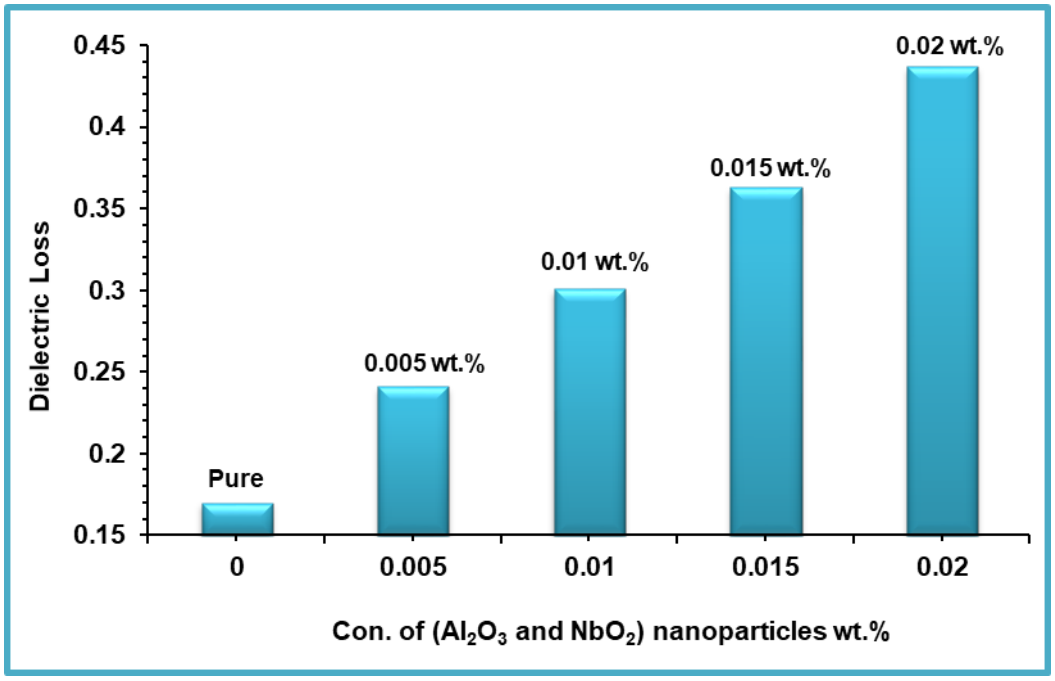

Figure (4.34): Effect the concentrations of (Al_2O_3 and NbO_2) NPs on dielectric loss at 100Hz.

4.4.3 The A.C Electrical Conductivity

Figures (4.35) and (4.36) show A.C electrical conductivity with frequency for (PVP-PVA-Ag_2O-NbO_2) and (PVP-PVA-Al_2O_3-NbO_2) nanocomposites. The conductivity is shown in this figure rises as a frequency rises, it can be attributable to increase the number of charge carriers transmitted by the hopping mechanism, and consequently, by increasing the frequency, the mobility of charge carriers and their number increases. In the low frequency, more charge accumulation occurred at the electrode and electrolyte interface, leading to a decrease in the number of the ionization processes for Ag_2O, Al_2O_3 and NbO_2 nanoparticles and oxygen vacancies for (PVP-PVA) blend. As high frequency region; the mobility of charge carriers was higher. Hence the electrical conductivity increases with frequency for (PVP-PVA-Al_2O_3-NbO_2) and (PVP-PVA-Ag_2O-NbO_2) nanocomposites. The prepared nanocomposites can be applied in various electronic devices, this is similar with the results of Bohara *et al.* [194].

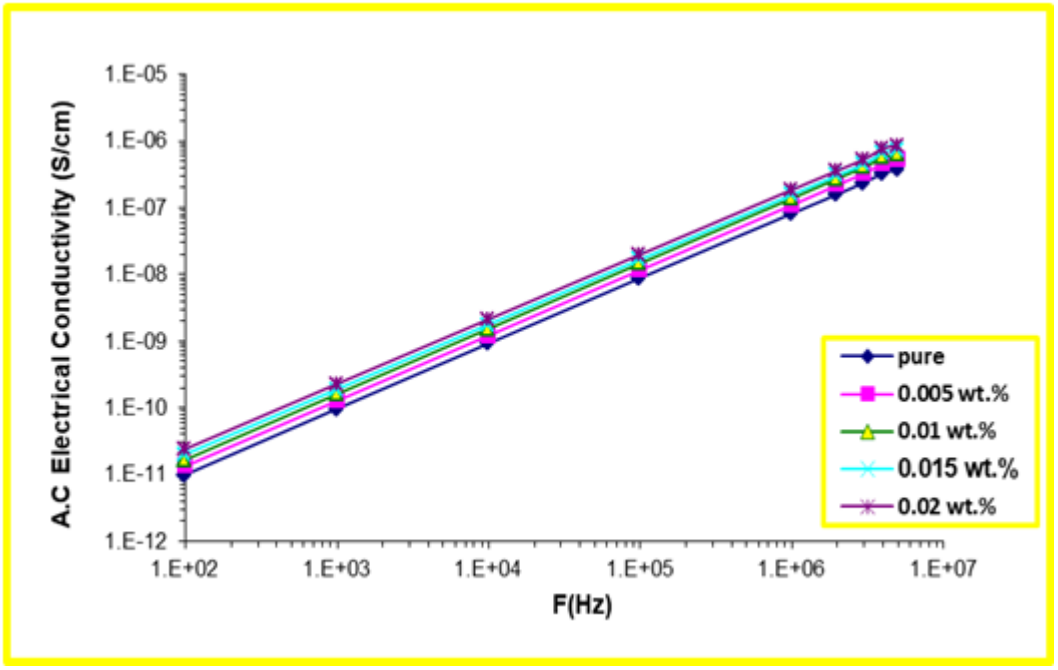

Figure (4.35): The σ A.C. variation with frequency of (PVP- PVA- Ag_2O-NbO_2) nanocomposites at room temperature.

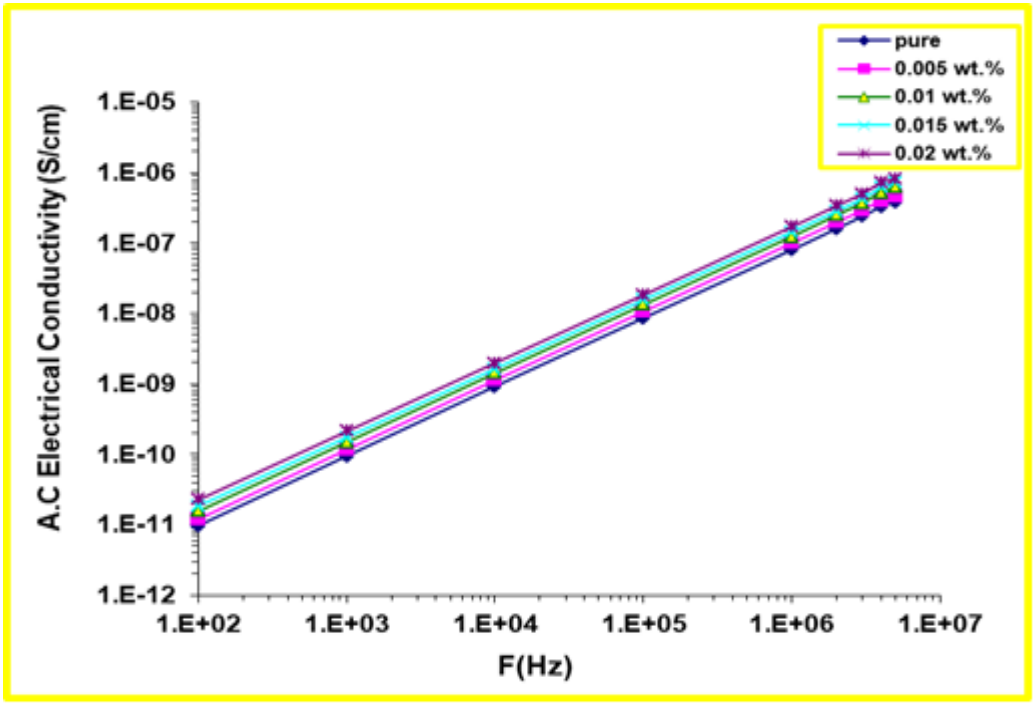

Figure (4.36): The σ A.C. variation with frequency of (PVP- PVA- Al_2O_3-NbO_2) nanocomposites at room temperature.

Figure (4.37) and (4.38) depicts the impact of the weight percentages of (Ag_2O, Al_2O_3 and NbO_2) nanoparticles on σ A.C for nanocomposites (PVP-PVA-Ag_2O-NbO_2) and (PVP-PVA-Al_2O_3-NbO_2). The conductivity is shown in this figure rises as a frequency rises, it can be attributable to polarization and hopping's impact. When a ratio of the (Ag_2O, Al_2O_3) and (Ag_2O, NbO_2) nanoparticles is increased, the conductivity of (PVP-PVA) increases. This is because conducting charge carriers have a hopping mechanism. Where with increasing weight percentages of (Ag_2O, Al_2O_3 and NbO_2) nanoparticles, the σ A.C of nanocomposites increases. This is because in nanocomposites, a rise in the number of charge carriers, this is similar with the results of Hashim and Habeeb [195].

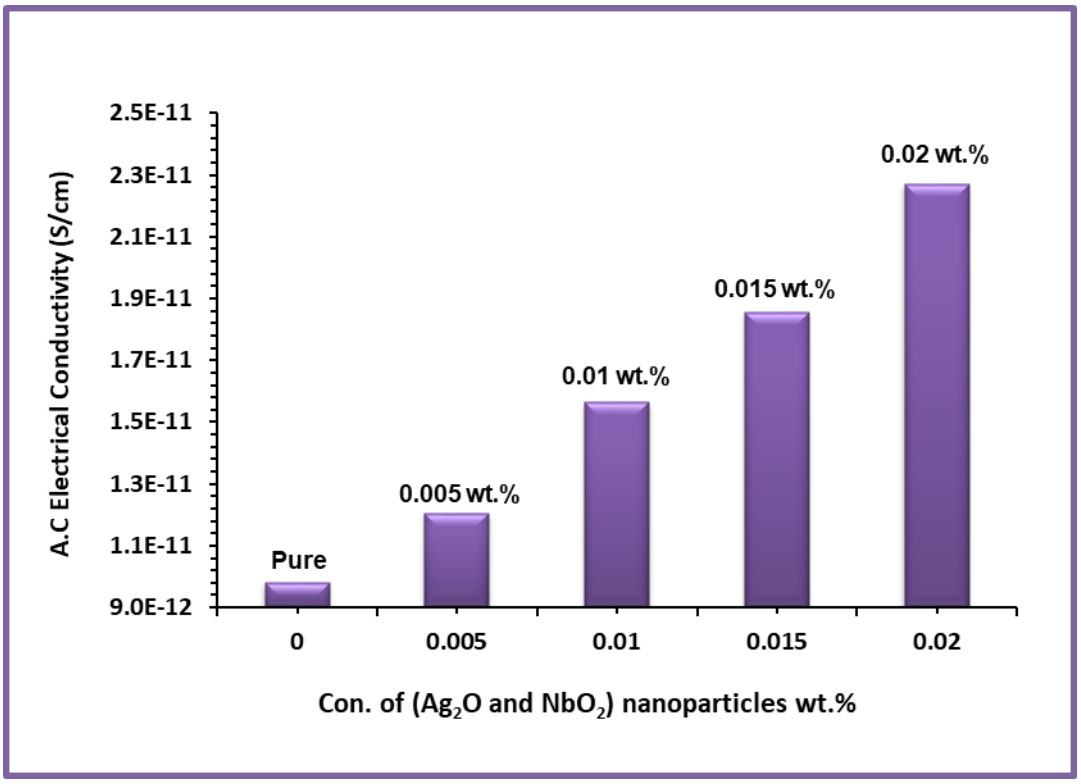

Figure (4.37): Effect of ($Ag_2O$and NbO_2) nanoparticles concentrations on A.C electrical conductivity for (PVP-PVA-Ag_2O_3-NbO_2) nanocomposites at 100Hz.

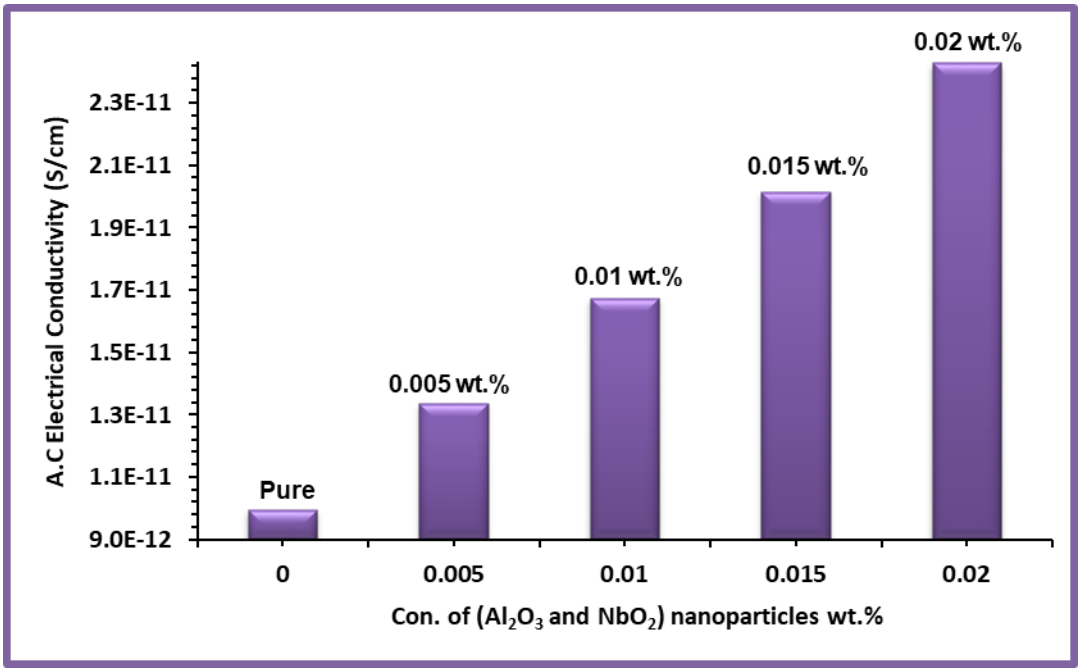

Figure (4.38): Effect of (Al_2O_3 and NbO_2) nanoparticles concentrations on A.C electrical conductivity for (PVP-PVA-Al_2O_3-NbO_2) nanocomposites at 100Hz.

4.5 Application for Antibacterial Activity

The antibacterial activity of the (PVP-PVA-Ag_2O-NbO_2) and (PVP-PVA-Al_2O_3-NbO_2) samples tested against gram positive (*S. aureus* and *E. fecials*) and gram negative (*E. coli* and *K. pneumonia*) as shown in images (4.39), (4.40) Figures (4.41 to 4.48) and tables (4.5) and (4.6). From the figures and tables, the inhibition zone increases with increase in (Ag_2O-Al_2O_3-NbO_2) nanoparticles concentrations. The reason for the antibacterial activity of (PVP-PVA-Ag_2O-NbO_2) and (PVP-PVA-Al_2O_3-NbO_2) nanocomposites may be due to the presence of reactive oxygen species (ROS) generated with different concentration of (Ag_2O and NbO_2) and (Al_2O_3 and NbO_2) nanoparticles. Chemical interaction between hydrogen peroxide and membrane proteins could be the reason for the antibacterial activity of nanocomposites. The hydrogen peroxide produced enters the cell membrane of bacteria and kills them. The other possible mechanism of action is that the (Ag_2O and NbO_2) and (Al_2O_3

and NbO_2) nanoparticles in nanocomposites are carrying the positive charges and the microbes are having the negative charges which create the electromagnetic attraction between the nanoparticles and the microbes. When the attraction is made, the microbes get oxidized and die instantly. The results indicated that (PVP-PVA-Ag_2O-NbO_2) and (PVP-PVA-Al_2O_3-NbO_2) films possessed a strong antibacterial activity with the increase in the weight percentages of (Ag_2O and NbO_2) and (Al_2O_3 and NbO_2) nanoparticles, this is similar with the results of Prabhu *et al.* [196], kumar and krishnan [197] and Khandanlou *et al.* [198].

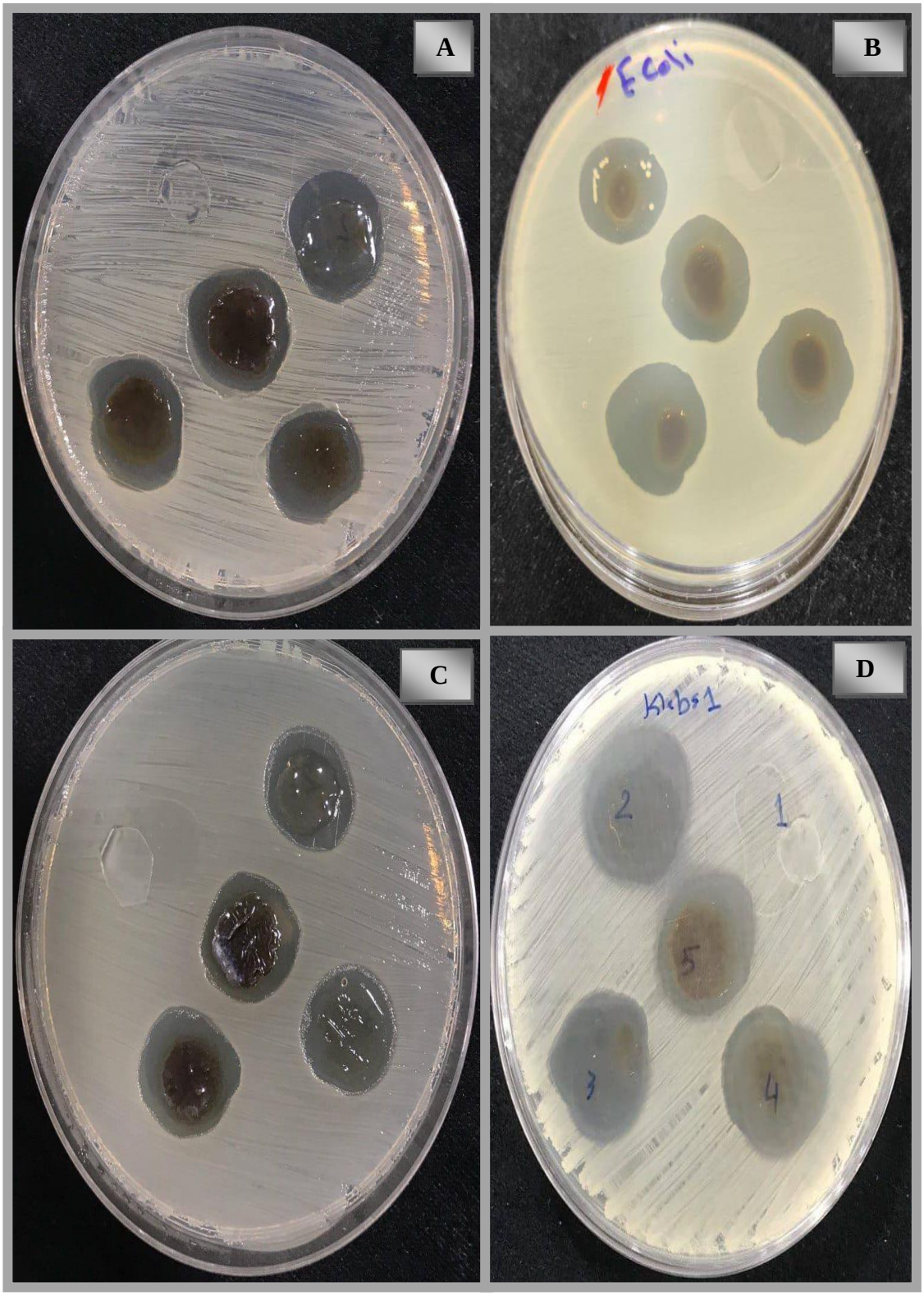

Figure (4.39): Images of (PVP-PVA-Ag_2O-NbO_2) nanocomposites anti-bacterial against: (A) *S. aureus*, (B) *E. coli*, (C) *E. faecalis* and (D) *K. pnenmoniae*.

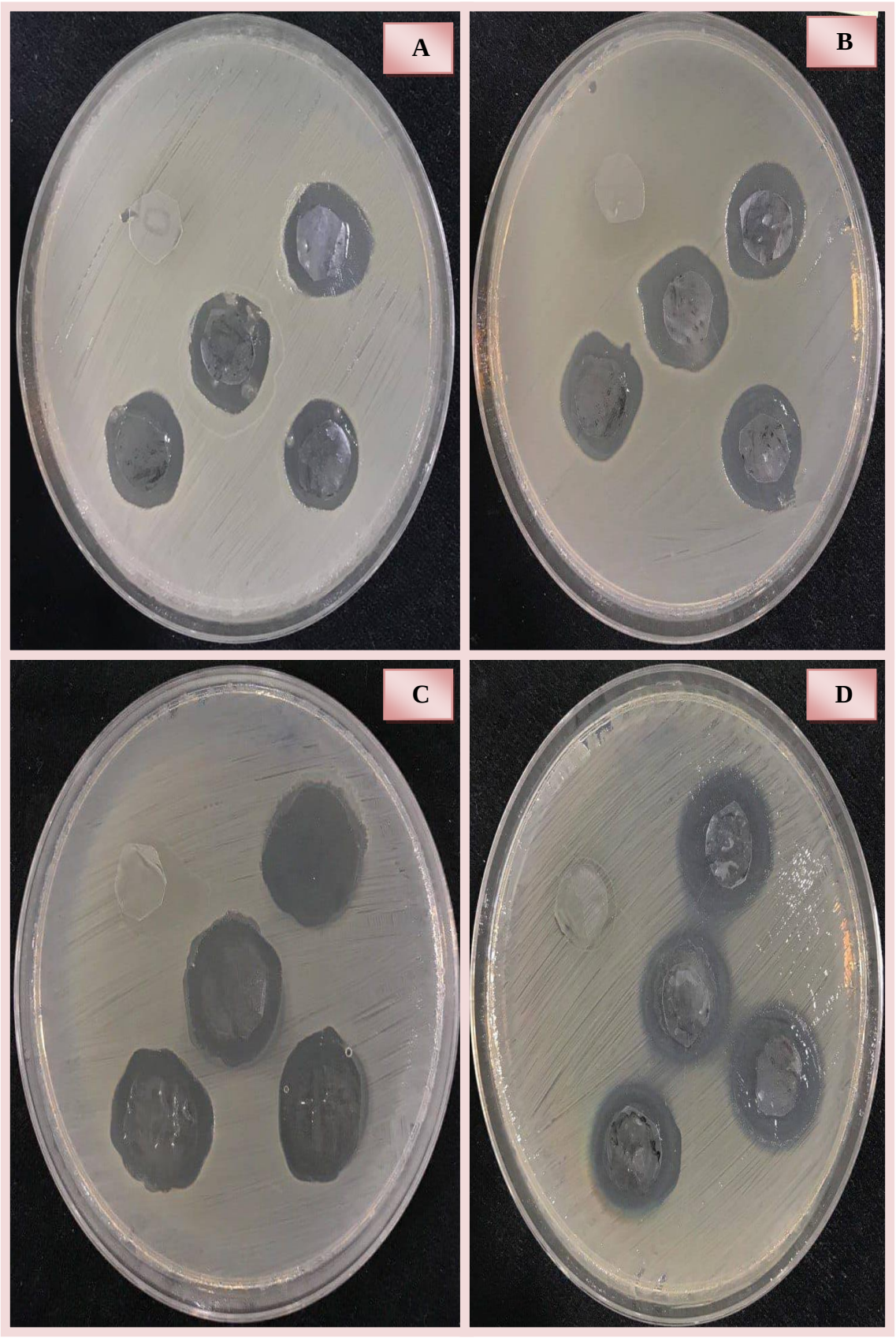

Figure (4. 40): Images of (PVP-PVA-Al_2O_3-NbO_2) nanocomposites anti-bacterial against: (A) *S. aureus*, (B) *E. coli*, (C) *E. faecalis* and (D) *K. pnenmoniae*.

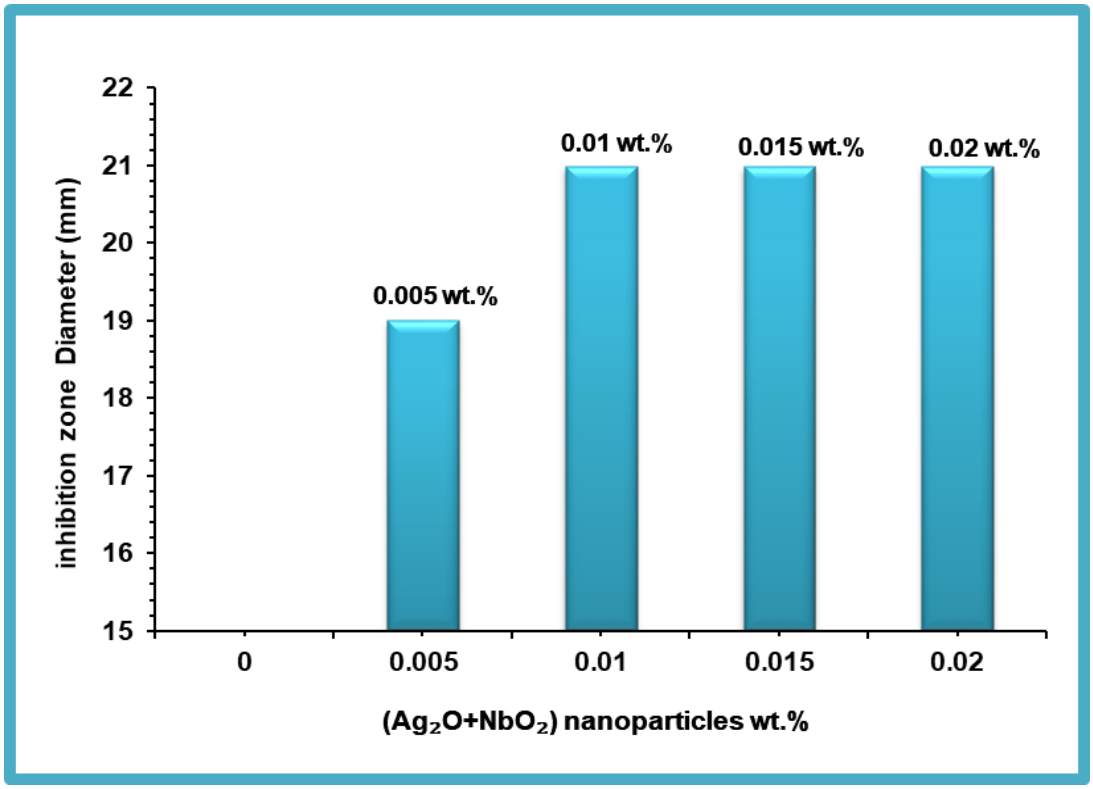

Figure(4.41): Antibacterial effect of (PVP-PVA) blend as a function of (Ag_2O and NbO_2) NPs concentrations on *S. aureus*.

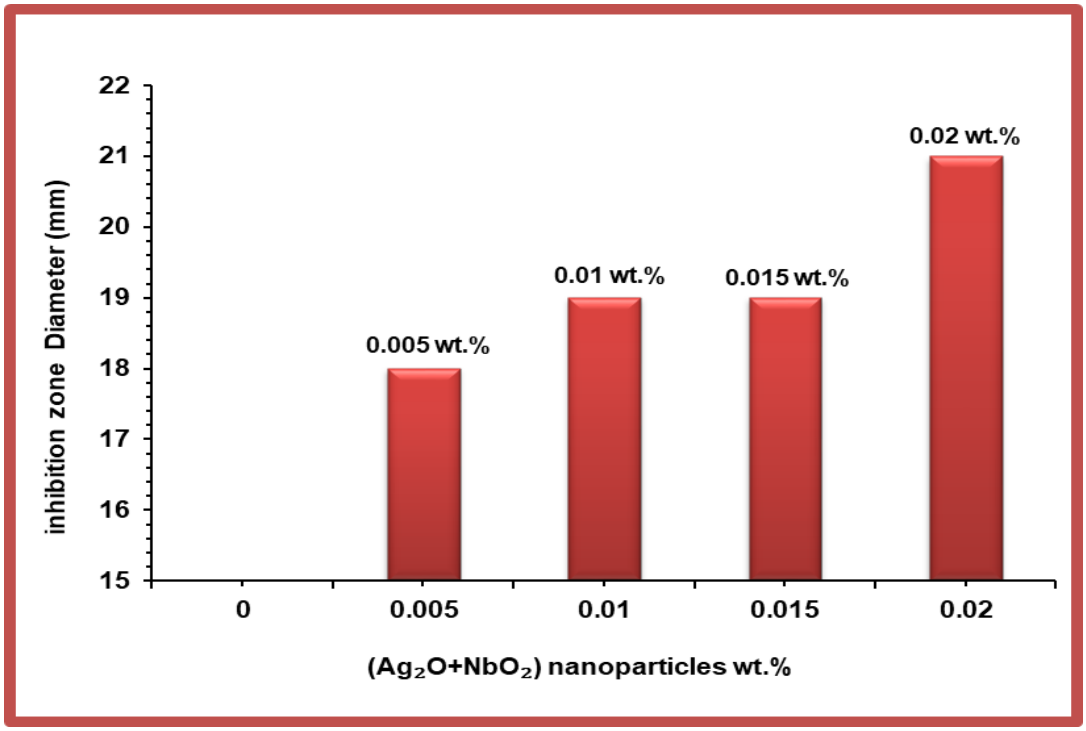

Figure(4.42): Antibacterial effect of (PVP-PVA) blend as a function of (Ag_2O and NbO_2) NPs concentrations on *E. coli*.

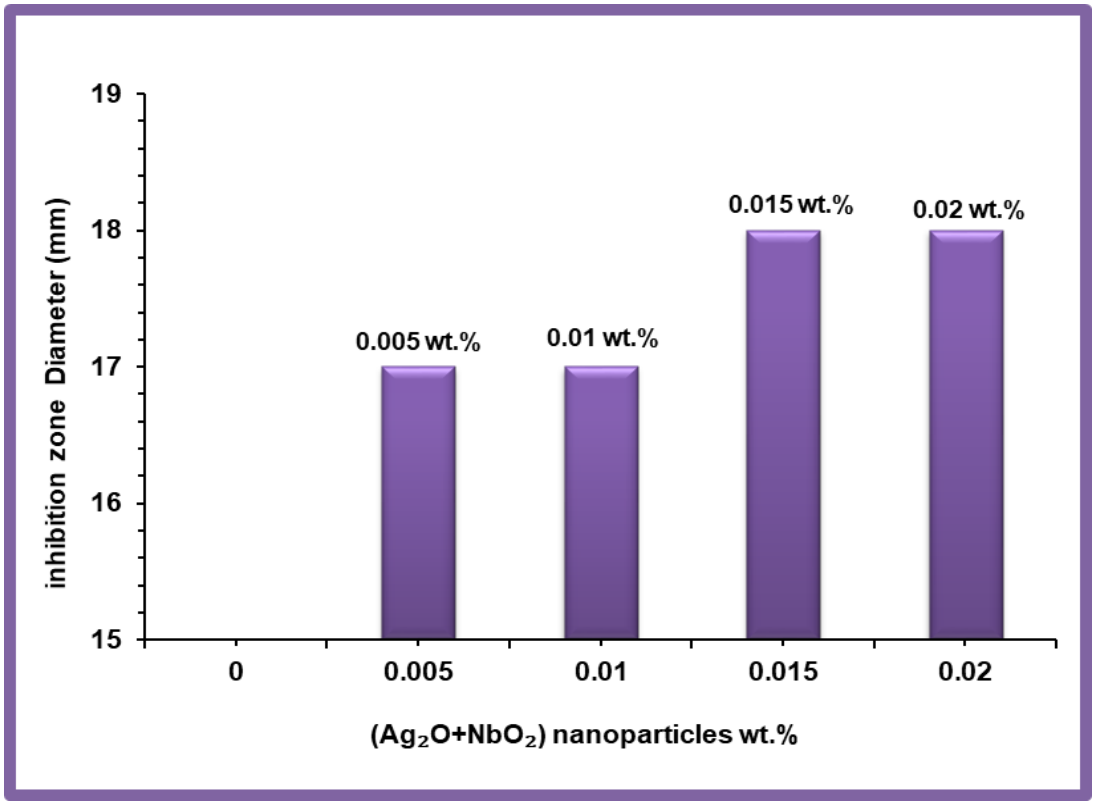

Figure(4.43): Antibacterial effect of (PVP-PVA) blend as a function of (Ag_2O and NbO_2) NPs concentrations on *E. facials*.

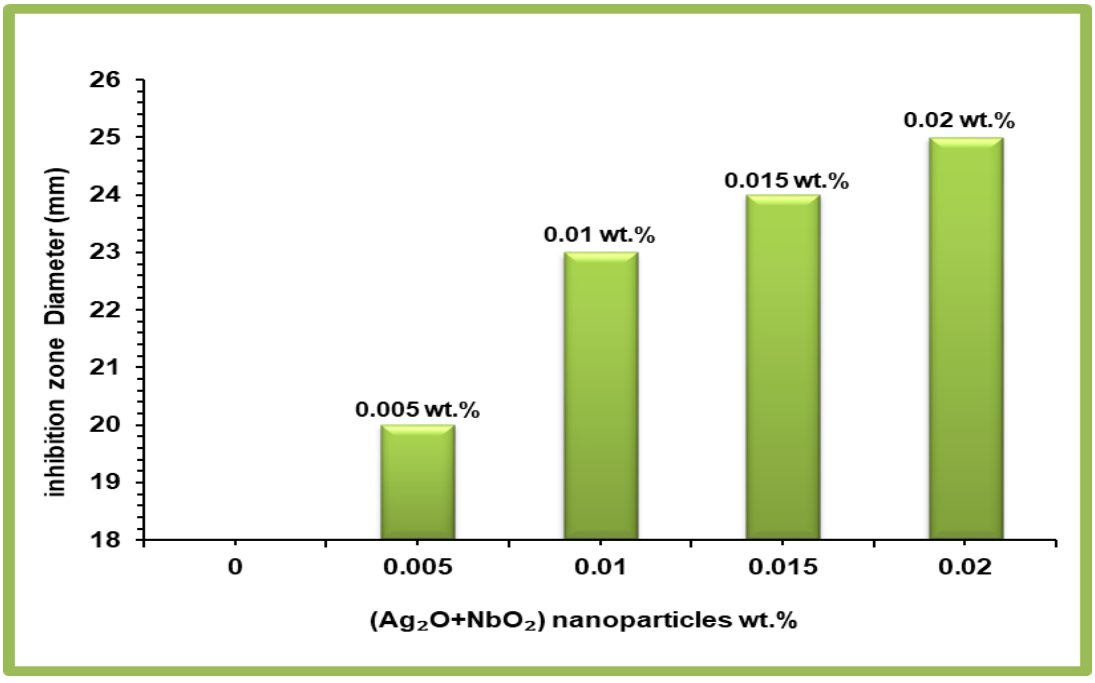

Figure(4.44): Antibacterial effect of (PVP-PVA) blend as a function of (Ag_2O and NbO_2) NPs concentrations on *K. pneumonia*.

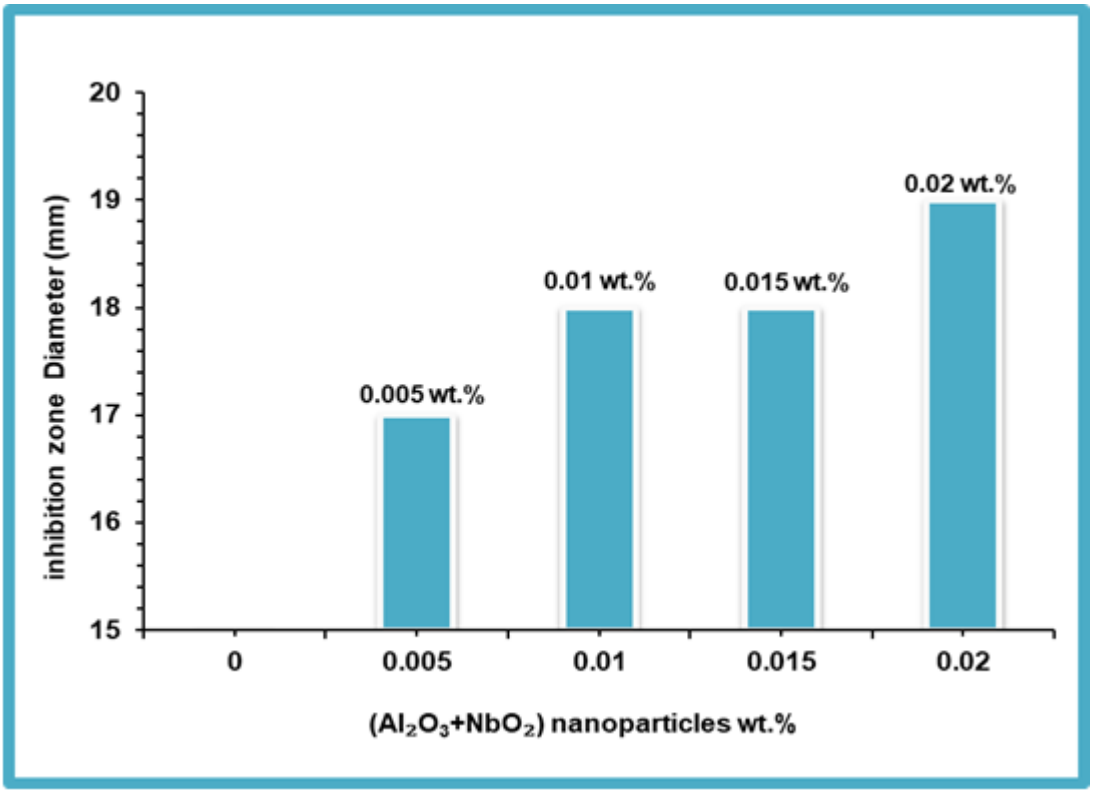

Figure(4.45): Antibacterial effect of (PVP-PVA) blend as a function of (Al_2O_3 and NbO_2) NPs concentrations on *S. aureus*.

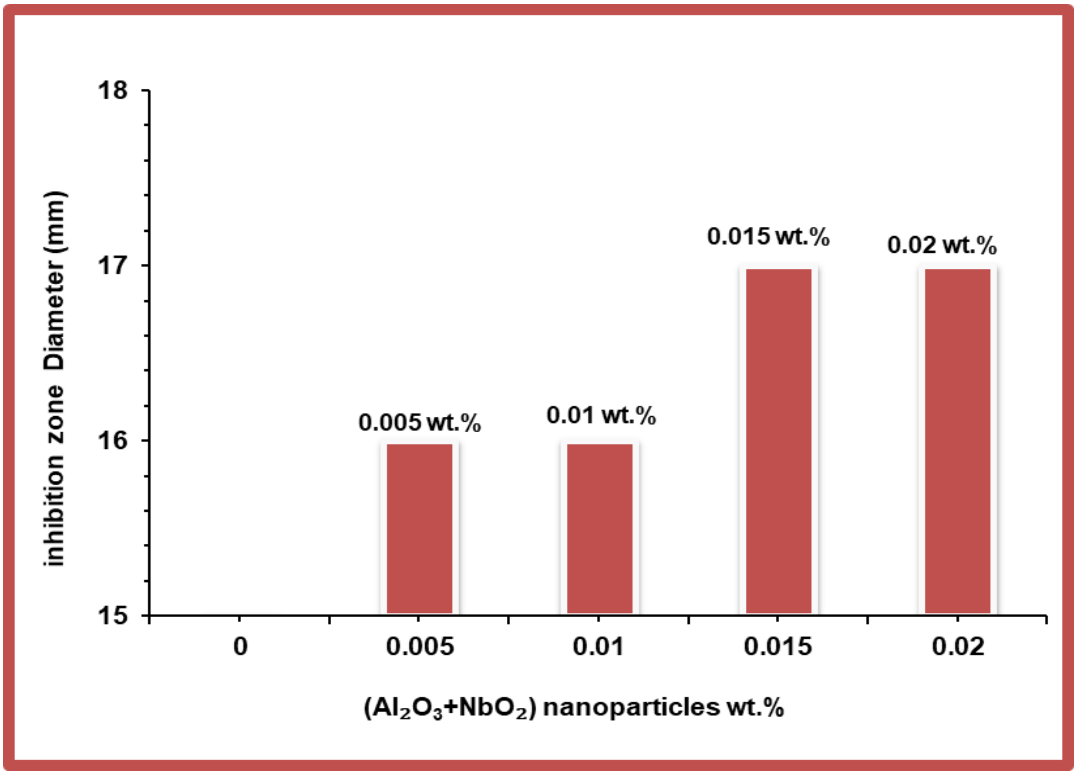

Figure(4.46): Antibacterial effect of (PVP-PVA) blend as a function of (Al_2O_3 and NbO_2) NPs concentrations on *E. coli*.

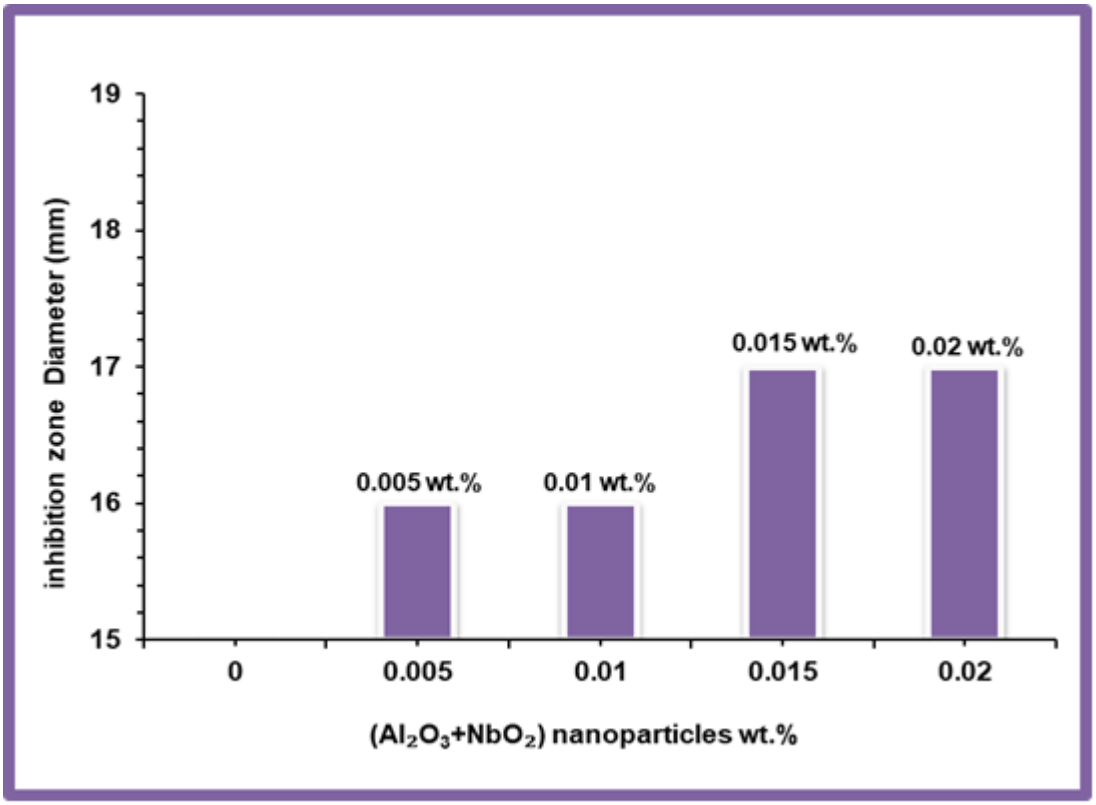

Figure(4.47): Antibacterial effect of (PVP-PVA) blend as a function of (Al_2O_3 and NbO_2) NPs concentrations on *E. facials*.

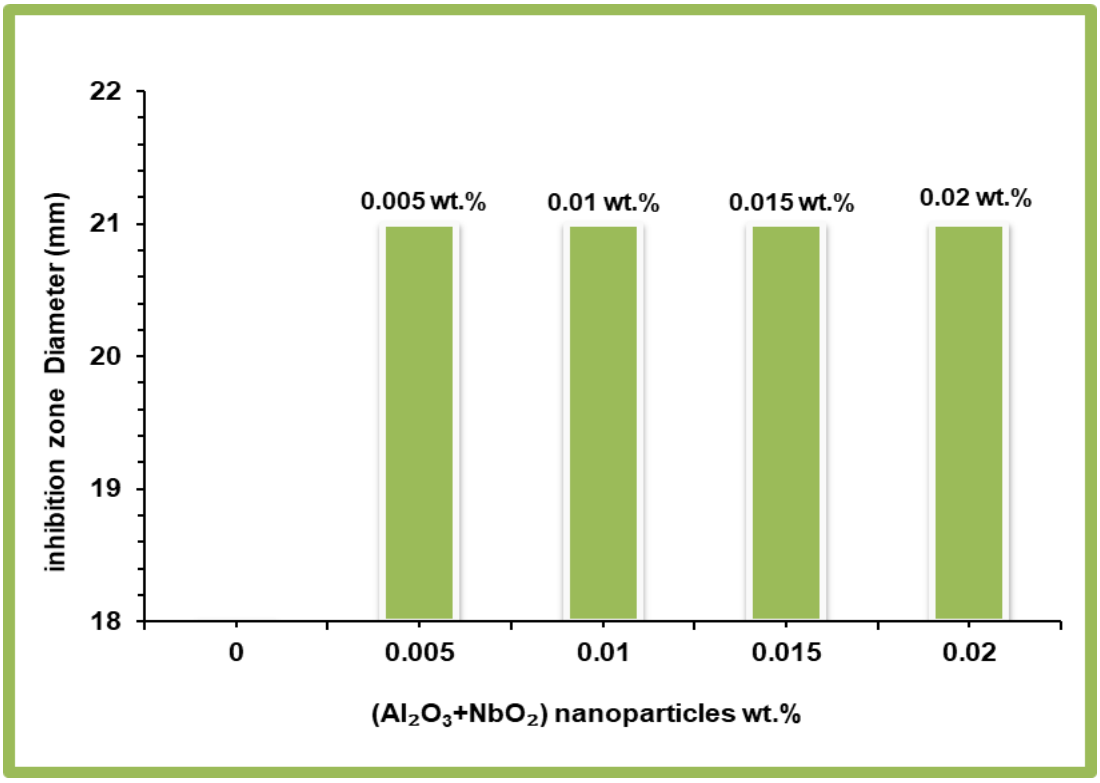

Figure(4.48): Antibacterial effect of (PVP-PVA) blend as a function of (Al_2O_3 and NbO_2) NPs concentrations on *K. pnenmoniae*.

Table (4.5): The diameter of inhibition zone for (PVP-PVA-Ag_2O-NbO_2) nanocomposites anti-bacterial against: (*S. aureus*, *E. coli*, *E. faecalis* and *K. pnenmoniae*.

con.	*S. aureus* (mm)	*E. coli* (mm)	*E. faecalis* (mm)	*K. pnenmoniae* (mm)
0	0	0	0	0
0.005	19	18	17	20
0.01	21	19	17	23
0.015	21	19	18	24
0.02	21	21	18	25

Table (4.6): The diameter of inhibition zone for (PVP-PVA-Al_2O_3-NbO_2) nanocomposites anti-bacterial against: (S. aureus, E. coli, E. faecalis and K. pnenmoniae.

con.	*S. aureus* (mm)	*E. coli* (mm)	*E. faecalis* (mm)	*K. pnenmoniae* (mm)
0	0	0	0	0
0.005	17	21	16	21
0.01	18	21	16	21
0.015	18	22	17	21
0.02	19	22	17	21

Chapter Five

Conclusions and Future Works

5.1 Conclusions

1. The optical properties of (PVP-PVA) blend which are included (absorbance, absorption coefficient, extinction coefficient, refractive index, real and imaginary dielectric constants and optical conductivity) were improved with adding of the (Ag_2O, Al_2O_3 and NbO_2) NPs can be useful in different optical and electronic field. The results showed that concentration is best of (0.02 wt.%) also (PVP-PVA-Ag_2O-NbO_2) nanocomposites have higher absorbance of (PVP-PVA-Al_2O_3-NbO_2) nanocomposites.
2. The transmittance and energy band gap of (PVP-PVA) blend decrease with increasing the (Ag_2O, Al_2O_3 and NbO_2) nanoparticles concentrations, except energy gap for (PVP-PVA-Al_2O_3-NbO_2) increase at (0.005 wt.%).
3. The dielectric properties (dielectric constant, dielectric loss and A.C electrical conductivity) were with increase in the (Ag_2O, Al_2O_3 and NbO_2) NPs which made of (PVP-PVA-Ag_2O-NbO_2) and (PVP-PVA-Al_2O_3-NbO_2) nanocomposites are suitable for different electronic application. The results showed that concentration is best of (0.02 wt.%) have higher the dielectric properties of (PVP-PVA-Al_2O_3-NbO_2) nanocomposites.
4. The dielectric constant and dielectric loss of nanocomposites are decreased with the increase of the frequency.
5. The A.C electrical conductivity of nanocomposites is increased with increase of the frequency.

6. The inhibition zone of (PVP-PVA-Ag_2O-NbO_2) and (PVP-PVA-Al_2O_3-NbO_2) nanocomposites against *S. aureus*, *E. faecalis*, *K. pneumonia* and *E. coli* is increased with the increasing the concentrations of (Ag_2O, Al_2O_3 and NbO_2) NPs. The results showed that the (PVP-PVA-Ag_2O-NbO_2) and (PVP-PVA-Al_2O_3-NbO_2) nanocomposites may be used as coating materials for high antibacterial activity applications.

5.2 Future works

1. Studying the effect of (Ag_2O, Al_2O_3 and NbO_2) nanoparticles on thermal properties of (PVP-PVA) blend.
2. Studying the mechanical properties of (PVP-PVA-Ag_2O-NbO_2) and (PVP-PVA-Al_2O_3-NbO_2) nanocomposites.
3. Studying the A.C electrical properties of (PVP-PVA-Ag_2O-NbO_2) nanocomposites.
4. Studying the D.C electrical conductivity at different temperatures of (PVP-PVA-Ag_2O-NbO_2) nanocomposites.
5. Studying the D.C electrical conductivity at different temperatures of (PVP-PVA-Al_2O_3-NbO_2) nanocomposites.
6. Studying the dielectric properties of (PVP-PVA-Ag_2O-NbO_2) and (PVP-PVA-Al_2O_3-NbO_2) nanocomposites.
7. Studying the humidity sensors application of (PVP-PVA-Ag_2O-NbO_2) and (PVP-PVA-Al_2O_3-NbO_2) nanocomposites.

References

[1] A. Kumar, K. Kaur and S. Sharma, "Synthesis, characterization and antibacterial potential of silver nanoparticles by Morus nigra leaf extract", Indian Journal of Pharmaceutical and Biological Research, Vol. 1, No. 4, PP. 16-24, 2013.

[2] A. Ruhal, J. S. Rana, P. Ruhal, A. Kumar and M. Ruhil, "Antimicrobial nanocomposite of silver and gelatin nanofibers for medical applications", International Journal for Technological Research in Engineering, Vol. 1, No. 4, PP. 177-182, 2013.

[3] K. Jhansi, S. Chandralingam, N. M. Reddy, P. Suvarna, A. Chinthakuntla and K. V. Rao, "CuO nanoparticles synthesis and characterization for humidity sensor application", Journal of Nanotechnology and Materials Science, Vol. 3, No. 1, 2016.

[4] Sh. Kaushik, "Application of nanotechnology in textile", Asian Journal of Home Science, Vol. 9, No. 2, PP. 580-583, 2014.

[5] B. A. M. A. Al-Salihi, " Effect of nano-copper oxide on the electrical and optical properties of (PMMA) polymer", Ph. D. Thesis, University of Babylon, College of Education for Pure Sciences, Department of Physics, (2016).

[6] L. M. Armijo, S. J. Wawrzyniec, M. Kopciuch, Y. I. Brandt, A. C. Rivera, N. J. Withers, N. C. Cook, D. L. Huber, T. C. Monson, H. D. C. Smyth and M. Osinski, "Antibacterial activity of iron oxide, iron nitride and tobramycin conjugated nanoparticles against seudomonas aeruginosa biofilms", Journal of Nanobiotechnology, Vol. 18, No. 35, PP. 2-27, 2020.

[7] R. Singh, M. S. Smitha, and S. P. Singh, "The Role of Nanotechnology in Combating Multi-Drug Resistant Bacteria", Journal of Nanoscience and Nanotechnology, Vol. 14, PP. 4745-4756, 2014.

[8] S. Mussa and F. Basheer, " Material Technology", Tripoli, 2003.

[9] D. Paul and L. Robesonb, "Polymer nanotechnology nanocomposites", Vol. 49, No. 15, PP. 3187-3204, 2008.

[10] D. Lukhassen and A. Meide,"A advanced materials and structures and them fabrication process", Third Edition, Narvik university college, HIN, 2003.

[11] R. G. Kadhim, M. H. Shinen and M. S. Abdali, "Electrical properties of polyaniline/multi-walled carbon nanotubes nano films", AL-Qadisiyah Journal of pure Science, Vol. 22, No. 2, 2017.

[12] K. M. Ziadan, H. F. Hussein and K. I. Ajeel "Study of the electrical characteristics of poly(otoluidine) and application in solar cell", Energy Procedia, Vol. 18, PP. 157-164, 2012.

[13] A. S. Hussein, "Influence of adding polyethylene oxide on some polymer properties for medical applications", Ph. D. Thesis, University of Babylon, College of Science, Department of Physics, 2016.

[14] B. Horst, N. S. Moiemen and L. M. Grover, "Natural polymers: biomaterials for skin scaffolds", Biomaterials for Skin Repair and Regeneration, PP. 151-192, 2019.

[15] F. Rodriguez, C. Cohen, Ch. K. Ober and L. Archer "Principles of polymer systems", Second Edition, McGraw- Hill, New York, PP. 810-406, 2015.

[16] E. Al-Bermany, D. Qais and S. Al-Rubaye "Graphene effect on the mechanical properties of poly (ethylene oxide)/graphene oxide nanocomposites using ultrasound technique", Journal of Physics: Conference Series, Vol. 1234, PP. 1-12, 2019.

[17] A. I. Abdelamir, E. Al-Bermany and F. S. Hashim, "Important factors affecting the microstructure and mechanical properties of PEG/GO-based nano-graphene composites fabricated applying assembly-acoustic method", AIP Conference Proceedings, Vol. 2213, PP. 1-13, 2020.

[18] G. A. Kontos, A. L. Soulintzis, P. K. Karahaliou, G. C. Psarras, S. N. Georga, C. A. Krontiras and M. N. Pisanias, "Electrical relaxation dynamics in TiO_2-Polymer matrix composites", Express Polym Lett, Vol. 1, PP. 781-9, 2007.

[19] S. Al-Rubaye, E. Al-bermany, M. Habeeb and R. Rajagopalan, "Electrochemical performance evaluation of Ni foam/$NiCo_2O_4$-CNTs for energy storage applications", Test Engineereing and Management, Vol. 83, PP. 12828-41, 2020.

[20] E. Sharifzadeh, I. Ghasemi, M. Karrabi and H. Azizi, "A New approach in modeling of mechanical properties of nanocomposites: effect of interface region and random orientation", Iranian Polymer Journal, Vol. 23, PP. 835-45, 2014.

[21] E. Jawad, S. H. Khudhair and H. N. Ali, "A Thermodynamic study of adsorption of some days on Iraqi bentonite modified clay" European Journal of Scientific Research, Vol. 60, PP. 63-70, 2011.

[22] E. Al-Bermany, "Polymer/graphene oxide nanocomposites: surface adsorption and interfaces", Ph. D. Thesis, University of Sheffield, 2017.

[23] V. C. Tung, M. J. Allen, Y. Yang and R. B. Kaner, "High-Throughput solution processing of large-scale graphene", Nature Nanotechnology, Vol. 4, PP. 25-9, 2009.

[24] N. Mahmood, "Graphene-based nanocomposites for energy storage and conversion in lithium batteries", supercapacitors and fuel cells Vol. 2, PP. 15-32, 2014.

[25] M. A. Kadhim and E. Al-Bermany, "Structural and D.C-electrical properties of novel PMMA-PVA nanocomposites reinforced with graphene nanosheets", 4th International Conference on Engineering Sciences, IOP Conf. Series: Materials Science and Engineering, Vol. 1067, PP. 1-14, 2021.

[26] Sh. S. Al-Abbas, R. A. Ghazi, A. K. Al-shammari, N. R. Aldulaimi, A. R. Abdulridha, S. H. Al-Nesrawy and E. Al-Bermany, "Influence of the polymer molecular weights on the electrical properties of Poly(vinyl alcohol)-Poly(ethylene glycols)/Graphene oxide nanocomposites", Materials Today: Proceedings, Vol. 42, PP. 2469-2474, 2021.

[27] E. Al-Bermany, B. Chen, "Preparation and characterization of Poly(ethylene glycol)-adsorbed graphene oxide nanosheets", Polymer International, Vol. 70, No. 3, PP. 341-351, 2021.

[28] H. Kasim, M. Yazici, "Electrical properties of graphene/natural rubber nanocomposites coated nylon 6.6 fabric under cyclic loading, Period. Polytech. Chem. Eng. Vol. 63, PP. 160-169, 2019.

[29] A. Adeniyi, O. Agboola, E. R. Sadiku, M.O. Durowoju, P.A. Olubambi, A. B. Reddy, I. D. Ibrahim and W. K. Kupolati, "Chapter2thermoplastic-thermoset nanostructured polymer blends", book, PP. 1-23, 2016.

[30] R. Muthuraj, M. Misra and A. K. Mohanty, "Biodegradable compatibilized polymer blends for packaging applications: A literature review ", Journal of Applied Polymer Sciences, Vol. 135, No. 24, PP. 1-35, 2017.

[31] A. H. O. Alkhayatt, A. H. Al-Azzawi and Z. Alakayashi, "Rheological and optical characterization of polyvinyl pyrrolidone (PVP) - polyethylene glycol (PEG) polymer blends", Journal of Applied Physics, Vol. 8, No.1, PP. 11-18, 2016.

[32] S. P. Masti and R. B. Chougale, "Influence of polyvinyl pyrrolidone on binary blend films made from polyvinyl alcohol/chitosan", International Research Journal of Environment Sciences, Vol. 3, No. 3, PP.11-13, 2014.

[33] M. A. Kader and A. K. Bhowmick, "Effect of filler on the mechanical, dynamic mechanical, and aging properties of binary and ternary blends of acrylic rubber, fluorocarbon rubber, and polyacrylate", Journal of applied polymer science, Vol. 90, No. 1, PP. 278-286, 2003.

[34] A. Y. Ban, "Development and characterization of ternary thermosetting polymer blends", Ph. D thesis, University of technology, 2010.

[35] M. N. Subramanian, "Basics of polymers fabrication and processing technology", India, Printed in the United States of America, Momentum Press, LLC, PP. 5-108, 2015.

[36] S. A. Jabbar, F. L. Rashid, A. Hadi, M. A. Habeeb and A. Hashim "Enhancement of optical properties for poly vinyl alcohol by addition of biomaterial", Journal of Chemical and Pharmaceutical Sciences, Vol. 10, No.1, PP. 0974-2115, 2017.

[37] E. D. J. Ali, "Study some Physical Properties of Post-Irradiation for Polystyrene Dissolved in Toluene", American Journal of Scientific Research, Vol. 29, PP. 130-141, 2011

[38] J. B. Bhaiswar, M. Salunkhe, S. P. Dongre and B. T. Kumbhare, "Comparative study on thermal stability and optical properties of PANI/Cds and PANI/Pbs nanocomposite", Journal of Applied Physics, International Conference on Advances in Engineering & Technology, Vol. 80, PP. 79-82, 2014.

[39] I-Yup Jeon and J. Beom Baek, "Nanocomposites Derived from Polymers and Inorganic Nanoparticles", Journal of Materials, Vol. 3, P. 3654-3674, 2010.

[40] H. Hu, L. Onyebueke and A. Abatan, "Characterizing and modeling mechanical properties of nanocomposites-review and evaluation", Journal of minerals & materials characterization& engineering, Vol. 9, No.4, PP.275-319, 2010.

[41] H. M. Shanshool, M. Yahaya, W. M. Yunus and b. Y. Abdullah, "Optical properties of PMMA/ZnO nanocompositesas foils prepared by casting method", Australian Journal of Basic and Applied Sciences, Vol. 9, No. 5, PP. 401-409, 2015.

[42] A. Jaafari and A. S. Ayesh, "Effect of ZnO nanoparticles on the dielectric relaxation behavior and thermal stability of polycarbonate host", Journal of Thermoplastic Composite Materials, Vol. 24, PP. 837-852, 2011.

[43] W. Al-Taay, M. A. Nabi, R. M. Yusop, E. Yousif, B. M. Abdullah, J. Salimon, N. Salih, and S. I. Zubairi, "Effect of nano ZnO on the optical properties of polyvinyl chloride films", International Journal of Polymer Science, Article ID 697809, Vol. 2014, PP. 1-6, 2014.

[44] M. E. Gouda and T. Y. Elrasasi, " Impact of gamma irradiation on structural and dielectric properties of CuI-PVA/PEDOT: PSS polymer nanocomposite", IOSR Journal of Applied Physics, Vol. 7, No. 6, PP. 22-30, 2015.

[45] G. E. William, B. A. Aldo and Z. Jinwen, "Polymer nanocomposites: synthetic and natural fillers", Maderas. Ciencia y tecnología, Vol. 7, No. 3, PP. 159-178, 2005.

[46] A. Kaur and N. Shahi, "How nanotechnology works in medicine", Nternational Journal of Electronics and Computer Science Engineering, Vol. 1, No. 4, PP. 2452-2459, 2012.

[47] P. Boisseaua and B. Loubaton , "Nanomedicine, nanotechnology in medicine", Comptes Rendus Physique , Vol. 12, No. 7, PP. 620-636, 2011.

[48] A. P. Nikalje,"Nanotechnology and its applications in medicine", Medicinal chemistry, Vol. 5, No. 2, PP.81-89, 2015.

[49] S. B. Somwanshi, R. T. Dolas, S. S. Siddheshwar, A. N. Merekar, R. K. Godge and S. R. Pattan, "Nanomedicine drug delivery system", Asian Journal of Biomedical and Pharmaceutical Sciences, Vol. 3, No. 22, PP. 9-15, 2013.

[50] S. Radha, "Medical application of nanotechnology in nanomedicine", Journal of Science, Vol. 3, No. 1, PP. 28-34, 2013.

[51] SK. Sh. Basha, G. S. Sundari and K. V. Kumar, "Optical, thermal and electrical studies of PVP based solid polymer electrolyte for solid state battery applications", International Journal of Chem Tech Research, Vol. 9, No. 2, PP. 165-175, 2016.

[52] E. M. Abdelrazek, H. M. Ragab and M. Abdelaziz, "Physical characterization of poly (vinyl pyrrolidone) and gelatin blend films doped with magnesium chloride", Plastic and Polymer Technology, Vol. 1, No. 1, PP. 1-8, 2013.

[53] K. Sivaiah, K. N. Kumar, V. Naresh and S. Buddhudu, "Structural and optical properties of Li^+: PVP & Ag^+ : PVP polymer films", Materiales sciences and Application, Vol. 2, PP. 1688-1696, 2011.

[54] J. Marijana, S. Igor, Z. Zoran and M. Stjepan, "Effect of polyvinyl pyrrolidone on the formation AgBr grains in gelatine media", Croatica Chemica Acta, Vol. 85, No. 3, PP. 269-276, 2012.

[55] H. Qina, Sh. Niea, Ch. Chenga, F. Rana, Ch. Hea, L. Maa , Z. Yina and Ch. Zhao, "Insights into the surface property and blood compatibility of polyethersulfone/polyvinyl pyrrolidone composite membranes: toward high-performance hemodialyzer", Polymers for Advanced Technologies, Vol. 25, No. 8, PP. 851-860, 2014.

[56] H. Hakim, A. Hashim, G. Abdul-Hafidh, H. A. Alyaa and S. Mohammed, "Study the optical properties of polyvinyl pyrrolidone (PVP) doped with Kbr", European Scientific Journal, Vol. 3, PP. 132-137, 2013.

[57] L. Wang, M. WeiChang, Z. Ahmad, H. Zheng and J. SongLi, "Mass and controlled fabrication of aligned PVP fibers for matrix type antibiotic drug delivery systems", Chemical Engineering Journal, Vol. 307, PP. 661-669, 2017.

[58] J. M. H. Jabir, "The optical properties of (PVA+PVP) + PANI blends", Iraqi Journal of Physics, Vol. 13, No. 28, PP. 162-169, 2015.

[59] C. Liew, N. HM, A. Numan and S. Ramesh, "Poly(Acrylic acid)-based hybrid inorganic–organic electrolytes membrane for electrical double layer capacitors application", Polymers. Vol. 8, No. 5, PP. 179, 2016.

[60] Sk. M. Begum , M. C. Rao and R. V. S. S. N. Ravikumar, "Cu_2+ doped PVA passivated ZnSe nanoparticles-preparation, characterization and properties", Journal of Inorganic and

Organometallic Polymers and Materials, Vol. 23 , No. 2, PP. 350-356, 2013.

[61] N. B. R. Kumar, V. Crasta and B. M. Praveen, "Advancement in microstructural, optical, and mechanical properties of PVA (Mowiol 10-98) doped by ZnO nanoparticles", Physics Research International, Vol. 2014, PP. 1-9, 2014.

[62] A. A. M. Shehab, E. Y. Abid and S. H. Salman, "Studying the structural and optical properties of PVA doped with CuO and $FeCl_3$ composites films", Engineering & Technology Journal, Vol. 33, No. 9, PP. 1712-1722, 2015.

[63] J. Selvi, S. Mahalakshmi and V. Parthasarathy, "Synthesis, structural, optical, electrical and thermal studies of poly(vinyl alcohol)/CdO nanocomposite films", Journal of Inorganic and Organometallic Polymers and Materials, Vol. 27, PP. 1918-1926, 2017.

[64] S. K. Das, M. Hasan, J. M. M. Islam, M. A. Khan, Md. A. Gafur and E. Hoque, "Characterization of solution casting derived carbon nanotube reinforced poly(vinyl alcohol) thin films", International Journal of Plastics Technology, Vol. 21, No. 2, PP. 338-350, 2017.

[65] A. Chaturvedi, A. K. Bajpai and J. Bajpai, "Preparation and characterization of polyvinyl alcohol Cryogel-silver nanocomposites and evaluation of blood compatibility, cytotoxicity, and antimicrobial behaviors", Polymer Composites, Vol. 36, No.1, PP. 1983-1997, 2015.

[66] P. Jayakrishnan and M. T. Ramesan , "Synthesis, characterization, electrical conductivity and materialn properties of magnetite/ polyindole /poly(vinyl alcohol) blend nanocomposites", Journal of Inorganic and Organometallic Polymers and Materials, Vol. 27, No.1, PP. 323-333, 2017.

[67] J. A. Al-Kareem, K. B. Yahya and F. N. Lamis, "Study of some mechanical properties of PVA/ZnO composites byultrasonic waves", Journal of Babylon University/Pure and Applied Sciences, Vol. 21, No. 1, 2013

[68] A. J. Al-bermany, B. Y. Kadem and E. D. J. Al-bermany, "Study of some mechanical properties of PVA/TiO_2 composite at different ultrasonic frequencies", World Academy of Science, Engineering and Technology 61, Vol. 62, No. 6, 2012.

[69] M. Abdul and E. Al-bermany, "Enhance the electrical properties of the novel fabricated PMMA-PVA/graphene based nanocomposites", Journal of Green Engineering, Vol. 10, PP. 3465-83, 2020.

[70] T. W. Clyne and D. Hull, "An introduction to composite materials", Cambridge university press, book, 2019.

[71] ED. Jawad, S. Khudhair and H. Ali "A thermo dynamic study of adsorption of some days on Iraqi bentonite modified clay", Journal of Social Sciences, No. 60: PP. 63-70, 2011.

[72] S. S. Devangamath, B. Lobo, S.P. Masti and S. Narasagoudr, "Thermal, mechanical, and A.C electrical studies of PVA-PEG-Ag_2S polymer hybrid material", Journal of Materials Science: Materials in Electronics, Vol. 31, PP. 2904-2917, 2020.

[73] Z. Guo, D. Zhang, S. Wei, Z. Wang, A. B. Karki, L. Yuehao, P. Bernazzani, D.P. Young, J. A. Gomes, D. L. Cocke and C. H. Thomas, "Effects of iron oxide nanoparticles on polyvinyl alcohol: interfacial layer and bulk nanocomposites thin film", Journal of Nanoparticle Research, Vol. 12, PP. 2415-2426, 2010.

[74] A.R. Abdulridha, E. Al-Bermany, F.S. Hashim and A.H.O. Alkhayatt, "Synthesis and characterization and pelletization pressure effect on the properties of $Bi_{1.7}Pb_{0.3}Sr_2W_{0.2}$ Ca_2Cu_3 $O_{10+\delta}$ superconductor system ", Intermetallics, Vol. 127, PP. 1-8, 2020.

[75] E. D. Jawad, S.H.S.H. Khudhair and H. N. H. N. Ali, "A thermodynamic study of adsorption of some days on Iraqi Bentoniet modified clay", European Journal of Scientific Research, Vol. 60, PP. 63-70, 2011.

[76] N. T. A. Azeez, "Spectroscopic study of some new prepared organic dyes as optical limiting", Ph. D thesis, University of Babylon, 2019.

[77] T. S. Gaaz, A. B. Sulong, M. N. Akhtar, A. A. H. Kadhum, A. B. Mohamad and A. A. Al-Amiery, " Properties and applications of polyvinyl alcohol, halloysite nanotubes and their nanocomposites", Molecules, Vol. 20, PP. 22833-22847, 2015.

[78] H. N. Friedlander, H. E. Harris and J. G. Pritchard, "Structure-property relationships of poly(vinyl alcohol).i.influence of polymerization solvents and temperature on the structure and properties of poly(vinyl alcohol) derived from poly(vinyl acetate)", Journal of Polymer Science, Vol. 4, No. 3, PP. 649-664, (1966).

[79] P. Sivakumar, C. Nethra Devi and S. Renganathan," Synthesis of silver nanoparticles using lantana camara fruit extract and its effect on pathogens" , Asian Journal of Pharmaceutical and Clinical Research, Vol. 5, No. 3, PP. 97, 2012.

[80] G. M. Sulaimana, A. A.W. Mohammada, H. E. Abdul-Waheda and M. M. Ismail, "Biosynthesis, antimicrobial and cytotoxic effects of silver nanoparticles using rosmarinus officinalis extract", Digest Journal of Nanomaterials and Biostructures Vol. 8, No. 1, 2013, PP. 273-280, 2013.

[81] G. M. Sulaimana, E. H. Alia, I. I. Jabbarb and A. H. Saleema, "Synthesis, characterization, antibacterial and cytotoxic effects of silver nanoparticles", Digest Journal of Nanomaterials and Biostructures, Vol. 9, No. 2, PP. 787-796, 2014.

[82] S. Moaddab, H. Ahari, D. Shahbazzadeh, A. A. Motallebi, A. A. Anvar, J. Rahman-Nya and M. R. Shokrgozar, " Toxicity study of nanosilver (nanocid®) on osteoblast cancer cell line", International Nano Letters, Vol.1, No. 11, PP. 11-16, 2011.

[83] K. Satyavani, S. Gurudeeban, T. Ramanathan and T. Balasubramanian, "Biomedical potential of silver nanoparticles synthesized from calli cells of Citrullus colocynthis (L.) Schrad", Journal of Nanobiotechnology, Vol. 9, No. 2, 2011.

[84] N. Ch. Emeka, P. E. Imoisili and T. Ch. Jen, "Preparation and characterization of NbxOy thin films: a review", Coatings, Vol. 10, No. 1246, PP. 1-28, 2020.

[85] K. T. Jacob, Ch. Shekhar, M. Vinay and Y. Waseda, "Thermodynamic properties of niobium oxides", Journal of Chemical & Engineering Data, Vol. 55, No. 11, PP. 4854-4863, 2010.

[86] S. Iqbal, M. Fakhar Alam, F. Akbar, M. Shafiq, M. Atif, N. Amin, M. Ismail, A. Hanif and W. A. Farooq, "Application of silver oxide nanoparticles for the treatment of cance", Journal of Molecular Structure, Vol. 1189, No. 5, PP. 203-209. 2019.

[87] K. T. Jacob, C. Shekhar, M. Vinay and Y. Waseda, "Thermodynamic properties of niobium oxides", Journal of Chemical & Engineering Data, Vol. 55, PP. 4854-4863, 2010.

[88] G. Ramírez, S.E. Rodi, S. Muh, D. Turcio-Ortega, J. J. Olaya, M. Rivera, E. Camps and L. Escobar-Alarcon, "Amorphous niobium oxide thin films", Journal of Non-Crystalline Solids, Vol. 356, PP. 2714-2721, 2010.

[89] J. H. Xu, T. Jarlborg and A. J. Freeman, "Self-consistent band structure of the rutile dioxides NbO_2, RuO_2 and IrO_2", The American Physical Society, Vol. 40, PP. 7939-7947, 1989.

[90] A. Tarlani, M. Isari and A. Khazraei, "New sol-gel derived aluminum oxide-ibuprofen nanocomposite as a controlled releasing medication", Nanomedicine Research Journal , Vol. 2, No. 1, PP. 28-35, 2017.

[91] P. Hassanpour, Y. Panahi, A. Ebrahimi-Kalan, A. Akbarzadeh, S. Davaran, A. N. Nasibova, R. Khalilov and T. Kavetskyy, "Biomedical applications of aluminium oxide nanoparticles", Micro & Nano Letters, Vol. 13, No. 9, PP. 1227-1231, 2018.

[92] Material Properties Data: Alumina (Aluminum Oxide) Archived 2010-04-01 at the Wayback Machine. Makeitfrom.com. Retrieved on 2013-04-17.

[93] Y. Zhao, Y. Zhou, W. Xiaomian, L. Wang, X. Ling, and W. Shicheng, "A facile method for electrospinning of Ag nanoparticles/poly(vinylalcohol)/carboxymethyl-chitosa nanofibers", Applied Surface Science, Vol. 258, PP. 8867-8873, 2012.

[94] W. H. Eisa, Y. K. Abdel-Moneam, A. A. Shabaka, and A. M. Hosam, "In situ approach induced growth of highly monodispersed Ag nanoparticles within free standing PVA/PVP films", Spectrochimica Acta Part A: Molecular and Biomolecular Spectroscopy, Vol. 95, PP. 341-346, 2012.

[95] M. H. AL-humairi, "Study the optical and electrical properties of (PVA-Ag) and (PVA-TiO_2) nanocomposites", M.Sc. Thesis, University of Babylon, College of Education for Pure Sciences, 2013.

[96] H. N. Chandrakala, B. Ramaraj, Shivakumaraiah, G.M. Madhu and Siddaramaiah," Investigation on the influence of sodium zirconate nanoparticles on the structural characteristics and electrical properties of polyvinyl alcohol nanocomposite films", Journal of Alloys and Compounds, Vol. 551, PP. 531–538, 2013.

[97] M. Ghanipour and D. Dorranian, "Effect of Ag-nanoparticles doped in polyvinyl alcohol on the structural and optical properties of PVA films", Journal of Nanomaterials, Vol. 2013, PP. 1-10, 2013.

[98] R. Augustine, H. N. Malik, D. K. Singhal, A. Mukherjee, D. Malakar and S. Thomas, "Electrospun polycaprolactone /ZnO nanocomposite membranes as biomaterials with antibacterial and cell adhesion properties", Journal of Polymer Research, Vol. 21, PP. 347, 2014.

[99] S. Azizi, M. B. Ahmad, M. Z. Hussein, N. A. Ibrahim and F. Namvar, "Preparation and properties of poly(vinyl alcohol)/chitosan blend bionanocomposites reinforced with cellulose nanocrystals/ ZnO-Ag multifunctional nanosized filler", International Journal of Nanomedicine, Vol. 9, PP. 1909-1917, 2014.

[100] H. Hakim, Z. Al- Ramadhan and A. Hashim, "The effect of aluminum oxide nanoparticles on the optical properties of (PVP-PEG) blend", Research Journal of Cell and Molecular Biology, Vol. 5, No. 1, PP. 15-18, 2015.

[101] R. G. Kadhim, "Study the electrical and structural properties of (PMMA-TiO_2) nanocomposites", Chemistry and Materials Research, Vol.7, No.9, pp.37- 48, 2015.

[102] R. T. Abdulwahid, O. Gh. Abdullah, S. B. Aziz, S. Hussein, F. Muhammad and M. Yahya, "The study of structural and optical properties of PVA:PbO_2 based solid polymer nanocomposites", Journal Mater Science: Mater Electron, Vol. 27, No.11, ISSN 0957-4522, PP. 1-15, 2016.

[103] M. Karpuraranjith and S. Thambidurai, "Chitosan/zinc oxide-polyvinylpyrrolidone (CS/ZnO-PVP) nanocomposite for better thermal and antibacterial activity", International Journal of Biological Macromolecules, Vol. 104, PP. 1753-1761, 2017.

[104] M. E. Diken, S. Doğan, Y. Turhan and M. Doğan, "Synthesis and characterization of poly(acrylicacid)/organo-modified hydroxyapatite nanocomposites: thermal, optical and biocompatibility properties", Advances In Materials Science, Vol. 18, No. 3, PP. 57, 2018.

[105] R. M. Tripathi, R. N. Pudake, B. R. Shrivastav and A. Shrivastav, "Antibacterial activity of poly(vinyl alcohol)-biogenic silver nanocomposite film for food packaging material", Advances in Natural Sciences: Nanoscience and Nanotechnology, Vol. 9, PP. 1-5, 2018.

[106] I. A. Hamad, R. I. Khaleel and A. M. Raoof, " Structural and optical properties for nanostructure (Ag_2O/Si & Psi) films for photodetector applications", Baghdad Science Journal, Vol. 16, No. 4, 2019.

[107] A. Hazim, A. Hashim and H. M. Abduljalil," Novel (PMMA-ZrO_2-Ag) nanocomposites: structural, electronic, optical properties as antibacterial for dental industries", International Journal of Emerging Trends in Engineering Research, Vol. 7, No. 8, PP. 68 - 84, 2019.

[108] R. M. Mohammed, M. A. Habeeb and A. Hashim,"Effect of antimony oxide nanoparticles on structural, optical and A.C electrical properties of (PEO-PVA) blend for antibacterial applications", International Journal of Emerging Trends in Engineering Research, Vol. 8, No. 8 PP. 4726 -4738, 2020.

[109] A. Hashim, A. J. Kadham, A. Hadi and M. A. Habeeb, "Determination of optical parameters of polymer blend/ nanoceramics for electronics applications", Nanosistemi, nanomaterial, nanotechnology, Vol. 19, No. 2, PP. 327-336, 2021.

[110] M. H. Meteab, A. Hashim and B. H. Rabee, "Controlling the structural and dielectric characteristics of PS-PC/Co_2O_3-SiC hybrid nanocomposites for nanoelectronics applications", Silicon, No. 10, 2022.

[111] R. Divya, M. Meena, C. K. Mahadevan and C. M. Padma, "Investigation on CuO dispersed PVA polymer films", Journal of Engineering Research and Applications, Vol. 4, No. 5, PP. 1-7, 2014.

[112] I. R. Agoo, K. J. Kadhim and A. Hashim, "Synthesis of (PVA-PEG-PVP-ZrO_2) nanocomposites for energy release and gamma shielding applications", International Journal of Plastics Technology, Vol. 21, No. 2, PP. 444-453, 2017.

[113] M. H. M. Zaid, K. A. Matori, S. H. Abdul Aziz, A. Zakaria and M. S. M. Ghazali, "Effect of ZnO on the physical properties and optical band gap of soda lime silicate glass", International Journal of Molecular Sciences, Vol. 13, PP. 7550-7558, 2012.

[114] M. A. Habeeb , H. M. Mohssen and R. G. Kadhim , "Effect of (CoO) nanoparticles on someoptical properties of (PVA-PAAM) composite", International Journal of Engineering Research & Technology, Vol. 3, No. 5, PP. 2050-2053, 2014.

[115] N. Wilkinson, A. Metaxas, E. Ruud, E. Raethke , S. Wickramaratn, Th. M. Reineke and C. S. Dutcher , "Internal structure visualization of polymer-clay flocculants using fluorescence", Colloids and Interface Science Communications, Vol. 10, No. 11, PP. 1-5, 2016.

[116] A. Hashim, M. Ali and B. H. Rabee, "Optical properties of (PVA-CaO) composites", American Journal of Scientific Research, No.69, PP. 5-9, 2012.

[117] M. A. Habeeb, A. Hashim and N. Hayder, " Structural and Optical Properties of Novel (PS-Cr_2 O_3 / $ZnCoFe_2$ O_4) Nanocomposites For UV and Microwave Shielding", Egyptian Journal of Chemistry, Vol. 62, No. 2, PP. 697-708, 2019.

[118] V. N. Reddy, K.S. Rao, M.C Subha and K. C. Rae "Miscibility behavior of dextrin/PVA blends in water at 35 Cº", International Conference on Advances in Polymer Technology, India, PP. 356-368, 2010.

[119] K. J. Kadhim, I. R. Agool and A. Hashim, "Enhancement in optical properties of (PVA-PEG-PVP) blend by the addition of titanium oxide nanoparticles for biological application", Advances in Environmental Biology, Vol. 10, No.1, PP. 81-87, 2016.

[120] A. Begum, A. Hussain and A. Rahman, "optical and electrical properties of doped and Un doped Bi_2S_3–PVA films prepared by chemical drop method", Journal of Materials Sciences and Applications, Vol. 2, PP. 163-168, 2011.

[121] K. C. Lalithambika, K. Shanthakumari and S. Sriram, "Optical Properties of CdO thin films deposited by chemical bath method", International Journal of Chem. Tech. Research, Vol.6, No. 5, PP. 3071-3077, 2014.

[122] S. F. Wei, "Research on the characterization of hydrogenated silicon thin film using constant photocurrent method", Thesis M.Sc, Department of Optics and Photonics, National Central University, 2009.

[123] O. Gh. Abdullah1, B. K. Aziz, and S. A. Hussen, "Optical characterization of polyvinyl alcohol-ammonium nitrate polymer electrolytes films", Journal of Chemistry and Materials Research, Vol. 3, No. 9, PP. 84-90, 2013.

[124] C. Mwolfe, N. Holouyak and G. B. Stillman, "Physical properties of semiconductor", prentice Hall, New York, 1989.

[125] J. I. Pankove, "Optical process in semiconductors", Dover Publishing, Inc., New York, 1971.

[126] Y. N. Al-Jamal, "Solid state physics", Al-Mosel University, 2nd Ed., Arabic Version, (2000).

[127] J. H. Nahida, "Spectrophotometric analysis for the UV- irradiated (PMMA)", International Journal of Basic & Applied Sciences, Vol. 12, No. 2, PP. 58-67, 2012.

[128] A. Essahlaoui, H. Essaoudi, A. Hallaoui, M. Bouhadda, A. Labzour and A. Housni, "Calculation of the thickness and optical constants of lead titanate thin films grown on MgO from their transmission spectra", Journal of Materials and Environmental Sciences, Vol. 9, No. 1, PP. 228-234, 2018.

[129] O. Abdullah, D. A. Tahir, S. S. Ahmad, and H. T. Ahmad, "Optical properties of PVA: $CdCl_2$. H_2O polymer electrolytes", Journal of Applied Physics, Vol.4, No. 3, PP. 52-57, 2013.

[130] S. A. Salman, M. H. Abdu-allah and N.A. Bakr, "Optical characterization of red methyl doped poly (vinyl alcohol) films", International Journal of Engineering and Technical Research, Vol. 2, No. 4, PP. 126-128, 2014.

[131] M. Noweel, NR. Pandel and X. Liu, "characterization of sputtered CdTe thin films electron bactter diffraction and correlation with device performance ", Journal Microscopy and Microanalysis, Vol. 21, No. 4, PP. 27-35, 2015.

[132] M. Akram, A. Javed and T. Zahra, "Dielectric properties of industrial polymer composite materials", Turkish Journal of Physics, Vol. 29, PP. 355-362, 2005.

[133] S. Prasher, M. Kumer and S. Singh, "Analysis of electrical properties of Li^{3+} ion beam irradiated lexan polycarbonate", Chemistry: An Asian Journal, Vol. 21, No. 10, PP. 43-46, 2009.

[134] B. B. Bohara, A. Kassu, J. Brinkley, A. K. Batra and M. D. Aggarwal, "Dielectric properties of lead magnesium niobate-lead titanate/cement nanocomposites", Advanced Science, Engineering and Medicine, Vol. 10, PP. 1260-1264, 2018.

[135] D. Oliveira , A. Borges , M. Simoes , "*Staphylococcus aureus* toxins and their molecular activity in infectious diseases", Toxins, Vol. 10, No. 6, P. 252, 2018.

[136] H. Jacquemyn, M. Lenaerts, R. Brys, K. Willems, O. Honnay and B. Lievens, "Among-population variation in microbial community structure in the floral nectar of the bee-pollinated forest herb *Pulmonaria officinalis*L", PLOS ONE, Vol. 8 , No. 3, 2013.

[137] H. W. Boucher , G. H. Talbot, J. S. Bradley, J. E. Edwards, D. Gilbert, L. B Rice, M. Scheld, B. Spellberg and J. Bartlett, "An Update from the Infectious Diseases Society of America", Clinical Infectious Diseases, Vol. 48, No. 1, PP. 1-12, 2009.

[138] H. Andersson, C. Lindholm, B. Fossum, "MRSA-Global threat and personal disaster: Patients experiences", International Nursing Review, Vol. 58, PP. 47-53, 2011.

[139] N. A. Turner, B. K. Sharma-Kuinkel, S. A. Maskarinec, E. M. Eichenberger, P. P. Shah and M. Carugati, "Methicillin-resistant *Staphylococcus aureus*: an overview of basic and clinical research", Nature reviews Microbiology, Vol. 17, No. 4, PP. 203-18, 2019.

[140] D. Nurjadi, A. O. Olalekan, F. Layer, A. O. Shittu, A. Alabi, B. Ghebremedhin, F. Schaumburg, J. Hofmann-Eifler, P. J. Van Genderen, E. Caumes, "Emergence of trimethoprim resistance gene

dfrG in *Staphylococcus aureus* causing human infection and colonization in sub-Saharan Africa and its import to Europe", Journal of Antimicrobial Chemotherapy, Vol. 69, PP. 2361-2368, 2014.

[141] T. Jin, M. Mohammad, R. Pullerits and A. Ali, " Bacteria and host interplay in Staphylococcus aureus septic arthritis and sepsis", Pathogens, Vol. 10, No. 158, PP. 2-25, 2021.

[142] M. D. Willcox, "Characterization of the normal microbiota of the ocular surface", International Society for Eye Research, Vol. 117, PP. 99-105, 2013.

[143] A. P. Dale, N. Woodford, "Extra-intestinal pathogenic *Escherichia coli* (ExPEC): Disease, carriage and clones", Journal of Infection, Vol. 71, PP. 615-626, 2015.

[144] E. Denamur, O. Clermont, S. Bonacorsi and D. Gordon, "The population genetics of pathogenic *Escherichia coli*", Nature Reviews Genetics, Vol. 19, No. 1, PP. 37-54, 2021.

[145] C. J. Murray, K. S. Ikuta, F. Sharara, L. Swetschinski, G. R. Aguilar, A. Gray, C. Han, C. Bisignano, P. Rao, E. Wool and E. Global burden of bacterial antimicrobial resistance in 2019: A systematic analysis", Vol. 399, PP. 629-655, 2022.

[146] R. Laxminarayan , A. Duse, Ch. Wattal, A. K. M. Zaidi, H. F. L. Wertheim, N. Sumpradit, E. Vlieghe, G. L. Hara, I. M. Gould, H. Goossens, Ch. Greko, M. Bigdeli, G. Tomson, , E. Ombaka, A. Q. Peralta, F. N. Qamar, F. Mir, S. Kariuki, Z. A. Bhutta, A. Coates, R. Bergstrom, G. D Wright, E. D. Brown, "Antibiotic resistance-the need for global solutions", The Lancet Infectious Diseases ,Vol. 13, No. 12, PP. 1057-98, 2013.

[147] R. Smith and J. Coast, "The true cost of antimicrobial resistance", The BMJ, Vol. 346, PP. 1493, 2013.

[148] A. Vasudevan, B. I. Memon, A. Mukhopadhyay, P. A. Tambyah, "The costs of nosocomial resistant gram negative intensive care unit infections among patients with the systemic inflammatory response syndrome-a propensity matched case control study", Antimicrobial Resistance & Infection Control , Vol. 4, No. 3, 2015.

[149] E. Morales, F. Cots, M. Sala, M. Comas, F. Belvis, M. Riu, M. Salvadó, S. Grau, J. P. Horcajada, M. M. Montero, "Hospitalcosts of nosocomial multi-drug resistant Pseudomonas aeruginosa acquisition", BMC Health Services Research, Vol. 12, No. 122, 2012.

[150] R. Laxminarayan, A. Malani, D. Howard, D. L. Smith, "Extending the cure: policy responses to the growing threat of antibiotic resistance", Taylor & Francis Group: Abingdon, UK, 2010.

[151] N. Gupta, A. Jain, R. Sen, Sh. Mishra and M. Gupta, "A study on isolation of *E. coli* bacteria from different human clinical specimens", International Journal of Health Sciences and Research, Vol. 12, No. 6, P. 260, 2022.

[152] A. Gomez-Simmonds and A. Uhlemann, "Clinical implications of genomic adaptation and evolution of carbapenem-resistant *Klebsiella pneumoniae*", The Journal of Infectious Diseases, Vol. 215, No. 1, PP. 18-27, 2017.

[153] K. L. Wyres, M. M. C. Lam, K. E. Holt, "Population genomics of *Klebsiella pneumoniae*. Nature Reviews Microbiology, Vol. 18, PP. 344-359, 2020.

[154] N. Girometti, R. E. Lewis, M. Giannella, S. Ambretti, M. Bartoletti, S. Tedeschi, F. Tumietto, F. Cristini, F. Trapani, and P. Gaibani, "*Klebsiella pneumoniae* bloodstream infection: epidemiology and impact of inappropriate empirical therapy", Medicine, Vol 93, PP. 298-309, 2014.

[155] L. Chen, B. Mathema, K. D. Chavda, F. DeLeo, R. A. Bonomo and B. N. Kreiswirth, "Carbapenemase-producing *Klebsiella pneumoniae*: molecular and genetic decoding",Trends Microbiol, Vol. 22, PP. 686-696, 2014.

[156] S. P. Henson, C. J. Boinett, M. J. Ellington, N. Kagia, S. Mwarumba, S. Nyongesa, N. Mturi, S. Kariuki, J. A. G. Scott, and N. R. Thomson, "Molecular epidemiology of *Klebsiella pneumoniae* invasive infections over a decade at Killifish County Hospitalin Kenya", International Journal of Medical Microbiology, Vol. 307, PP. 422-429, 2017.

[157] D. Rawat and D. Nair, "Extended-spectrum ß-lactamases in gram negative bacteria" Journal of Global Infectious Diseases, Vol. 2, No. 263- 274, 2010.

[158] S. Kishibe, Y. Okubo, S. Morino S, et al. "Pediatric hypervirulent Klebsiella pneumoniae septic arthritis", Pediatrics International, Vol. 58, PP. 382-385, 2016.

[159] V. Arato, M. M. Raso, G. Gasperini, F. B. Scorza and F. Micoli, "Prophylaxis and treatment against *Klebsiella pneumoniae*: current insights on this emerging anti-microbial resistant global threat", International Journal of Molecular Sciences, Vol. 22, No. 8, PP. 4-20, 2021.

[160] C. V. d. Almeida, A. Taddei and A. Amedei, "The controversial role of Enterococcus faecalis in colorectal cancer", Therapeutic Advances in Gastroenterology, Vol. 11, 2018.

[161] P. M. G. Upadhyaya, K. L. Ravikumar, B. L. Umapathy, " Review of virulence factors of enterococcus: an emerging nosocomial pathogen", Indian Journal of Medical Microbiology, Vol. 27, No. 4, PP. 301-5, 2009.

[162] I. N. Rocas , J. F. Siqueira, K. R . N. Santos, " Association of Enterococcus faecalis with different forms of periradicular diseases", Journal of Endodontics, Vol. 30, No. 5, PP. 315-20, 2004.

[163] H. J. Rolph, A. Lennon, M. P. Riggio, W. P. Saunders, D. M. Kenzie, L. Coldero and J. Bagg, Molecular identification of microorganisms from endodontic infections", Journal of Clinical Microbiology, Vol. 39, No. 9, PP. 3282-9, 2001.

[164] J. F. Siqueira and I. N. Roças, "Uncultivated phylotypes and newly named species associated with primary and persistent endodontic infections", Journal of Clinical Microbiology, Vol. 43, N0. 7, PP. 3314-9, 2005.

[165] I. N. Roças, I. Y. Jung, C. Y. Lee and J. F. Siqueira, "Polymerase chain reaction identification ofmicroorganisms in previously root-filled teeth in a South Korean population", Journal of Endodontics, Vol. 30, PP. 504-8, 2004.

[166] J. F. Siqueira and I. N. Roças, "Polymerase chain reaction-based analysis of microorganisms associated with failed endodontic treatment", Oral Surg Oral Med Oral PatholOral Radiol Endod, Vol. 97, PP. 85-94, 2004.

[167] I. N. Roças, J. F. Siqueira, M. C. Aboim and A. S. Rosado, "Denaturing gradient gel electrophoresis analysis of bacterial communities associated with failed endodontic treatment", Oral Surg Oral Med Oral Pathol Oral Radiol Endod, Vol. 98, PP. 741-9, 2004.

[168] A. Azam, A. S. Ahmed, M. Oves, M. S. Khan, S. S. Habib and A. Memic, "Antimicrobial activity of metal oxide nanoparticles against gram-positive and gram-negative bacteria: A comparative

study", International Journal of Nanomedicine", Vol. 7, PP. 6003-6009, 2012.

[169] Z. Si-Wei, G. Chong-Rui, H. Ying-Zhu, G. Yuan-Ru and P. Qing-Jiang, "The preparation and antibacterial activity of cellulose/ZnO composite: A review", Open Chemistry, Vol. 16, No.1, PP. 9-20, 2018.

[170] N. Tran, A. Mir, D. Mallik, A. Sinha, S. Nayar and TJ. Webster, "Bactericidal effects of iron oxide nanoparticles on staphylococcus aureus", International Journal of Nanomedicine ,Vol. 5, PP. 277-283, 2010.

[171] A. Azam, A. Ahmed, M. Oves, M. Khan and A. Memic, "Size-dependent antimicrobial properties of CuO nanoparticles against gram-positive and -negative bacterial strains", International Journal of Nanomedicine, Vol. 7, PP. 3527-3535, 2012.

[172] KR. Raghupati, RT. Koodali and AC. Manna, "Size-dependent bacterial growth inhibition and mechanism of antibacterial activity of zinc oxide nanoparticles", Langmuir, Vol. 27, PP. 4020-4028, 2011.

[173] M. Singh, S. Singh, S. Prasada and I. Gambhir, "Nanotechnology in medicine and antibacterial effect of silver nanoparticles", Digest Journal of Nanomaterials and Biostructures, Vol. 3, No. 3, PP. 115-122, 2008.

[174] V. Monzillo, C. D. Valle, M. Corbella, E. Percivalle, D. Sassera, D. Scevola and P. Marone, "Antibacterial activity and cytotoxic effect of SIAB-GV3", Journal New of Microbiology, Vol. 37, PP. 535-541, 2014.

[175] M. A. Ansari, H. M. Khan, A. A. Khan, A. Sultan, A. Azam, M. Shahid and F. Shujatullah, "Antibacterial activity of silver nanoparticles dispersion against mssa and mrsa isolated from

wounds in a tertiary care hospital of north india", International Journal of Applied Biology and Pharmaceutical Technology, Vol. 2, No. 4, PP. 34-42, 2011.

[176] C. Srikanth, C. Sridhar, B. M. Nagabhushana and R. D. Mathad, "Characterization and D.C conductivity of novel CuO doped polyvinyl alcohol (PVA) nano-composite films", Journal of Engineering Research and Applications, Vol. 4, No. 10, PP. 38-46, 2014.

[177] J. Ramesh Babu and K. Vijaya Kumar, "Studies on structural and electrical properties of $NaHCO_3$ doped PVA films for electrochemical cell applications", International Journal of Chemistry Technology Research, Vol.7, No. 1, PP. 171-180, 2014.

[178] O. Abdullah, D. R. Saber and L. O. Hamasalih, "Complexion formation in PVA/PEO/$CuCl_2$ solid polymer electrolyte", Universal Journal of Materials Science, Vol. 3, No. 1, PP. 1-5, 2015.

[179] A. Pal Indolia and M. S. Gaur, "Optical properties of solution grown PVDF-ZnO nanocomposite thin films", Journal of Polymer Research, Vol. 20, No. 43, PP. 1-8, 2013.

[180] P. Phukan and D. Saikia, "Optical and structural investigation of CdSe quantum dots dispersed in PVA matrix and photovoltaic applications", International Journal of Photoenergy, Vol. 2, PP. 6, 2013.

[181] Y. Feng, N. Dong, G. Wang, Y. Li, S. Zhang K. Wang, L. Zhang, W. J. Blau, and J. Wang, "Saturable absorption behavior of free-standing graphene polymer composite films over broad wavelength and time ranges", Journal of Optics Express, Vol. 23, No.1, PP. 559-569, 2015.

[182] S. Salman, N. Bakr and M. H. Mahmood, "Preparation and study of some optical properties of (PVA-Ni($CH_3COO)_2$) composites", International Journal of Current Research, Vol. 6, No. 1, PP. 9638-9643, 2014.

[183] A. M. Abdelghany, E .M. Abdelrazek and D. Rashad, "Impact of in situ preparation of CdS filled PVP nano-composite", Journal of Spectrochimica Acta Part A: Molecular and Biomolecular Spectroscopy, Vol. 130, PP. 302-308, 2014.

[184] D. Hegazy, M. Eid and M. Madani, "Effect of Ni nano particles on thermal, optical and electrical behaviour of irradiated PVA/AAC films", Arab Journal of Nuclear Science and Applications, Vol. 47, No. 1, PP. 41-52, 2014.

[185] Z. H. E. M. Ghanipour and D. Dorranian, "Effect of dye concentration on the optical properties of red-BS dye-doped PVA film", Journal of theoretical Applied Physics, Vol. 8, No. 139, PP. 117-121, 2014.

[186] M. Ali, "Dielectric and optical properties of (PVAC-PEG-Ber) biocomposites", Australian Journal of Basic and Applied Sciences, Vol. 8, No. 13, PP. 623-629, 2014.

[187] A. M. El Sayed and W. M. Morsi, "α-Fe_2O_3 /(PVA + PEG) nanocomposite films; synthesis, optical, and dielectric characterizations", Journal of Materials Science, Vol. 49, PP. 5378-5387, 2014.

[188] O. Gh. Abdullah, "Influence of barium salt on optical behavior of PVA based solid polymer electrolytes", European Scientific Journal, Vol. 10, No. 33, PP. 406-417, 2014.

[189] N. K. Abbas, M. A. Habeeb, and A. J. Kadham Algidsawi, "Preparation of chloro penta amine cobalt(III) chloride and study of Its influence on the structural and some optical properties of

polyvinyl acetate", International Journal of Polymer Science, Vol. 2015, PP. 1-10, 2015.

[190] M. Venkatarayappa, S. Kilarkaje, A. Prasad and D. Hundekal, "Refractive index and dispersive energy of $NiSO_4$ doped poly (ethylene oxide) films", Journal of Materials Science and Engineering, Vol. 1, PP. 964-973, 2011.

[191] Hashim A and Hadi A "Novel pressure sensors made from nanocomposites (biodegradable polymers–metal oxide nanoparticles): fabrication and characterization", *Ukr. J. Phys, Vol.* 63 , No. 8, PP. 754, 2018.

[192] Habeeb M A, Hashim A, and Hadi A, "Fabrication of new nanocomposites: cmc-paapbo$_2$ nanoparticles for piezoelectric sensors and gamma radiation shielding applications", Sensor Lett, Vol. 15, No. 9, PP. 785-990, (2017).

[193] M. H. Harun, E. Saion, A. Kassim, M. Y. Hussain, I. Sh. Mustafa and M. A. A. Omer, "Temperature dependence of A.C electrical conductivity of PVA-PPy-$FeCl_3$ composites polymer Films", Malaysian Polymer Jounal, Vol. 3, No. 2, PP. 24-31, 2008.

[194] B. B. Bohara, A. Kassu, J. Brinkley, A. K. Batra and M. D. Aggarwal, "Dielectric properties of lead magnesium niobate-lead titanate/cement nanocomposites", Advanced Science, Engineering and Medicine, Vol. 10, PP. 1260-1264, 2018.

[195] A. Hashim and M. A. Habeeb, "Synthesis and characterization of polymer blend-$CoFe_2O_4$ nanoparticles as a humidity sensors for different temperatures", Transactions on Electrical and Electronic Materials, Vol. 20, No. 9. 2019.

[196] Y. T. Prabhu, K. V. Rao, B. Siva Kumari, V. S. S. Kumar and T. Pavani, "Synthesis of Fe_3O_4 nanoparticles and its antibacterial application", International Nano Letters, Vol. 5, No. 2, PP. 85-92, 2015.

[197] S. R. Kumar, R. G. krishnan, "The inhibitory effect of metal oxide nanoparticles against poultry pathogens", International Journal of Pharmaceutical Sciences and Drug Research, Vol. 4, No. 2, PP. 157-159, 2012.

[198] R. Khandanlou, M. B. Ahmad, K. Shameli, E. Saki and K. Kalantari, "Studies on properties of rice straw/polymer nanocomposites based on polycaprolactone and Fe_3O_4 nanoparticles and evaluation of antibacterial activity", International Journal of Molecular Sciences, Vol. 15, PP. 18466-18483, 2014.